USING VHSR MULTISPECTRAL IMAGERY AND OBJECT-BASED EXTRACTION TO DISCOVER VERNAL MEADOWS THROUGH VEGETATIVE PERSISTENCE AT FORT ORD, CALIFORNIA

by

Charles Joseph Hanley III

A Thesis Presented to the
FACULTY OF THE USC GRADUATE SCHOOL
UNIVERSITY OF SOUTHERN CALIFORNIA
In Partial Fulfillment of the
Requirements for the Degree
MASTER OF SCIENCE
(GEOGRAPHIC INFORMATION SCIENCE AND TECHNOLOGY)

August 2015

DEDICATION

I dedicate this document to my beautiful and amazingly patient wife, Shannon, without whom I could never have completed this project. You are my true one and only, my soulmate, and I am profoundly lucky to call you my best friend. And to my crazy little rugrat Connor, who is the constant source of inspiration and joy in my life. I do this all for the two of you!

ACKNOWLEDGMENTS

There are too many people to which I owe a debt of gratitude to mention them all here. On a personal note, I must first thank my wife for putting up with the two-year disappearance of her husband into a computer screen. I am so thankful to have returned to you from my long digital sojourn. Your love and support are the cornerstones of my life, and I am profoundly grateful to have you. To Connor, thank you for being the driving force that impels me on in life. Dad and Gina, what can I even begin to say? I could not have gotten anywhere without you. You both know very well the road I have traveled, and deserve thanks and praise for paving it ahead of me. To my Mom, who has always lent an ear and had a kind supportive word, you have my eternal appreciation. Thank you. To Doug and Jackie, you have been so supportive throughout this process. I owe you a great debt of gratitude. To Dan O'Rourke, the generous donation of your aircraft and piloting were an important part of this research project, and were greatly appreciated.

Professionally, I would like to thank Professor John Wilson. For agreeing to advise my project, I am forever grateful. Not often in life does one receive tutelage from someone whom is truly at the top of their respective field. I have always felt encouraged by your feedback. All the backing I required to complete this work was graciously provided to me, at the behest of Dr. Wilson. Thank you also to Professors Travis Longcore and Su Jin Lee, both for sitting on my committee and for providing invaluable feedback. Professor Robert Vos deserves many thanks as well, for serving as my *de facto* advisor while I conceived of this project. To Richard Tsung, thanks for the amazing all-hours tech support. Thanks also go to Cary Steibel and Lyle Shurtleff from the U.S. Army BRAC office, for being amenable and providing invaluable GIS data. And last, but certainly not least, many sincere thanks to Devon Libby and the Digital Globe Foundation, for graciously providing an imagery grant for this project.

CONTENTS

LIST OF TABLES

LIST OF FIGURES

LIST OF ABBREVIATIONS

B&W	Black And White (Panchromatic)
BLM	Bureau of Land Management
BG	Bare Ground/Dirt Track
BRAC	Base Realignment and Closure
CERCLA	Comprehensive Environmental Response, Compensation and Liability Act
CIR	Colorized Infrared
CVP	Confirmed Vernal Pool
DT	Dead Transition
ETM/ETM+	Enhanced Thematic Mapper/Enhanced Thematic Mapper Plus
FB	Fire Break/Burn
FD	Fractal Dimension
FNEA	Fractal Net Evolution Approach
GIS	Geographic Information Systems
HD	High Definition
HSR	High Spatial Resolution
IV	Invasive
KML	Keyhole Markup Language
LL	Lowland
LT	Live Transition
MO	Model Object
MRS-BLM	Munitions Response Site-Bureau of Land Management
MSR	Medium Spatial Resolution

NDVI	Normalized Difference Vegetation Index
NIR	Near Infrared
NN	Nearest Neighbor
OBIA	Object-Based Image Analysis
OT	Oak Tree
P or PERI	Perimeter
PAR	Perimeter to Area Ratio
PI	Persistence Index
PR	Paved Road
PVP	Potential Vernal Pool
SI	Shape Index
SPOT-5	*Satellite Pour l'Observation de la Terre 5*
TTA Mask	Test and Training Area Mask
UL	Upland
USGS	United States Geological Survey
VHSR	Very High Spatial Resolution
WIPI	Weighted Intervals Persistence Index
WV2	WorldView 2

ABSTRACT

Vernal pools are rare, seasonal pools that form in landscape depressions and create temporary habitat for many floral and faunal taxa. In California, as much as 90% of historic vernal pool area has been displaced by agriculture and urbanization. Pools are commonly inhabited by endemic, threatened, and endangered plants and animals, and are critical breeding areas for California tiger salamanders (*Ambystoma californiense*) and fairy shrimp (*Linderiella occidentalis*). Seasonal inundation and desiccation are driving factors behind the biotic community structure around pools, both spatially and compositionally.

At Fort Ord, California, a rare subset of vernal pools occur perched atop relict sand dunes in an arid chaparral environment. Fifteen vernal pools have been previously identified within the base's historic firing range impact area. At least 45 other lowland meadows within the impact area meet pool topographic requirements and were evaluated for their potential to be vernal habitats. This thesis proposes an object-based method of extracting vegetative patterns from VHSR Ikonos and WorldView 2 satellite imagery, to compare persistence in vegetative patterns over time. Classification results from three aerials collected over an 80-year interval were subjected to a geospatial change analysis, and used to make short- and long-term comparisons of known vernal meadows to themselves and other meadows in the study area. Two new metrics, the Persistence Index and Weighted Intervals Persistence Index, were created for this study. These indices normalize changes in geometric properties, enabling comparisons between known vernal areas and study sites, and between self-same sites sampled at different times. PI and WIPI results were consistent with the results from other analyzed metrics.

Strong persistence in several study sites, comparable to that of the known vernal areas, likely indicates latent presence of a seasonal hydric regime and an elevation-based hydrological gradient. The results of this study show that there is no statistically significant difference between the way that vernal and other meadows change shape and size over time. This result means that a number of lowland meadows in the impact area may have active or dormant vernal pools because the two groups cannot be empirically differentiated from one another. This study also positively confirmed the presence of at least five previously unrecognized vernal areas through the detection of water in multiple aerial images. These findings merit further on-the-ground investigation, as well as a geographical reconsideration of current conservation efforts.

CHAPTER 1: INTRODUCTION

Vernal pools are ephemeral wetlands that are geographically isolated from other water bodies and inundated only on a seasonal basis. They provide habitat for a rich variety of endemic, threatened, and endangered taxa of flora and fauna (Bauder 2005; Burne 2001; Carpenter, Stone, and Griffin 2011; Keeler-Wolf et al. 1998; Lathrop et al. 2005; Reed and Amundson 2007; Stone 1992; Van Meter, Bailey, and Grant 2008; Van Thomme 2011; Zedler 1987). Though variations of vernal pools occur worldwide, in most cases these environments have been drastically reduced in number (Bauder 2005; Burne 2001; Carpenter, Stone, and Griffin 2011; Gibbes et al. 2010; Keeler-Wolf et al. 1998; Kneitel 2014; Mattoni and Longcore 1997).

The primary threats to all temporary wetlands are urban and agricultural development (Bauder 2005; Cormier 2001; Cutler 2006; Keeler-Wolf et al. 1998). In California alone, as much as 90% of vernal habitat has been lost to development and farmland (Ferren et al. 1996; Keeler-Wolf et al. 1998; Tannourji 2009). Of these remaining few, a rare subset exist in isolated depressions amongst thickets of cismontane central maritime chaparral, a narrowly distributed plant community with drought- and fire-resistant characteristics. An even more uncommon subset of chaparral vernal pools, many of which may now be dormant or extinct, can be found within the relict sand dunes of Monterey Bay's Fort Ord. Because they are unusually unique and occur inside an area of heavily restricted access, it is critical that these rare but diverse habitats be identified for study and conservation.

Fort Ord's vernal pools occur in both oak savanna and chaparral landscapes. Vernal pools in the base's northern zones typically develop in large, flat plains. These plains alternate

between grasslands and oak groves, and are densely dotted with large gopher mounds (mimas) (Cox 1986; Reed and Amundson 2007). By contrast, vernal pools at the southern end of the base are found isolated in grassy lowland depressions amongst dense stands of manzanita (*Arctostaphylos* spp.) chaparral. In such circumstances, competition for space is intense and in many locations there is a sharp break between upland chaparral and grassy lowland meadow habitats. Vernal pools in particular develop strong, lasting vegetative patterns in and around their margins because of the intermittent flooding to which their plant communities are subjected. Likewise, non-vernal meadows in the area appear to resist the encroachment of chaparral recruits as well, but the explanation as to why is less-readily apparent.

Patterning characteristic of vernal vegetation is also evident in some non-vernal lowland meadows and raises the possibility that these meadows may have some latent potential to act as vernal pools. It is possible that these areas are, or once were, ephemeral wetlands that have not been previously recognized. The simplest explanation for the similarity in patterning is that the same underlying process is happening in both types of location. That is, soil moisture gradients are dictating the local floral distributions. This project primarily asked whether persistent vegetation patterns could be measured and correlated to an inundation regime. Specifically, have the shapes and sizes of vernal meadows changed over time in a way that is significantly different than that of non-vernal meadows? How then would it be possible to quantify and compare such changes? Moreover, are there remaining vernal meadows that have gone unnoticed or been missed in previous site surveys that are discoverable using the methods demonstrated here?

One objective of this study was to create a single index number, henceforth referred to as the Persistence Index (PI), to encapsulate the gross degree of size and shape change an ecological patch undergoes over time. To make this evaluation, which required very high resolution aerial

photography and fine-scale classification, a method of object-based image analysis was employed. The resulting classification outputs were analyzed at the patch level for a variety of shape and size metrics. Changes in metric values were computed over short-term (10-year) and long-term (70-year) difference intervals. The degrees of change in several key metrics were then combined and normalized in a novel equation to create the Pl value for each study site. A comparison of PI distributions for known vernal and non-vernal meadows was used to determine if any differences between the two populations existed. If water is the factor controlling the vegetation patterns in lowland meadows, as hypothesized, the relative magnitudes and variances in PI values were expected to be significantly smaller for those areas that pool vernally, as compared to those that do not.

1.1 Aerial Wetland Surveillance

Wetlands are frequently surveyed using flyovers and aerial image data. Panchromatic (B&W), colorized infrared (CIR), and true-color aerial imagery have all been employed to this end (Burne 2001; Carpenter, Stone, and Griffin 2011; Cutler 2006; Stone 1992; Tiner 2003). Manual image interpretation via a stereoscope is a well-established but laborious method (Burne 2001; Drägut and Blaschke 2006; Fallon 2013; Lathrop et al. 2005; Stone 1992). More recently, supervised and unsupervised algorithms for automatic image classification have been developed, and in the past several decades used routinely for wetlands surveying (Cutler 2006; Cormier 2001; Dissanska, Bernier, and Payette 2009; Fallon 2013; Frohn et al. 2009, 2012; Gibbes et al. 2010; Lichvar et al. 2006). Most of these perform pixel-based classifications on images that offer no better than 15-30 m resolution (e.g. Landsat TM and ETM+ datasets). Because some vernal pools may be smaller than three meters across (Zedler 1987), an alternative approach amenable to use with higher resolution datasets, such as OBIA, is necessary.

Medium (15–5 m), high (5–1 m), and very high spatial resolution (<1 m) (MSR, HSR, VHSR, respectively) satellite imagery in many spectral channels is now routinely available through missions like Quickbird, Ikonos, WorldView-2, and SPOT-5. These higher resolution images present highly-complex spectral components that confound typical pixel-based classification processes (Blaschke 2010; Burnett and Blaschke 2003; Corcoran, Winstanley, and Mooney 2010; Mallinis, Pleniou, and Koutsias 2010; Thompson and Gergel 2008; Yu and Zhang 2008). By comparison, object-based classification has been demonstrated to be highly accurate, but is still an area of ongoing research and development (Corcoran, Winstanley, and Mooney 2010; Drägut and Blaschke 2006). OBIA utilizes texture, color, and spatial orientation to first segment (outline), then classify objects in an image (Blaschke 2010; Burnett and Blaschke 2003; Corcoran, Winstanley, and Mooney 2010; Drägut and Blaschke 2006; Hsu, Chua, and Pung 2000; Johansen et al 2007; Mallinis, Pleniou. and Koutsias 2010; Yu and Zhang 2008). OBIA has been used to classify wetland areas, as well as to map vegetation patterns in landscapes (Blaschke 2010; Cutler 2006; Dissanska, Bernier, and Payette 2009; Fallon 2013; Frohn et al. 2009, 2012; Gibbes et al. 2010; Johansen et al. 2007; Lichvar 2006; Mayer et al. 1997). This thesis demonstrates a technique for integrating OBIA results with the analytical power of a Geographic Information System (GIS) to extract vegetation patterns around potential and confirmed vernal lowland meadows, and measure changes in those patterns over time. Historic and contemporary aerial and satellite imagery were used to measure spatial persistence and compare vernal lowlands with other lowland meadows.

1.2 Wetlands and Vernal Pools at Fort Ord

Fort Ord (Figure 1) occupies a plateau of relict Pleistocene and Holocene sand dunes on the southeastern crescent of California's Monterey Bay (Smith et al. 2002). The former U.S. Army

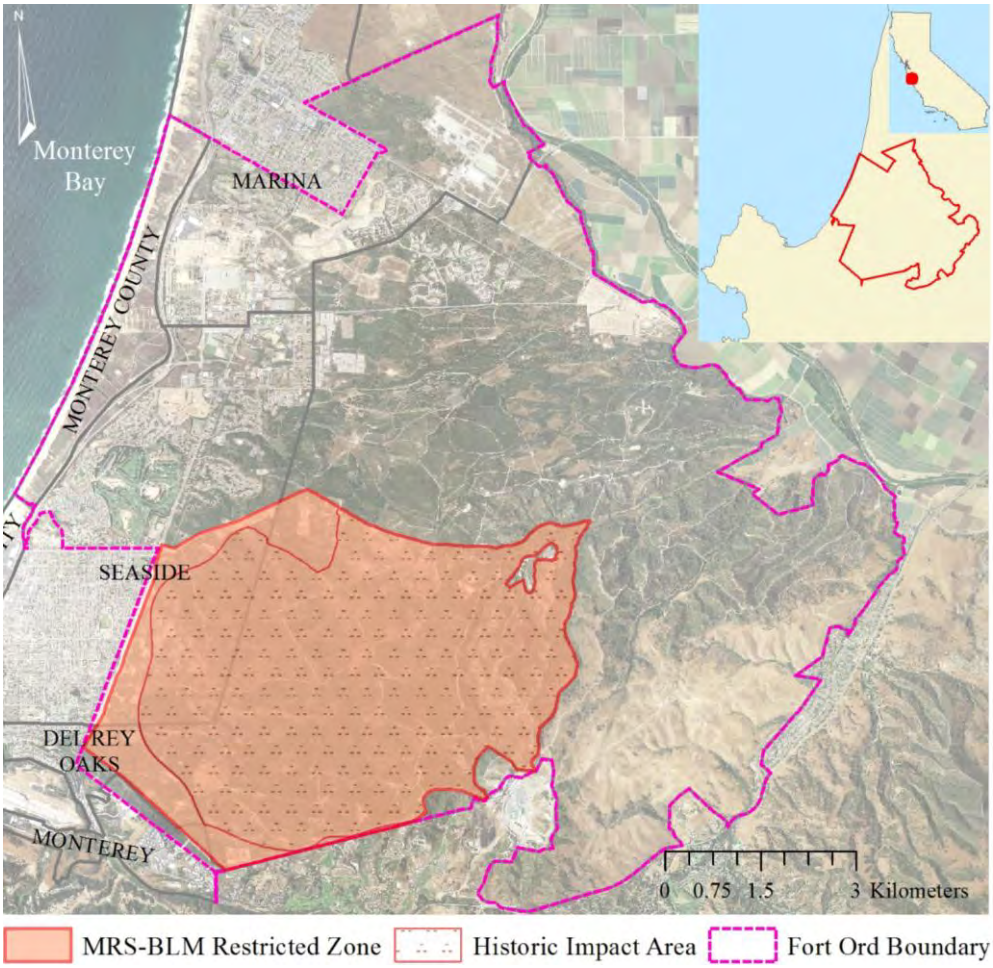

Figure 1: Fort Ord MRS-BLM Restricted Site

base is a 28,000 acre (~45 square mile) CERCLA Superfund site with legacy pollution left over from nearly 100 years of intense military activity (EMC Planning Group 2012; EMC Planning Group and EDAW, Inc. 2001a; LFR, Weston Solutions, and Westcliffe Engineering, Inc. 2008). While under Army control, over 8,000 ha (approximately 20,000 acres) of undeveloped wilderness were restricted and used for historic firing ranges and training areas. Much of that wilderness is in the impact area (Figure 1), and remains entirely off limits because it is still polluted with dangerous munitions and unexploded ordnance. Ironically, the restricted area is also habitat for several important ecosystems with significantly reduced ranges, including central

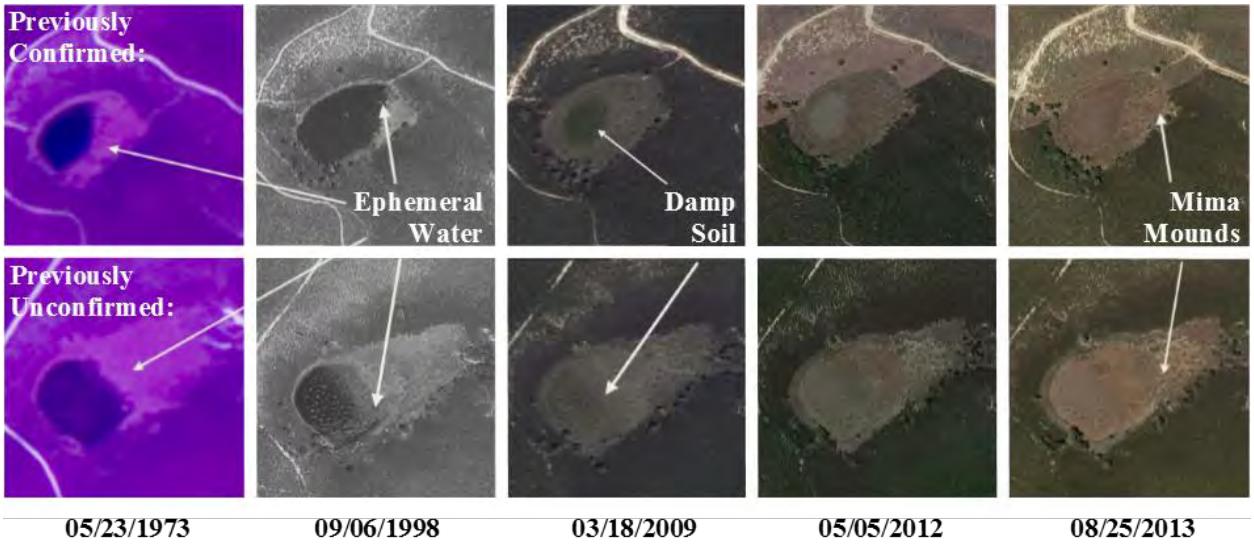

Figure 2: Previously Confirmed (ID # 80C02) Versus Previously Unconfirmed (ID # 80P03) Vernal Pool Meadows (Source Imagery: USGS EarthExplorer, Google Earth, 8/25/2014)

maritime chaparral and collocated vernal pools (Burleson Consulting, Inc. 2006; Keeler-Wolf et al. 1998). An unintentional consequence of the Army's 75 year occupation of the land is that many of the Fort Ord vernal pools have been protected from development (Bauder 2006; Keeler-Wolf et al. 1998; Van Meter, Bailey, and Grant 2008), as can often happen with natural landscapes near to noxious land uses (Longcore and Rich 2008). Yet, the Army's treatment of the land may have also led to a shift from natural wetlands and vernal pools to stock ponds and artificial pools formed in artillery craters (Keeler-Wolf et al. 1998; Smith et al. 2002).

As visible from medium- and high-resolution imagery, there remain many depressions in the restricted area's landscape that are marked only as meadows or grasslands, but which bear a strong visual resemblance to already-mapped vernal areas. Some of these grasslands (bottom row, Figure 2) were confirmed as vernal pools during this analysis, through multiple water sightings and extreme visual similarities. Other non-pooling meadows with similar appearances, if they exist in lowland depressions, may themselves be dormant vernal areas. As such, they should be examined thoroughly to assess their hydrologic potential.

Vernal pools, as well as much of their constituent biota, are protected by both federal and state statutes, and they are recognized as highly valuable habitat areas for freshwater crustaceans and amphibians (Keeler-Wolf et al. 1998; Kneitel 2014; TetraTech and Ecosystems West Consulting Group 2014; USFWS 2005; Zedler 1987, 2003). At present, military installations with *de facto* wilderness refuges, like that at Fort Ord, offer the best opportunity to reclaim and restore vernal areas (Cooper and Perlman 1997; Keeler-Wolf et al. 1998; USFWS 2005). Because vernal pools at Fort Ord are protected sites, knowing the locations of them is vital to any conservation efforts. They are critical habitat and breeding areas for endangered, threatened, and special status species like the California tiger salamander (*Ambystoma californiense*), fairy shrimp (*Linderiella occidentalis*), and Contra Costa goldfields wildflowers (*Lasthenia conjugens*) (Burleson Consulting, Inc. 2006; Keeler-Wolf et al. 1998; Lathrop et al. 2005; LFR, Weston Solutions, and Westcliffe Engineering, Inc. 2008; Smith et al. 2002; USFWS 2005; Wang et al. 2011). Some other vernal pool species may be largely endemic to Fort Ord. Identifying new vernal pool habitat areas would thus be a critical boon to local and statewide conservation efforts.

The specific definition of a vernal pool varies regionally, since they occur in a variety of landscapes all over the globe (Bauder 2005; Burne 2001; Carpenter, Stone, and Griffin 2011; Lathrop et al. 2005; Keeler-Wolf et al. 1998; Mattoni and Longcore 1997; Reed and Amundson 2007; Stone 2002; Van Meter, Bailey, and Grant 2008; Van Thomme 2011; Zedler 1987). In general, vernal pools are ephemeral waterbodies that collect in a depression in the landscape during late winter and early spring rains. They persist for at least two months, providing critical habitat for local flora and fauna, and then slowly desiccate during the hot months of summer (Burne 2001; Cormier 2001; Stone 1992). Importantly, because they are not permanent, they

cannot support fish populations that would otherwise predate upon the invertebrates and amphibians that breed in vernal waters (Burne 2001; Lathrop et al. 2005; Munoz et al. 2009; USFWS 2005; Zedler 2003). Pools can range in size from 1 m^2 to 36 ha, but are generally less than 1 m deep (Keeler-Wolf et al. 1998; USFWS 2005). They lack inlets and outlets, and either trap water with an impermeable horizon of clay or bedrock, or sit low enough to be below the surface level of a perched water table (Bauder 2005; Burne 2001; Lathrop et al. 2005, Stone 1992). Often, a characteristic array of wildflowers will colonize the margins of a pool, making them detectable even after surface waters are gone (Burne 2001; Burleson Consulting, Inc. 2006; USFWS 2005; Van Thomme 2001; Zedler 1987).

1.3 Scope

Fort Ord vernal pools are part of the Fort Ord Core Area (Figure 3), a subzone of the larger Central Coast vernal pool region (USFWS 2005). In the Fort Ord Core Area, vernal pools occur in three basic environments: (1) in steep valleys supporting oak woodlands and annual grasslands to the southeast; (2) in oak woodland savannas in the north; and (3) amongst the xeric (arid) sandy soils and central maritime chaparral of the southwest relict sand dunes (Smith et al. 2002). It is the last variety of pools that concern this study, as they reside in an uncommon vernal environment that has been altered by human actions. For this research, vegetative alliances described in the literature assisted in the identification of potential pool locations (Burleson Consulting, Inc. 2006; Jones & Stokes Associates 1992; Keeler-Wolf et al. 1998; USFWS 2005; Zedler 1987). The identification framework created here for characterizing dry or dormant pools in coastal chaparral will be useful in informing future attempts to use remote sensing similarly in other locations.

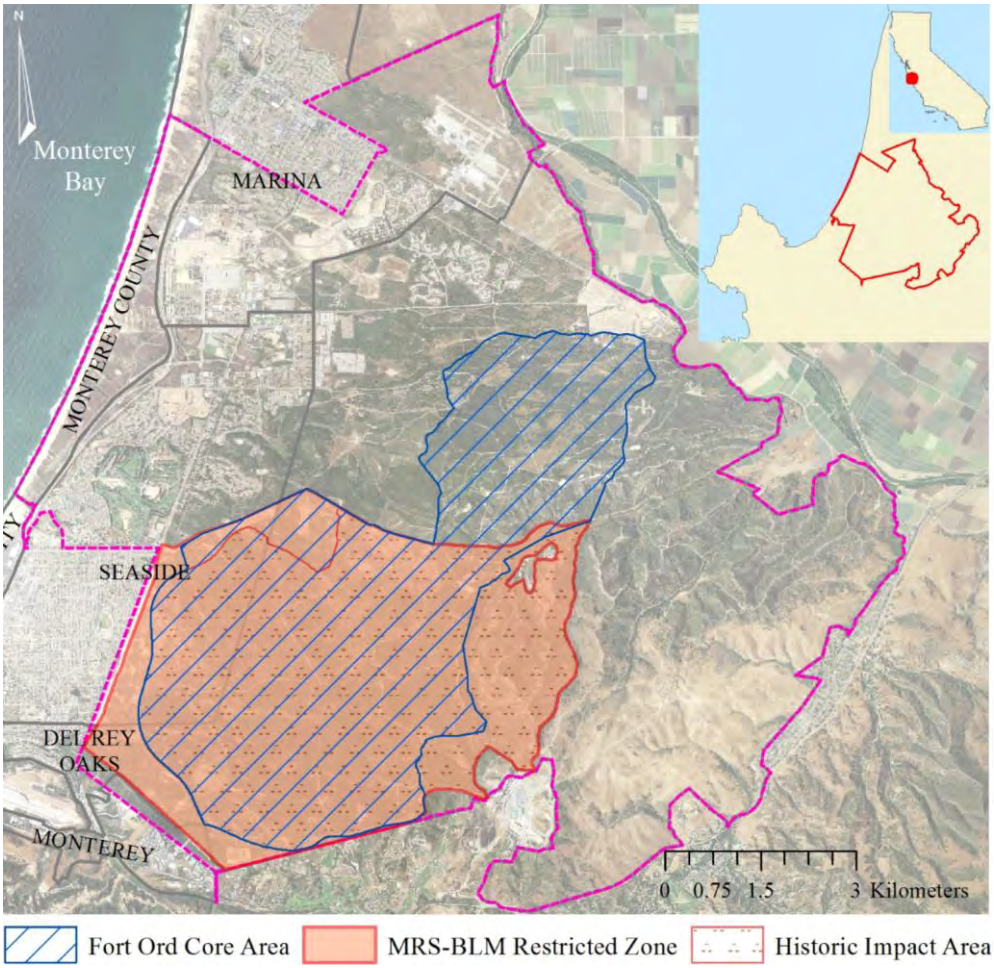

Figure 3: The Fort Ord Core Area (USFWS 2005)

A literature review uncovered no attempts to quantify Fort Ord's extinct or dormant vernal pool systems with aerial or remote sensing data. Although aerial imagery has been used elsewhere for vernal pool detection several times in the past, these studies have focused primarily on the identification of temporary waterbodies (Burne 2001; Carpenter, Stone, and Griffin 2011; Lathrop et al. 2005; Stone 2002; Van Meter, Bailey, and Grant 2008). Because Fort Ord has Mediterranean weather patterns (mild, moist winters and prolonged dry summers), however, its vernal pools exhibit variable hydrological cycles. In some years they may not fill with surface water at all, which makes water an unreliable indicator. Many organisms that use

vernal habitats in California are drought and fire adapted, and it is possible for pools to be dormant for decades before re-establishing themselves when appropriate conditions return (USFWS 2005; Van Dyke and Holl 2003; Van Dyke, Holl, and Griffin 2001).

This ability for vernal pools to lie dormant is particularly relevant at Fort Ord, where military activities have altered the landscape. Many of the natural vernal pools may have been degraded while, at the same time, artificial ones were being inadvertently created. Historical images therefore provide a baseline for calculating changes in confirmed and potential vernal pool sites, and OBIA offers an alternative method for examining the lasting effects of water and disturbance on plant communities in and around vernal pools.

Several ground studies have mapped portions of the base's extant vernal pools, but they do not agree entirely on the locations of vernal pool meadows (Burleson Consulting, Inc. 2006; Jones & Stokes Associates 1992; LFR, Weston Solutions, and Westcliffe Engineering, Inc. 2008; Tannourji 2009). Aerial imagery provides a different perspective not afforded to samplers working *in situ*. Landscape features such as the boundary between terrestrial and edge flora, depressions and swales, seasonal wildflowers, and mima mounds are strong indicators of the presence of latent hydric soil (Bauder 2000; Cormier 2001; Cutler 2006; Keeler-Wolf et al. 1998; Reed and Amundson 2007; TetraTech and Ecosystems West Consulting Group 2014; USFWS 2005, Wang et al. 2011; Zedler 1987, 2003), but may not always be discerned from the ground. While each of these indicators can be extracted using OBIA; this thesis primarily focused on mapping locations and characteristics of the boundaries of terrestrial-edge species (Burleson Consulting, Inc. 2006; Burne 2001; Keeler-Wolf et al. 1998; Montrone 2013; Reed and Amundson 2007; Zedler 1987). This boundary zone is typically represented by a band of constituent plants that undergo the most environmental stress of any in the localized vernal pool

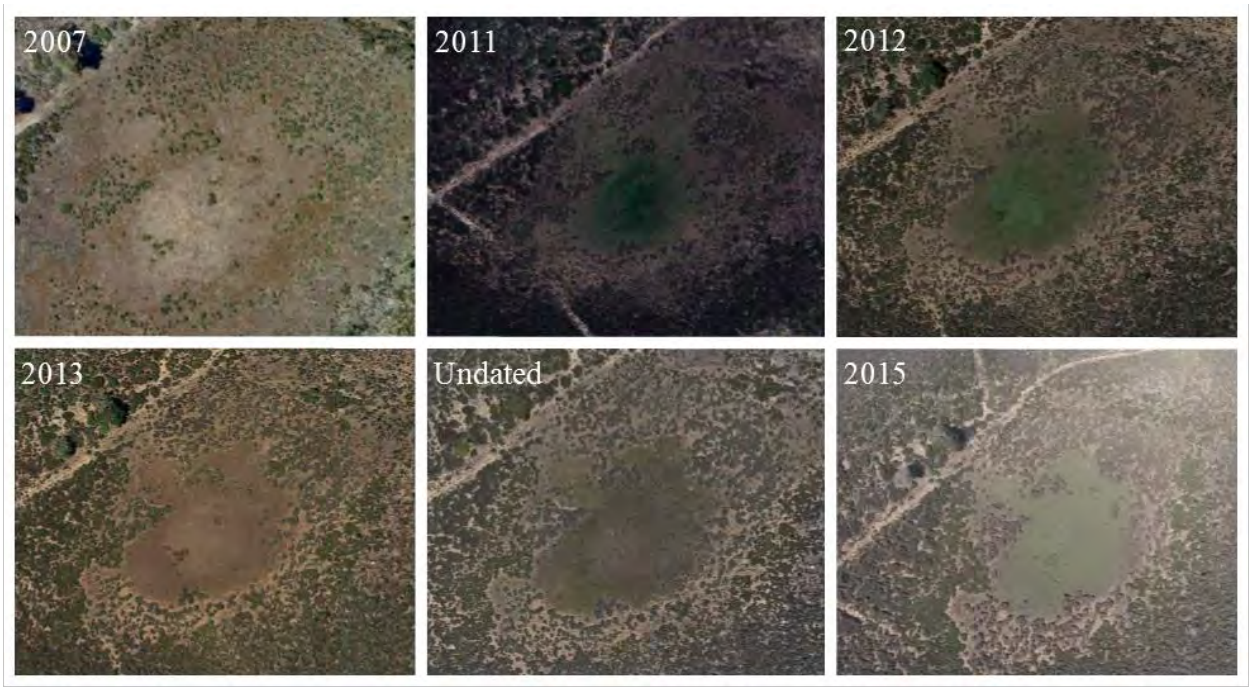

Figure 4: PVP Site 70P14 Vegetative Persistence and Hydrology Indicators (Photo Credits: Top Center, WorldView 2 2011; Bottom Right, C. Hanley 2015; All others, Google Earth)

community (Bauder 2000; Montrone 2013; Tannourji 2009; Zedler 1987). The boundary zone is an extreme environment that is highly vulnerable to alterations in hydrologic regime, making it an excellent indicator of change-over-time.

The underlying premise for this study was that vernal pools create a lasting imprint on the local environment. This imprint is difficult to erase, even through burning, bulldozing, or bombing. For example, a lowland meadow persists over an eight year time-series of photos, in spite of surrounding disturbance and encroaching chaparral (Figure 4). The center and right-hand panes show verdant springtime conditions that, upon close inspection, demonstrate vernal indicators like damp soil and wildflowers. The site shown (ID# 70P14) is not a confirmed vernal pool; whether or not it has vernal hydrology is unknown. It is, however, representative of other PVP in appearance and floral composition. It may be a relict or dormant pool site that is still imprinted on the land because of an ongoing subterranean hydrologic regime.

When a vernal pool disappears permanently due to a change in hydrology, it is possible for its physical signature to persist in the landscape for years or decades. This project advanced the hypothesis that vegetation patterns that persist in spite of repeated disturbances can be combined with topographical data to determine the historic extent of vernal pool systems at Fort Ord. The methodology adapted previously developed object-based image extraction techniques to identify and analyze potential vernal pool sites. The process whereby relict vernal pool areas were detected through OBIA is extensible to future studies of a similar nature. Discovering new sites in this manner can provide an avenue for better understanding California's coastal vernal pool ecosystems. Using the evidence produced by this study, researchers will be able focus survey effort on sites with the highest probability of having a vernal pool hydrology to collect soil and plant samples, which can then be used to verify the predictions. Finally, this thesis has produced the first comprehensive database of Fort Ord impact area vernal pool locations, which will be immediately useful in instructing continued conservation and future restoration efforts.

CHAPTER 2: BACKGROUND AND LITERATURE REVIEW

Wetlands are important national resources with high ecological, economic, and social value (Gibbes et al. 2010; Haas, Bartholomé, and Combal 2009). Remote sensing data has a long history of use in the inventory and delineation of wetland resources, at both continental and regional scales. Virtually every type of remote sensing data has been employed to study wetland areas. Because wetlands are often in remote, inaccessible places covering vast stretches, the acquisition of ground evidence might be impractical, or even impossible in many instances (Cormier 2001; Haas, Bartholomé, and Combal 2009; Munoz et al. 2009; Stone 1992). Remote sensing provides a solution to this problem and has proven to be a valuable tool for studying and mapping wetlands worldwide.

In resolutions ranging from low to very high, aerial and satellite imagery provide wide coverage, time-series data, and the ability to study remote sites *ex situ*. In particular, the availability of historic aerial imagery and satellite data collected at regular return intervals makes possible change assessments, and the detection of geographically isolated temporary waterbodies (e.g. vernal pools). It is common practice in this field to use the presence of water in an image as a wetland indicator (Burne 2001; Carpenter, Stone, and Griffin 2011; Dissanska, Bernier, and Payette 2009; Frohn et al. 2009; Yu and Zhang 2008). However, because temporary isolated waterbodies are ephemeral, they may not be flooded at the time of imaging (Andrew and Ustin 2008; Bauder 2000, 2005*)*. Fort Ord is a case in point, as the majority of photos reviewed for this project were taken while the landscape did not contain water features. Hence, other indicators were needed to remotely detect vernal pools.

Figure 5: Flyover Aerial of a Large Fort Ord Vernal Pool, 21 February, 2015 (Photo Credits: C. Hanley)

2.1 Vernal Pools

Vernal pools, like those found in woodlands (Figure 5), are a rare type of isolated ephemeral wetland. They are characterized physically as topographical depressions that flood seasonally and lack inlets or outlets (Bauder 2005; Burne 2001; Carpenter, Stone, and Griffin 2011; Cormier 2001; Kneitel 2014; Stone 1992). Inundation typically lasts two to six months and is followed by a lengthy desiccation period (Burne 2001; Cormier 2001; Stone 1992). Most pools trap water because they are either located on a shallow or exposed sill of bedrock, or underlain with a shallow clay aquitard (Carpenter, Stone, and Griffin 2011; Cormier 2001; Keeler-Wolf et al. 1998; Mayer et al. 1997; Montrone 2013; Smith et al. 2002; USFWS 2005, Zedler 1987, 2003). In some cases, pool bottoms may extend below the surface elevation of a locally perched water table (Ferren et al. 1996; Keeler-Wolf et al. 1998; Smith et al. 2002; Zedler 1987, 2003).

Biologically, vernal pools are richly diverse temporary habitats, and many pool taxa are specially adapted to their use (Bagella, Caria, and Zuccarello 2010; Burleson Consulting, Inc. 2006; Burne 2001; EMC Planning Group and EDAW, Inc.2001b; Tannourji 2009; USFWS 2005; Van Thomme 2001; Zedler 1987). California's vernal pools are known to be habitat for an assortment of endangered or threatened species of endemic flora and fauna. Such organisms have evolved to rely heavily upon specific ephemeral sites (Cormier 2001; Cutler 2006; Frohn et al. 2012; Gordon et al. 2012; Keeler-Wolf et al. 1998; Kneitel 2014; Lane, D'Amico, and Autrey 2012; Tannourji 2009; USFWS 2005). For instance, amphibians and freshwater crustaceans use vernal pools for breeding because their ephemeral nature precludes the presence of fish that would prey upon them and otherwise compete for resources (Burne 2001; Cormier 2001; Lathrop et al. 2005; Munoz et al. 2009; USFWS 2005; Zedler 2003). In addition, mammals use vernal pools as watering holes (Zedler 1987), migratory birds for temporary stopovers and breeding (Van Thomme 2001), and some plants are entirely restricted to the harsh environments of pool basins or edges (Rhazi et al. 2006; Tannourji 2009; Zedler 1987).

The inundation regime drives the structure of pool vegetation such that it often results in three distinct, concentric vegetative bands (i.e. aquatic, edge, and terrestrial plant taxa), although in some cases the banding may be non-concentric or fragmented (Bagella, Caria, and Zuccarello 2010; Keeler-Wolf et al. 1998; Montrone 2013; Schlising and Sanders 1982; Tannourji 2009; USFWS 2005). Because pool soils have a cyclical hydrological regime, their moisture content varies greatly throughout the year. Soil moisture also varies along an elevation gradient. The lowest local elevations flood first and for the longest, while higher elevations receive shorter-duration flooding that begins later in the year and ends earlier (Bagella, Caria, and Zuccarello 2010; Bauder 2000, 2005; Cormier 2001; Fernández-Aláez, Fernández- Aláez, and Bécares

1999; Rhazi et al. 2006). Both the timing and the duration of the inundation affect the development of pool vegetation, especially the location, size, and continuity of bands (Bagella, Caria, and Zuccarello 2010; Keeler-Wolf et al. 1998; Kneitel 2014; Rhazi et al. 2006; Zedler 1987).

2.2 Vernal Pools at Fort Ord

It could be argued that certain of Fort Ord's vernal pools are amongst the rarest of all varieties, and not just because they are part of the remaining 10% of California's historic cohort. These pools exist perched on a plateau of relict sand dunes that is uncommon in itself (Mattoni and Longcore 1997, Smith et al. 2002) and exhibits moderately to well-drained soil with little or no natural surface runoff (Smith et al. 2002). The local climate type is Mediterranean, which has a very limited worldwide distribution. Similarly, the dominant upland vegetation type, coastal central maritime chaparral (visible in the foreground of Figure 6), is a threatened ecosystem endemic to only a few small areas of California (Van Dyke and Holl 2003; Van Dyke, Holl, and Griffin 2001). In this environment, eggs and seeds of pool taxa can lay dormant within the soil's seedbank, awaiting the return of water before reviving (Gordon et al. 2012; USFWS 2005; Van Dyke and Holl 2003; Van Dyke, Holl, and Griffin 2001; Van Thomme 2001, Zedler 1987). This dormancy can last years or decades, and is critical in ensuring survival of pool species since hydric regimes may vary greatly from year to year and pool to pool (Gordon et al. 2012; USFWS 2005). In some years, as has been observed by the author, pools do not fill at all (Andrew and Ustin 2008; Bauder 2000). Vernal pools in California have also been demonstrated to have high within pool and pool to pool variation in terms of community structure (Bagella, Caria, and Zuccarello 2010; Barbour et al. 2003; Gordon et al. 2012; Rhazi et al. 2006; Tannourji 2009).

Figure 6: Mixed Chaparral and Oak Landscape inside the Restricted Area (Photo Credits: C. Hanley)

Central maritime chaparral is drought-resistant, woody vegetation dominated by manzanita (*Arctostaphylos* spp.) and coyote brush (*Baccharis pilularis*) (Smith et al. 2002; TetraTech and Ecosystems West Consulting Group 2014; Van Dyke and Holl 2003; Van Dyke, Holl, and Griffin 2001). At Fort Ord, the chaparral is also interspersed with Coast Live Oak (*Quercus agrifolia*), Monterey Pine (*Pinus radiata*), coastal sage scrub, and small lowland meadows (TetraTech and Ecosystems West Consulting Group 2014*)*. Although this region of California is both drought- and fire-prone and local plant taxa are well-adapted for it, current drought conditions are severe and the burn regime has been unnatural for 100 years or more (EMC Planning Group and EDAW, Inc.2001a; LFR, Weston Solutions, and Westcliffe

Engineering, Inc. 2008; Smith et al. 2002). A shift towards either climax terrestrial communities (e.g. mature chaparral or oak woodland) or disturbance species (e.g. invasive annuals grasses) should be measurable in the landscape at Fort Ord, in light of the current circumstances. If the size and shape of meadow areas exhibit measurable consistency over time, then water is likely playing a role. Regularly flooded soils can only support certain plant species, at the exclusion of all others (Bauder 2000, 2005; Tannourji 2009; Zedler 1987, 2003). Included on the exclusion list are terrestrial floral species such as chaparral plants, coast live oaks, and invasive annual grasses. In the absence of water and in the face of disturbance, vernal pool species should be locally extirpated in favor of the aforementioned terrestrial species.

Several ground studies of Fort Ord vernal pools have been conducted, most pursuant to the Fort Ord Reuse Plan (Burleson Consulting, Inc. 2006; Jones & Stokes Associates 1992; LFR, Weston Solutions, and Westcliffe Engineering, Inc. 2008; Tannourji 2009). These studies have variously characterized local flora and fauna, mapped the extents of known pools, and surveyed for characteristic species such as California tiger salamanders and fairy shrimp. No two studies are in agreement about the quantity or locations of vernal pool sites, however, and no remote sensing work has been conducted in this regard. Moreover, although some studies have discussed factors that have degraded vernal habitat at Fort Ord, there are few specific site locations described in the literature. The quantity and locations of degraded and lost vernal pools at Fort Ord are unknown. Sources of degradation include water diversions to holding ponds, erosion due to road and trail cuts, cratering from large explosions, soil contamination from remaining ordnance, and changes in climate (Keeler-Wolf et al. 1998; Smith et al. 2002). The study area, as described in the methods section, has 15 previously confirmed vernal pool sites and approximately 51 other lowland meadows that were viewed as having the potential to be

dormant or relict vernal pools. Henceforth, this document will refer to all previously known vernal pools as confirmed vernal pools (CVP). All other lowland meadows in the study area will interchangeably be referred to as either study sites or potential vernal pools (PVP) (*sensu* Burne 2001).

2.3 Remote Sensing of Wetlands and Vernal Pools

To classify vernal pools visually, images are usually selected based on optimal flyover time (generally spring, leaf-off imagery taken in wet years) (Burne 2001; Carpenter, Stone, and Griffin 2011; Cormier 2001; Lathrop et al. 2005; Stone 1992; Van Meter, Bailey, and Grant 2008). Time-series studies have either examined multiple images from the same year to verify sites by measuring inundation time, or assessed change between different years (Burne 2001; Frohn et al. 2012; Stone 1992). B&W and CIR images are preferred over true color photos because water has a much more distinct spectral signature in B&W and CIR (Burne 2001; Cormier 2001; Frohn et al. 2009; Lane, D'Amico, and Autrey 2012; Lathrop et al. 2005; Stone 1992; Van Dyke and Holl 2003; Van Meter, Bailey, and Grant 2008). Supplementary topographic and soil data from a GIS are routinely utilized to verify that PVP meet the basic physical requirements of a vernal pool (Burne 2001; Carpenter, Stone, and Griffin 2011; Cormier 2011; Haas, Bartholomé, and Combal 2009; Lichvar 2006; Munoz et al. 2009; Stone 1992; Van Meter, Bailey, and Grant 2008; Yu and Zhang 2008). The typical scale range employed in this type of manual classification varies form 1:30,000 to 1:4,800 (Burne 2001; Carpenter, Stone, and Griffin 2011; Cormier 2001, Stone 1992).

2.3.1 Surveying Wetlands Using Image Analysis

More recently, automatic classification using pixel- and object-based extraction algorithms have been shown to produce similarly accurate results with less subjectivity (Burnett and Blaschke

2003; Corcoran, Winstanley, and Mooney 2010; Drăgut and Blaschke 2006; Hsu, Chua, and Pung 2000). Supervised and unsupervised pixel-based classifications are often used on low to medium resolution data (Blaschke 2010; Haas, Bartholomé, and Combal 2009; Thompson and Gergel 2008). They are most effective when areas to be classified are locally homogenous and single-scale (Burnett and Blaschke 2003; Drăgut and Blaschke 2006; Johansen et al. 2007). Pixel-based classification schemes are well-developed, and used in many applications beyond wetlands research. Their limitation for use in land cover analysis stems from the advent of HSR and VHSR data, which exhibits increased heterogeneity at finer scales (Blaschke 2010; Burnett and Blaschke 2003; Corcoran, Winstanley, and Mooney 2010; Mallinis, Pleniou, and Koutsias 2010; Thompson and Gergel 2008; Yu and Zhang 2008). Frohn et al. (2011) attempted to overcome this problem with sub-pixel classification of isolated wetlands and vernal pools, using Landsat ETM+ hyperspectral data (30–15 m spatial resolution). They demonstrated better than 87% producer's and 97% user's accuracies. Conversely, Fallon (2013) used EO-1 Hyperion 60 m resolution hyperspectral data to perform sub-pixel classification of spectral endmembers in channeled scablands, with only limited success.

High resolution imagery is more spectrally complex than low resolution because of the increased detail (Burnett and Blaschke 2003; Coburn and Roberts 2004; Corcoran, Winstanley, and Mooney 2010; Frohn et al. 2009; Johansen et al. 2007). Spectral information alone cannot sufficiently describe images in which small objects and textures are resolvable. Object-based classification algorithms combine spectral data with texture, spatial context, size, and shape to first segment an image into homogenous polygons, then merge the polygons into objects and classify them according to some set of knowledge-based semantics (Baatz and Schäpe 1999; Blaschke 2010; Dissanska, Bernier, and Payette 2009; Forestier et al. 2012, Halounova 2004;

Hsu, Chua, and Pung 2000; Johansen et al. 2007; Mallinis, Pleniou, and Koutsias 2010; Smeulders et al. 2000; Yu and Zhang 2008). The divide that separates spectral interpretation from semantic interpretation is called the semantic gap; it represents the difference between automatically and manually extracted information (Dissanska, Bernier, and Payette 2009; Forestier et al. 2012; Smeulders et al. 2000). Object-based classification can be used to make the semantic gap smaller (Forestier et al. 2012). OBIA processes are built to mimic the manner in which the human eyes and brain interpret visual information, and have been demonstrated to produce more accurate results than pixel-based spectral analyses (Baatz and Schäpe 1999; Blaschke 2010; Hsu, Chua, and Pung 2000).

Frohn et al. (2009) demonstrated a technique for accurately distinguishing isolated wetlands using OBIA on medium resolution Landsat-7 imagery. More typically, high resolution data from satellite missions like Quickbird, Ikonos, WorldView 2, and SPOT-5 are used for OBIA. In another approach, historical B&W aerial photographs were subjected to OBIA by Dissanska, Bernier, and Payette (2009) to analyze changes in peatlands and patterned fens. Cutler (1998) applied OBIA to distinguish homogenous landscape areas for potential inclusion in a sampling pool. Random OBIA polygons were then chosen for comparison between field data and high-resolution satellite imagery. OBIA has also been applied more broadly in environmental science to classify topographic landform types (Drăgut and Blaschke 2006), forest and riparian habitat (Johansen et al. 2007), heterogenous and fragmented temperate rainforests (Thompson and Gergel 2008), type and age class of forest stands (Coburn and Roberts 2004), and vegetation patterns in African savannas (Gibbes et al. 2010).

CHAPTER 3: METHODOLOGY

This chapter details the process by which this thesis was constructed and the research it describes executed. Descriptions of the selection of the study area and period are provided first in Section 3.1. Section 3.2 provides an overview of the study design and details previous scientific studies that were particularly influential to the research described here. The next three sections, in sequence, discuss the system used to explore, pre-process, and segment/classify the datasets. Finally, the change analysis approach that was used is documented in Section 3.6.

The methods described below draw heavily upon previous scientific studies of chaparral ecosystems, remote wetlands surveillance techniques, and image analysis algorithms. Nonetheless, the route from concept to execution required much trial-and-error, a trait common to object-based image analyses (Fallon 2013; Frohn et al. 2009; Yu and Zhang 2008; Zhang and Maxwell 2006). Many details of the development of the segmentation and classification process trees have been omitted here for brevity's sake, and because they are inconsequential to the outcome of this analysis. The landscape patterns are easily enough discerned that similarly accurate OBIA results could be achieved in multiple ways.

Real-world objects vary in size, shape, texture, spectral signature, and spatial context, so OBIA must account for these factors (Baatz and Schäpe 2000; Dissanska, Bernier, and Payette 2009). However, humans are able to classify visual objects immediately and discretely, without consciously considering such things. For example, we know an automobile when we see one; our brains automatically classify motorcycles, sedans, and trucks into this category even though they do not look similar. It is much more difficult for computer software to do the same equally

well. Thus, according to Baatz and Schäpe (2000), the human eye is the ultimate judge of image classification results. OBIA attempts to mimic the human ability to classify objects, in imagery and video (Blaschke 2010; Hsu, Chua, and Pung 2000). Whereas pixel-based analyses utilize non-spatial histograms that suffer from lost spatial information, object-based systems are better-suited to handle the inherent spatial complexity of VHSR imagery (Hsu, Chua, and Pung 2000).

3.1 Selection of Study Area and Time-Period

This project's study extent includes the majority of the historic impact area, along with the interim action ranges and the Seaside munitions response area. In total, the 2,578 ha (6,371 acres) area is bounded by Eucalyptus Road to the north, General Jim Moore Boulevard to the west, South Boundary Road to the south, and Impossible Canyon to the East. This location, also known as MRS-BLM, was chosen because its terrain and dominant vegetation are distinctive compared to the majority of the base's grounds. Vernal pools in the impact area exhibit more visually obvious vegetation patterns than those found elsewhere on Ft. Ord. The primary upland vegetation is central maritime chaparral occasionally interspersed with coastal sage scrub, coast live oak trees, and mixed conifer stands (Burleson Consulting, Inc. 2006; Smith et al. 2002; TetraTech and Ecosystems West Consulting Group 2014; Van Dyke and Holl 2003). Lowlands, by contrast, are typically grassy meadows (TetraTech and Ecosystems West Consulting Group 2014). The climate is Mediterranean and prone to severe drought (Bauder 2000, 2005; Smith et al. 2002; USFWS 2005; Van Dyke, Holl, and Griffin 2001). The two soil complexes comprising the study area are Baywood and Arnold, both of which are varieties of well-drained relict sand dunes approaching 100 m deep (EMC Planning Group and EDAW, Inc.2001b; TetraTech and Ecosystems West Consulting Group 2014; Smith et al. 2002). Of note, however, is the fact that

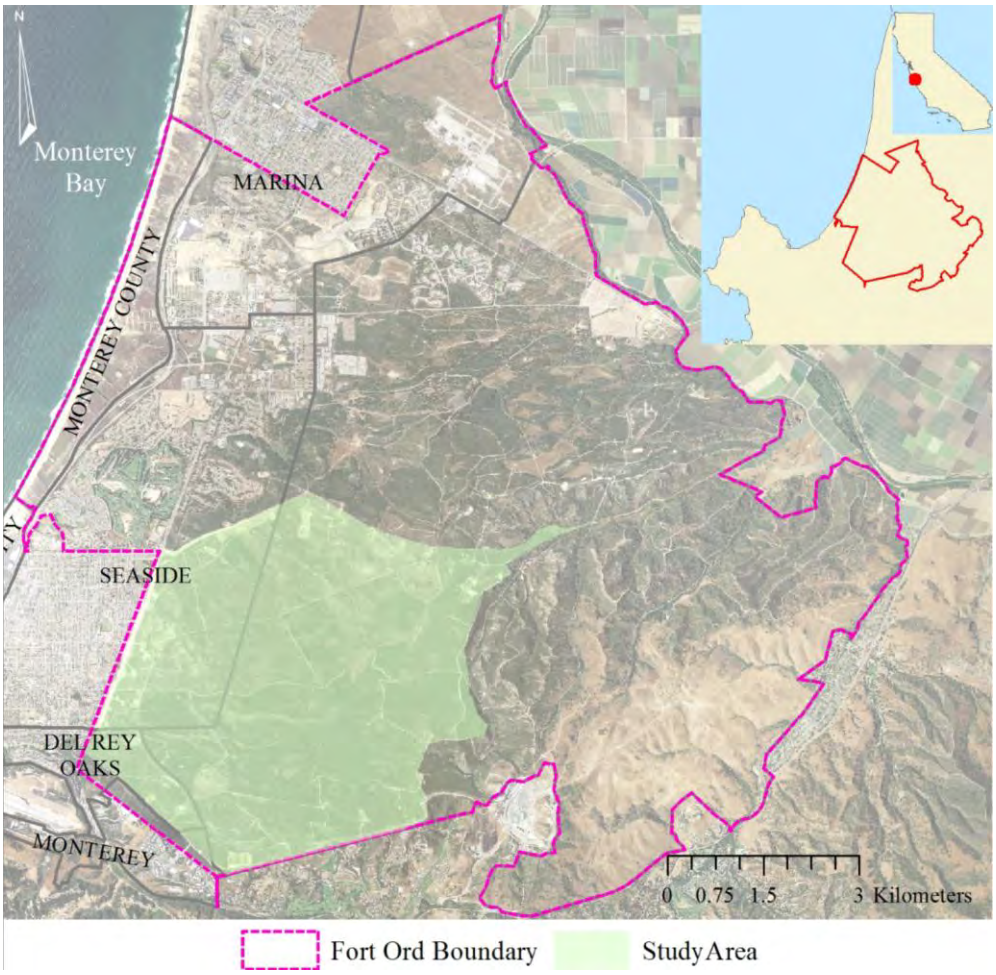

Figure 7: Study Area Extent

vernal soil samples taken within the study area by Burleson Consulting Inc. (2006) showed a predominant association with clay rich, low-permeability Antioch soils.

The study area (Figure 7) is about 2.4 km (1.50 mi) to 8.3 km (5.15 mi) from the coastline. The vertical range covers only around 215 m, from 60 to 275 m above mean sea level, but contains significant microtopographic relief. The area generally decreases in elevation from north to south and from east to west. However, the microtopography is such that hills and valleys appear to occur isotropically in localized areas, independently of elevation.

Image data were used for either exploratory or analytical purposes, depending on the type. Exploratory data were any historical aerial or satellite images that provided context or assisted in framing the study. There were three primary sources for exploratory images: the U.S. Army Base Realignment and Closure (BRAC) office at Fort Ord, the USGS EarthExplorer tool (earthexplorer.usgs.gov/, last accessed 25 September 2014), and Google Earth Pro (https://www.google.com/earth/, last accessed 31 March 2015). Data types included MSR B&W photos, low resolution CIR, and VHSR multispectral satellite imagery. Exploratory data were used to count and log historic inundation events, provide research context, support decision-making processes, and assess physical site characteristics. In most instances, exploratory images lacked complete metadata and did not include sensor information, spatial or spectral resolutions, or acquisition dates. In some cases they were not georeferenced. Yet they still provided a wealth of information and the opportunity for limited analysis. Unexpectedly, the images were utilized to confirm that certain PVP are in fact CVP (Figures 2 and 8).

3.1.1 Criteria for Selecting Analytical Datasets

Analytical data included two raw VHSR multispectral satellite datasets and one high resolution panchromatic aerial photograph. The project received a student research grant through the commercial vendor DigitalGlobe and the DigitalGlobe Foundation that provided the requisite data free of charge. The images were selected based upon the following six criteria:

1. Complete coverage of the study area;
2. Minimum of 10 years separation between datasets;
3. Maximum cloud cover of 1%;
4. Image acquisition date in late winter or early spring;

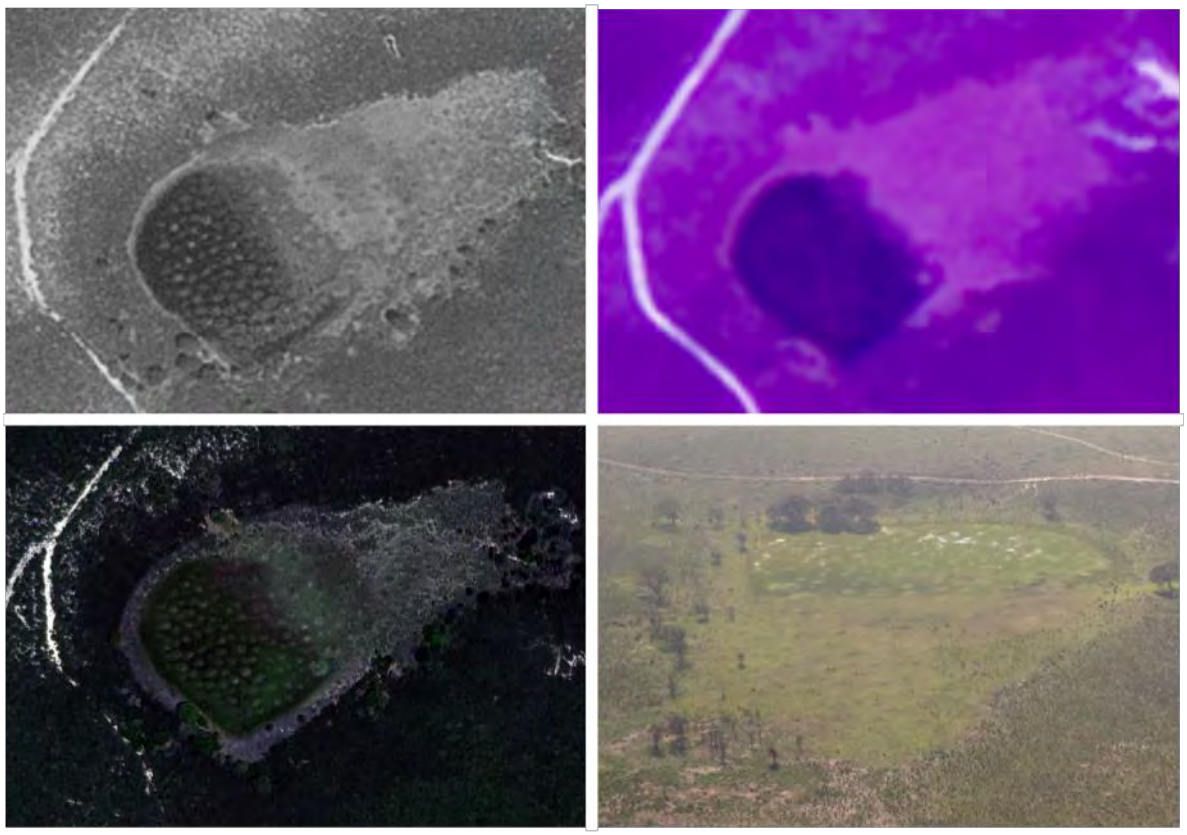

Figure 8: Exploratory Aerials Used to Confirm Site ID # 80P03 as Vernal (Photo credits, clockwise from top left: Google Earth, USGS EarthExplorer, C. Hanley, WorldView 2)

5. Panchromatic resolution finer than 1.0 m; and
6. Multispectral channels available.

Of the datasets from which to choose, one Ikonos (0.82 m panchromatic, 3.28 m blue, green, red, red edge, yellow, coastal, and near infrared) and one WorldView 2 (0.50 m panchromatic, 2.00 m blue, green, red, red edge, yellow, coastal, near infrared 1, and near infrared 2) dataset were selected. The Ikonos data was acquired 07 February, 2001, while that from WorldView 2 was obtained ten years later, on 15 April, 2011. Both presented 0% cloud cover and 100% aerial coverage of the study area. The analysis was restricted to the red, blue, green, and near infrared channels (NIR) for each multispectral dataset. The panchromatic aerial

mosaic was taken in 1941, and is of unknown but sufficiently high resolution to warrant inclusion as a baseline image for this study; it appears to have been resampled to a pixel resolution of 0.5 m.

Although the datasets did not have identical spatial resolutions, the OBIA was performed separately on each and the change analysis was based on vector polygons. Therefore all data were assumed to be functionally comparable in spite of the minor discrepancies in pixel scale. Positional differences that could not be resolved through georeferencing and geometric corrections were ignored because the final change analysis was based upon the geometry of polygons, not their absolute real-world positions. To wit, a change in polygon size or shape *implies* a change in boundary location, even if the precise coordinates of the new and old locations are not accurately known.

3.2 Study Design

This study began as an investigation of historical aerial imagery. It was rapidly evident that while the combination of anthropogenic disturbances and natural processes lead to short-term dynamism, at the landscape level the processes are largely deterministic. This study is based on the hypothesis that water explains the apparent tendency for localized climax communities to remain geographically bound, rather than expanding when disturbance presents an opportunity to do so.

An initial assumption that water would rarely be visible in historical aerials of the study area proved to be incorrect. Although looking for visible water surfaces directly is simpler and in line with approaches that have already been established in previous studies, this seemed poorly suited for use at the Fort Ord study area because the region is so arid. As fact would have it, numerous photographs show water surfaces in at least a few of the known vernal pool sites.

Surprisingly, water features were confirmed at five additional locations more than once (see Figures 2 and 8). These PVP locations also exhibited some of the same vegetative patterns as those visible around CVPs.

Such vegetation patterns were quantified in each analytical image, using Trimble eCognition Developer 9.0 for segmentation and classification, and ArcMap 10.3 for pre- and post-processing and analysis. The final datasets were also parametrically analyzed in IBM SPSS Statistics 21. These patterns were used as a proxy for water in the environment because plants must be specially adapted to survive in flooded soil. In theory, the way plant communities develop in areas with steep hydrologic gradients should be notably different than the way the same constituent species come together in the absence of standing water.

The postulate for this thesis is that relict or dormant vernal pool sites are still discoverable between historic and contemporary imagery, because the vegetation patterns in and immediately surrounding them appear strongly persistent. In this view, isolated lowland meadows with margins that are fixed in time and space are that way because of seasonal flooding. The persistence of vegetation patterns is not typical of a highly disturbed environment, such as the study area. The history of continual disturbance (e.g. fire, mastication, explosions, mowing, road and trail cuts, water diversions, and bulldozing) should be enough to shift the whole landscape toward a more homogenous state, via both primary and secondary forms of succession (Bauder 2000, 2005; Gopal 1986; TetraTech and Ecosystems West Consulting Group 2014; Van Dyke and Holl 2003; Van Dyke, Holl, and Griffin 2003). If meadow islands are permanent fixtures, it could be because some underlying process or processes are helping maintain the *status quo*. The presence of water at or just below the soil's surface could surely

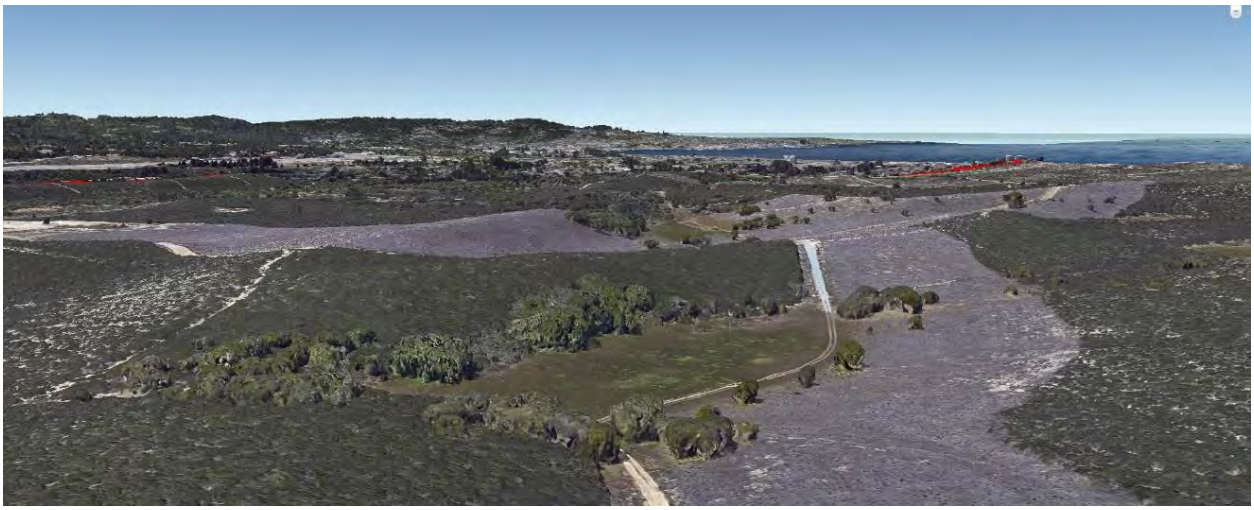

Figure 9: Oblique Camera Angle of CVP (ID # 80P07) from Google Earth Pro

account for such patterning, because it would restrict the nearby vegetation types to a much narrower cohort.

CVP site locations (n = 15) were compiled using previously published studies and maps as source information. An additional five meadows regularly developing water features were also noted, bringing the CVP total to 20. PVPs ($n \leq 51$) were identified through a manual examination of satellite imagery, aerial photographs, Google Earth Pro, and the digital USGS topographical base layer available through ArcGIS Online. Data exploration was primarily conducted with a dual approach that included the simultaneous use of ArcMap 10.3 and Google Earth Pro. Preliminary utilization of Google Earth included visual scrutiny of the study area, logging of historic inundation events using the timeline feature, and 2.5D visualization of the study area. Google Earth is excellent for studying spatial relationships when used in a decision-support role (Haas, Bartholomé, and Combal 2009; Jiang et al. 2012; Wang et al. 2011). For instance, the camera can be panned, tilted, and rotated (Figure 9) to view different perspectives

Figure 10: Analytical Rasters, Side by Side After Pre-processing

of image rasters draped over a 2.5D fine-scale model of the Earth's surface topography, and the vertical axis can be stretched by up to a factor of three.

Raster images were pan-sharpened and clipped to the boundaries of the study area before being uploaded into eCognition and subjected to OBIA. Figure 10 shows the three analytical rasters in B&W (1941, far left) and true color (2001 and 2011, from center to far right), as they appeared after the completion of post-processing. In a manner conceptually similar to that of Zhang and Maxwell (2006), the primary Model Object (MO) was determined to be the outermost edge of a study meadow, wherever chaparral and meadow habitats converged. Convergent regions typically constituted the boundary between upland and lowland vegetation types.

This study demonstrates a method for tracking changes in upland/lowland boundaries to allow a comparison between vernal pool-containing and other meadows. An *ad hoc* segmentation algorithm based on the Fractal Net Evolution Approach (FNEA), developed by Baatz and Schäpe (2000), was created for each set of rasters, after which supervised and visual methods were used to classify the image segments (Baatz and Schäpe 2000; Blaschke 2010; Halounova 2004; Mallinis, Pleniou, and Koutsias 2010). Objects were classified with input from

Figure 11: Site 80C03, the Single Study Area Vernal Pool Visible from Public Roads (Photo Credits: C. Hanley)

various components of the available feature space (discussed later in Section 3.5). Finally, the fully classified set of objects were exported to shapefiles and uploaded back into ArcMap. The patch analyst extension (Rempel, Kaukinen, and Carr 2012) was used to calculate area, perimeter (PERI), perimeter-to- area ratio (PAR), shape index (SI), and fractal dimension (FD). Patch metrics were then used to compare short- and long-term changes in CVP and PVP boundaries.

Attempts were made to collect ground evidence to verify OBIA results, but only one vernal meadow, 80C03 (Figure 11), is visible from a road or access point open to the public. A request to access the restricted zone was denied due to unsafe conditions relating to unexploded ordnance and munitions. Instead, a low-altitude flyover in a Piper PA-28 Cherokee was conducted above the study area on 21 February, 2015. The route traversed was an approximate north-south sawtooth pattern spanning the full extent of the study area. In flight, full HD video

of the ground was recorded from a GoPro HERO 3 digital camera mounted to the underside of the right wing, as photographs were taken from the cockpit. Conditions were clear and bright, with a flight time of 42 minutes at an altitude between 250 and 400 m above sea level.

3.3 Data Exploration

Persistent spatial patterns at the interface between meadow areas and chaparral habitats, mima mounds, and the regular occurrence of oak stands nearby, are noticeable landscape features common to many time-series images of the study area. Any location with a lasting meadow was initially considered for inclusion as a study site. Unlike other areas of Fort Ord, where oak trees mix with invasive annual grasses to create savanna ecosystems, the grassy lowland meadows in the study area invariably have no growth of oak trees within their margins. Interestingly, many meadows appear to coincide with small oak groves within the upland vegetation at their southern and western peripheries. By contrast, oaks tend to appear as isolated individuals throughout much of the remainder of the upland ecosystem.

A digital USGS topographic 10 m contour map, marked with depressions and drainage areas, was used to locate and log the locations of low spots in the landscape (n = 69) in an ArcGIS point feature class. The point file was converted to KML format, uploaded into Google Earth Pro, and used to confirm the physical feasibility of indicated sites. From the combination of topographical data and historical visual information, 54 PVPs were included in the first iteration.

Upon review of all the available datasets, it was determined through water sightings that the number of CVPs should be increased to 19, while the number of PVPs varied from image to image. The discrepancy in PVP count was due to disqualifications mediated by extreme disturbance. Namely, prescribed burns and mastications just prior to the 2001 and 2011 image

Table 1: Summary of Study Meadow Counts by Type and Year

Type	1941	2001	2011
CVP sites	18	17	18
PVP sites	41	38	7
Unique sites*	4	2	2

*Unique sites appear only in a single analytical image.

acquisition dates left more than 50% of the study area too denuded to perform accurate OBIA. For the purposes of this research, a minimum regrowth time of at least eight years was needed to see the re-establishment of a distinct upland/lowland boundary.

Recent disturbances were equal cause for jettisoning both CVP and PVP sites, except where a visible water feature existed in the analytical image. Sites were also eliminated when they did not persist from 1941 to 2001, or were not present in the 1941 image. The 2011 data included two unique sites, both of which are vernal pools. However, only one of these is a previously confirmed CVP. The study sites are summarized by year and type in Table 1.

3.4 Pre-Processing

Raw analytical data were projected and georeferenceed immediately upon acquisition. This study utilized the projected coordinate system WGS_1984_UTM_Zone_10N. The multispectral analytical images were pan-sharpened in ArcMap using a combination of their multispectral and panchromatic bands, with Gramm-Schmidt transformations. The default channel weights were chosen with respect to the sensor of acquisition.

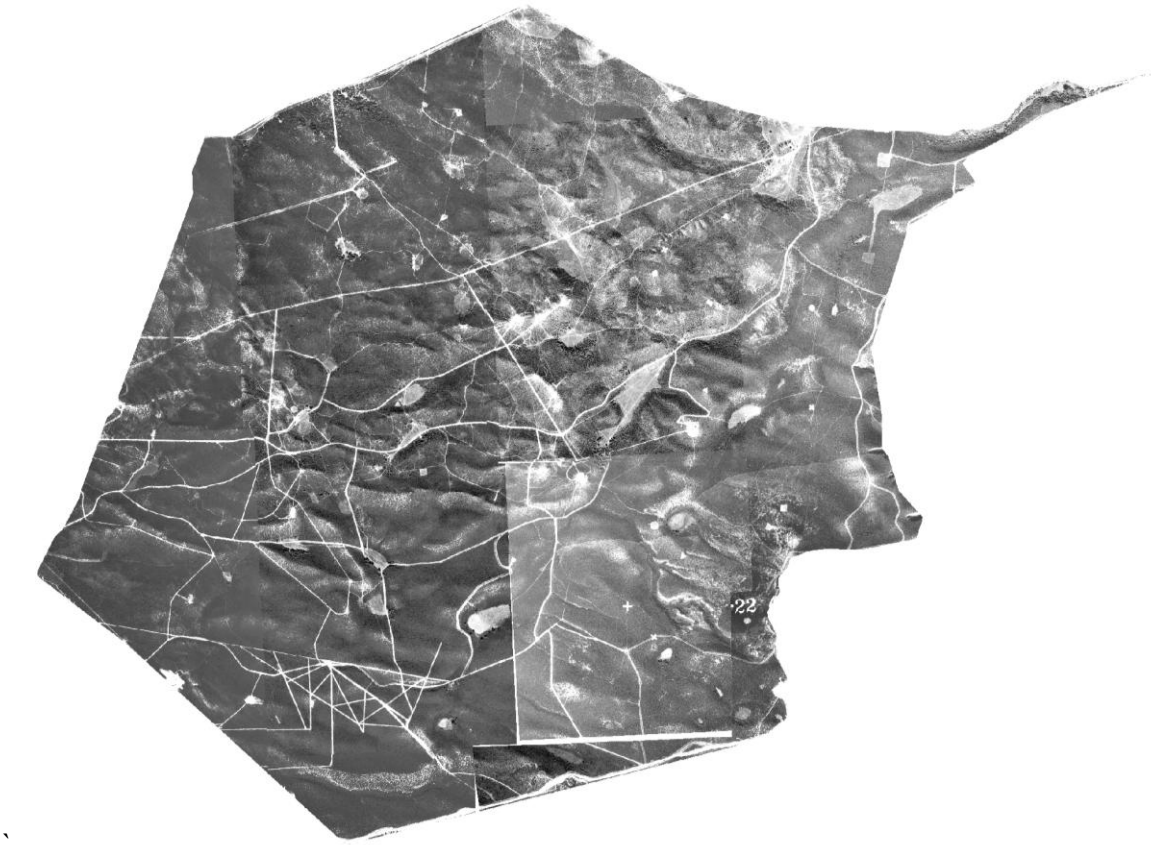

Figure 12: 1941 B&W Raster Reassembled mosaic, Post-geometric corrections

Prior to export, attempts were made to correct alignment issues between the three datasets. Since the panchromatic picture contained clear mosaic errors and the Ikonos data was acquired off-nadir, the WorldView 2 imagery was selected as the base layer to which the others were aligned. It was impossible to eliminate every alignment error, but most were significantly reduced. The Ikonos data was corrected using georeferenced control points. Control points were also used to align the 1941 raster, but the image contains some minor registration issues that are unresolvable due to slight mosaic misalignments. All attempts were made to correct the errors by first clipping the geotiff raster along the original mosaic lines, which are clearly visible in Figure 12, then georeferencing the new pieces and reassembling the mosaic. However, some distortion remained, in spite of these efforts.

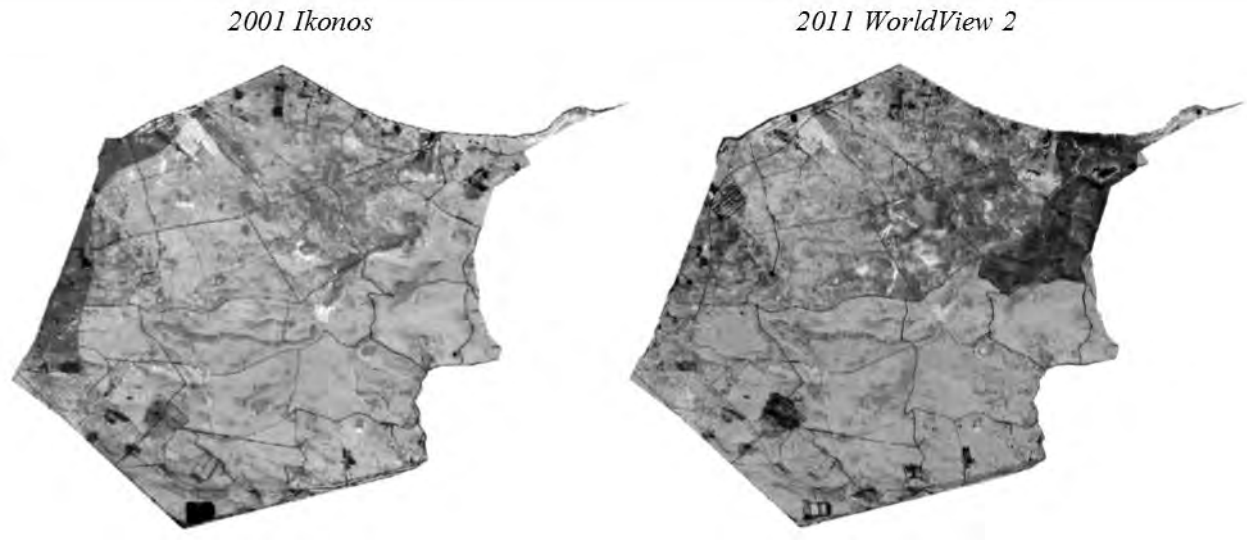

Figure 13: NDVI Comparison, 2001 Ikonos (left) versus 2011 WV2 (right)

The final pre-processing step performed in ArcMap was the creation of a Normalized Difference Vegetation Index (NDVI) band, which combines the Red and near-infrared (NIR) channels to create a new channel that is useful in assessing the health and state of vegetation (Fallon 2013; Highfield, Ward, and Laffan 2008). Red light is absorbed by chlorophyll during photosynthesis, while near infrared wavelengths are reflected by healthy plant cells. Most commonly, the brighter regions in Figure 13 coincide with areas of healthy flora. The NDVI band was calculated according to the standard NDVI equation:

$$NDVI = \frac{NIR - Red}{NIR + Red} \quad (1)$$

Image layers were mixed in eCognition using trial-and-error. The approach focused on the creation of clear visual distinctions between the most important image objects, like meadow margins, oak trees, and chaparral stands. The final weighted layer mixture was a variant of a weighted bands CIR mix. The mix included red, green, blue, NIR, NDVI, and panchromatic

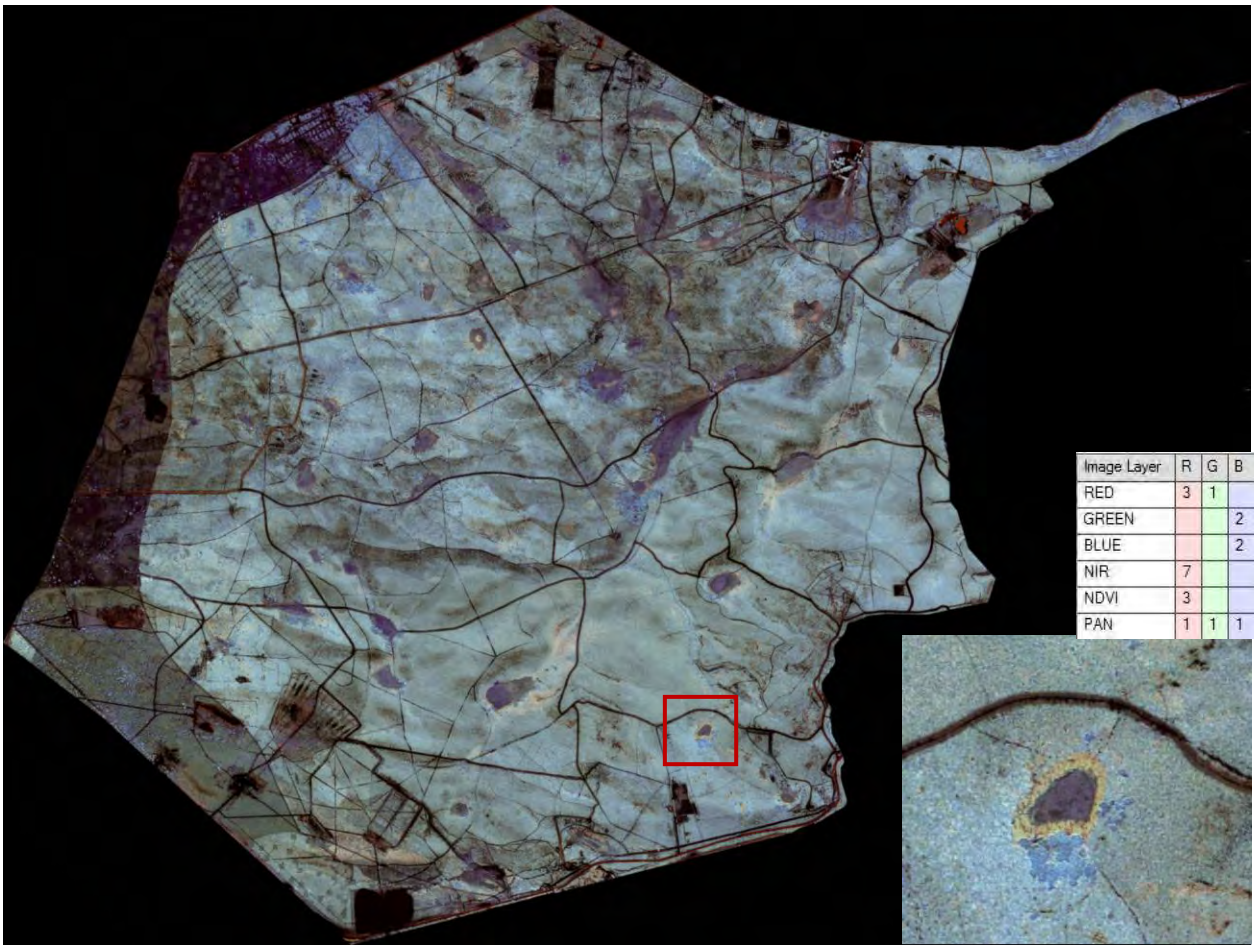

Figure 14: Novel False Color Composite of Ikonos 2001 Imagery

channels in order to enhance the separation between the feature spaces of different object classes, with each color gun having up to four layers used in combination (Figure 14).

Halounova (2004) recognized the need to perform signature space enhancement, doing so by using Gauss and median filters to reduce the amount of overlap in the spectral signatures of classes. Similar separation was achieved here manually, via noise-reducing contrast stretches produced with either inverse or negative gamma equalizations. An example of the novel false color composite mix, as it appeared when applied to the 2001 imagery, is visible in Figure 14. In the center of the inset is a CVP with a band of Dead Transition (orange) around the meadow

(purple). Oak trees are visible as blue objects, while the chaparral appears teal. Roads, bare ground, and fire break are the darkest objects visible.

3.5 Segmentation and Object-Based Classification

Typical OBIA workflows employ the Fractal Net Evolution Approach, which Baatz and Schäpe (2000) introduced commercially in eCognition software, followed by a Nearest Neighbor (NN) classification (Figure 15). FNEA has since been referenced numerous times in the literature, particularly in conjunction with multiresolution segmentation (Blaschke 2010; Burnett and Blaschke 2003; Halounova 2004; Mallinis, Pleniou, and Koutsias 2010, Smeulders et al. 2000).

In segmentation, grayscale texture is used to create polygons known as segments that represent homogenous regions. Multiresolution segmentation involves segmenting an image at multiple resolutions, in order to fuse homogenous lower level sub-objects into higher level model object classes. The result is a tessellation of polygons spanning the image extent, with each texture-based polygon ideally containing adjacent pixel groupings that represent cohesive real-world objects. Subsequently, classification of the segmented objects is performed. A NN algorithm (Blaschke 2010; Halounova 2004; Smeulders et al. 2000; Yu and Zhang 2008) is the most commonly applied classification technique. NN classifies horizontally across an image, assigning segments as semantic objects according to their spectral signatures, densities, and spatial contexts. The classification parameters one chooses to employ can be optimized in eCognition, but it is often easier to make the choices on a trial-and-error basis instead. The results of a simple linear FNEA and NN classification are depicted in Figure 15.

3.5.1 Fort Ord OBIA

Segmentation usually requires some supervision through the input of texture training areas, manual adjustments to segment boundaries, or the creation of additional dissolves not triggered

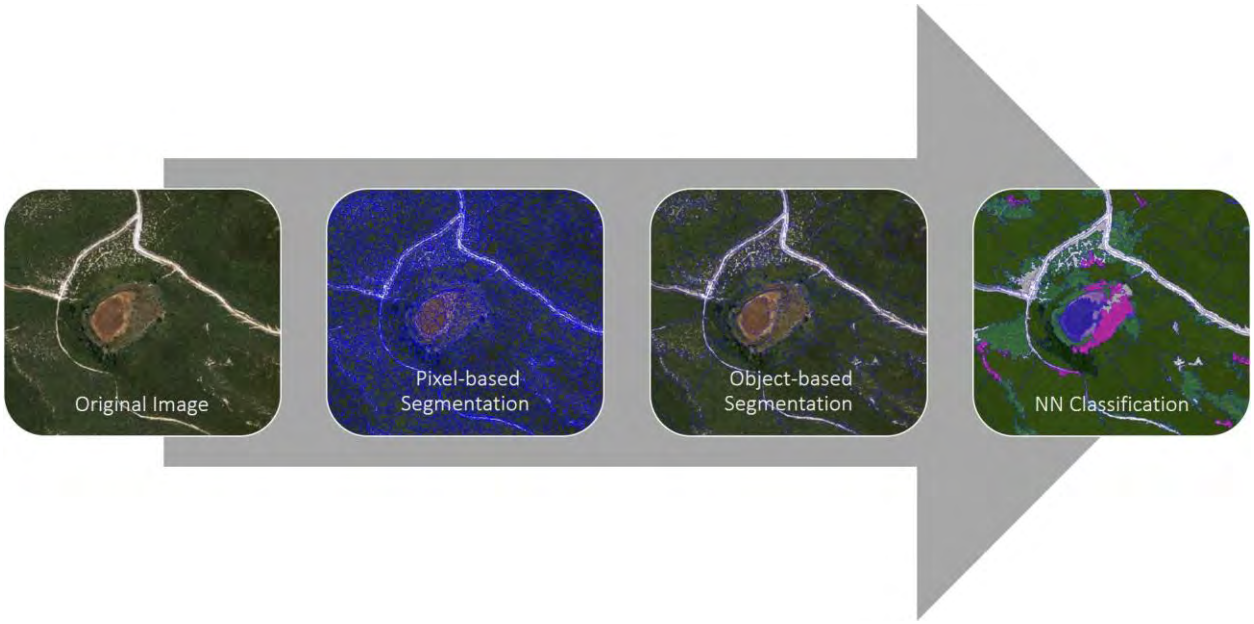

Figure 15: Typical Linear FNEA and NN Workflow

by the chosen algorithm (Dissanska, Bernier, and Payette 2009; Halounova 2004). Though object-based classification cannot be performed without first segmenting an image (Baatz and Schäpe 2000), it is possible to iterate through cycles of merging, re-segmenting, and re-classifying portions of an image to improve result accuracy. Several iterations may be necessary because noise in the image data can negatively impact segmentation if it occurs on a similar spatial scale as an object's texture (Baatz and Schäpe 2000). Per Zhang and Maxwell (2006), the segmentation of sub-objects can ultimately effect the drawn accuracy of the model objects. Thus it is preferable to over-segment the image with smaller polygons and merge upwards, stopping before the MO is merged with other objects.

The Fort Ord imagery was analyzed using a derivative of the FNEA approach that included a top-down, bottom-up scheme. Model objects were segmented and classified iteratively, going both forward and backwards as necessary. This multi-directional tactic allowed the small number of PVP and CVP sub-objects to be selected and merged into model

objects and classified manually, ensuring that lowland features and their boundaries were extracted with the highest precision possible. There was a conscious tendency to err on the side of commission and occasionally include adjacent sub-objects whenever the original segmentation was incorrect, as lowlands were later unclassified and re-segmented at a finer scale to improve the accuracy of the results. Spectral- and shape-related thresholds were then utilized to classify the remainder of the image because feature space optimization and the NN algorithms were computationally intensive and time-consuming. The cost in time was doubly important since the entire OBIA was constructed from scratch for each image, using trial-and-error.

To illustrate how thresholds were used, consider two equivalent road segments. Due to any number of chromatic aberrations or variations in the objects themselves, each road segment may attenuate differing proportions of a given wavelength of light. The reflected portion of said wavelength gives the object brightness in that color. Thus one road segment may have a brightness in the blue band, for instance, that overlaps the signature space of another object class while the other road segment does not. Adding a second threshold for another band, such as red, allows the first threshold to be adjusted while still excluding another object class that overlaps in blue (provided there is signature space separation in the new band).

While NN classification would have been easier to execute on a conceptual level, and the method described herein required more effort and direct input from the user, it also achieved much more accurate classification results. The scheme was refined using incremental changes in threshold values. Moreover, a shapefile of burn area polygons was created in ArcMap, exported to eCognition, and used to classify burn areas in the 2011 image. Integration of the two data streams significantly reduced the time required to perform the OBIA, as well as improved the

accuracy. Finally, the accuracies were assessed using error matrices created from Test and Training Area (TTA) masks, which were constructed from a carefully selected group of samples.

3.5.2 Semantic Considerations

Prudence dictates that segmentation and OBIA results must be visually inspected to ensure that classifications match the semantic knowledge base (Dissanska, Bernier, and Payette 2009). However, experience has shown that the semantic structure of the study is equally, if not more, important in producing accurate results. Choosing the optimal number of classes and naming them aptly was not easy to accomplish. The imagery was exclusively comprised of wilderness or natural landscapes, which increased the challenge because clear physical, as well as semantic, distinctions between object classes were often hard to achieve. For example, it was necessary to ask where the boundaries between transitional vegetation and lowland grasses were when a gradient existed rather than a break. Likewise, how many oak trees constituted an oak grove, or what was the appropriate classification of a study site that had water features but was not a previously confirmed vernal pool? What if object classes existed in one image but not others? These were some of the questions that needed answers.

Clearly, object class semantics are paramount to OBIA success. In this case, a structure was required that could be applied equally to every image in the time-series sequence. The Fort Ord impact area time-series presented many challenges because there was a high-degree of variation inherent in several object classes. For example, the "Invasive" class (Figure 16) included both iceplant (*Carpobrotus edulis*) and pampas grass (*Cortaderia jubata*), which differ considerably in texture and appearance. Another class, "Upland," likely encompassed anywhere from one to several species of *Arctostaphylos* manzanita, coyote brush, Monterey ceanothus (*Ceanothus cuneatus* var. *rigidus*), and chamise (*Adenostoma fasciculatum*). "Upland" probably

Figure 16: Iceplant and Pampas Grass Comprised the "Invasive" Class (Photo Credits: C. Hanley)

also included some unsegmented oak trees, small patches of bare ground, invasives, and the occasional coastal sage scrub community. Overall, there are more than 1,000 plant species that have been identified on the base, meaning that most categories had a catch-all component similar to the invasive and upland classes (BLM 2010). Table 2 details the overarching semantic structure employed during the analysis, as it was run in eCognition. Classes that related to lowland structures, such as Live Transition, Dead Transition, Lowland, and Water were later reclassified in ArcMap into a supra class, termed "Lowland Complex" (not described in Table 2). Although it was at times difficult to differentiate between within-meadow classes, it was rarely difficult to establish the lowland-upland boundary. Consequently, it was deemed appropriate to analyze lowlands as complexes, rather than at the constituent level. However, OBIA and classification required a more granular approach that necessitated the additional classes to reduce the semantic gap.

Table 2: Object Class Names, Acronyms, and Descriptions

Class Name	Description
Bare Ground/Dirt Track (BG)	Unpaved roads, tracks, paths, trails, and bare ground
Building	Buildings or similar human structures
Dead Transition (DT)	Band of grey (dead or senescent) upland vegetation surrounding vernal meadows
Fire Break/Burn (FB)	Any area that had been recently cleared of vegetation, but was not bare ground (e.g. recent burns, fuel breaks, youngest chaparral age classes)
Invasive (IV)	Typically iceplant or pampas grass
Live Transition (LT)	Areas where dead transition was reviving or chaparral was recruiting into meadow areas
Lowland (LL)	Local depression, grassy zone inside or adjacent to Dead/Live transition where water features may or may not develop
Oak Tree (OT)	Individual oak trees and groves
Paved Road (PR)	Any pavement, asphalt, or gravel surface
Upland (UP)	Chaparral vegetation that had reached minimum age class of 8 years
Upland Prairie	Any grassland not located in a lowland depression
Water (W)	Visible water features

3.6 Analyzing Change

From eCognition, the user is able to access and export over 100 spectral, geometric, or class-related metrics. However, these data were not used because the vernal pool analysis was not spectral in nature. More importantly, *post-hoc* corrections performed in ArcMap would have rendered eCognition's geometric values incorrect. The spatial metrics described below in this section were therefore calculated using ArcMap after *post-hoc* corrections had been made.

The change analysis approach that is presented in this section is novel in the sense that, unlike the other components of this study, it was not guided by previously published research. In essence, the *ad hoc* development of the change analysis arose from the problem of quantifying the spatial differences between an object and later versions of itself. Since the registration between the images was inexact, and the average offsets were far greater than the images' spatial resolutions, performing an overlay or examining changes in centroid positions were not considered appropriate analytical pathways. Instead, all lowland complexes were analyzed using the Patch Analyst extension, which computed values for several key geometric properties. In total, five initial metrics—area, perimeter, PAR, SI, and FD—were calculated for every meadow site (ID codes shown in Figure 17) in each analytical image, with PAR, SI, and FD being unitless numbers. A similar set of metrics was used by Backoulou et al. (2011) to evaluate island patches of aphid-stressed plants in wheat fields.

Changes in the geometric properties of polygons must be evaluated with caution because area and perimeter do not scale equally. Complicating the issue is the fact both segmentation granularity and landscape composition can lead to discrepancies in object smoothness. Changes in smoothness have a greater impact on perimeter than area. One way to handle the problem is to calculate a shape index. The SI equation normalizes the perimeter-to-area ratio of a polygon

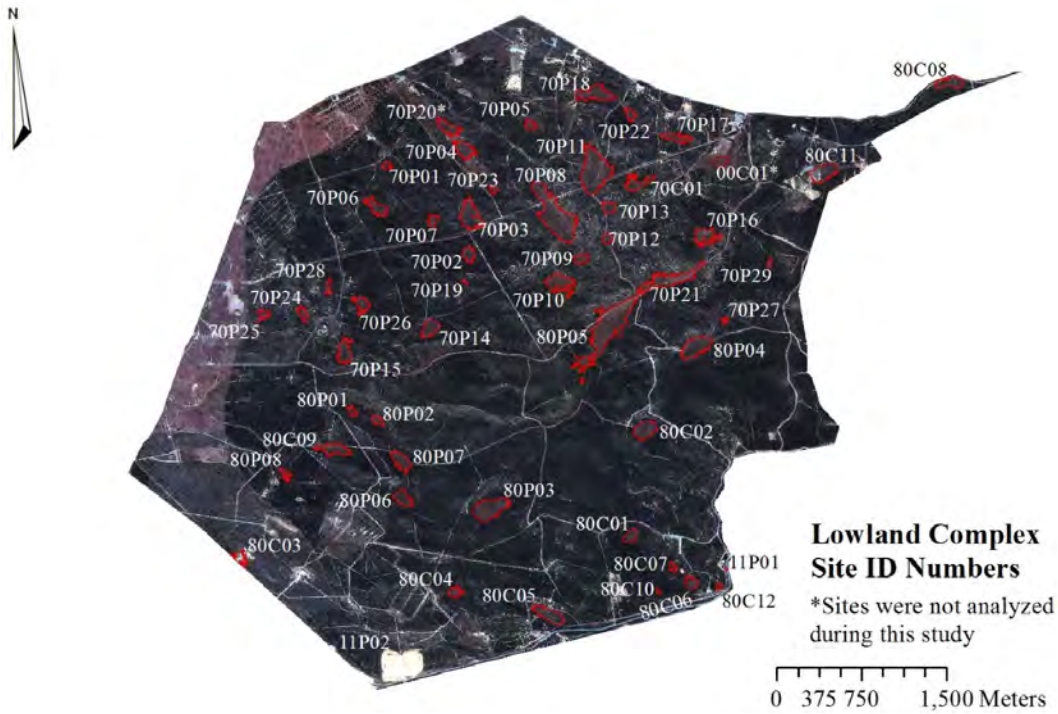

Figure 17: Lowland Complex Site ID Numbers

by comparing it to a simple shape, like a square, of equal size (Backoulou et al. 2011). SI also makes the PAR metric redundant. Instead another useful metric is the fractal dimension which, in simplest terms, is a measure of the degree of complexity of a shape's outline (Backoulou et al. 2011). The study meadows tend to have amorphous outlines that are relatively compact and simple, but the smoothness can exhibit some variance over time.

To compare images, differences in metric values for self-same sites were derived for the 1941–2001 and 2001–2011 intervals. The percent change in each category was calculated as well. Finally, a new metric introduced for the first time here, the Persistence Index, was determined for each site as follows:

$$PI = \left(\frac{1}{3}\right)\left(\frac{\Delta A_t}{A_i} + \frac{\Delta SI_t}{SI_i} + \frac{\Delta FD_t}{FD_i}\right) \quad (2)$$

where A_i = the initial area, ΔA_t = the area change at time t, SI_i = the initial shape index, ΔSI_t = the change in the *SI* at time t, FD_i = the initial fractal dimension, and ΔFD_t = the change in *the FD* at time t. Given that A_i, SI_i, and FD_i cannot equal or sum to zero, the range is $-\infty < PI < \infty$.

PI is also unitless, and can be interpreted as the mean of the change ratio across all three metrics. In theory, it can range to infinity in either direction. Shapes with PI values very close to zero have undergone very little change since the previous measurement. The index gives the relative degree of combined shape and size change of an object, either positive (i.e. expansion) or negative (i.e. contraction).

PI can also be weighted by interval (WIPI) by dividing by the number of intervals, allowing for groups with a variety of temporal ranges to be compared. For instance, 2011 WIPI value distributions were compared to 2001 WIPI values for self-same CVP locations, with an interval length of 10 years:

$$WIPI = \frac{\left(\frac{1}{3}\right)\left(\frac{\Delta A_t}{A_i} + \frac{\Delta SI_t}{SI_i} + \frac{\Delta FD_t}{FD_i}\right)}{C} \quad (3)$$

where C = the number of intervals and $C \neq 0$. Thus WIPI for the 7 decadal intervals from 1941–2001 is given by:

$$WIPI_{\Delta 01} = \frac{\left(\frac{1}{3}\right)\left(\frac{\Delta A_t}{A_i} + \frac{\Delta SI_t}{SI_i} + \frac{\Delta FD_t}{FD_i}\right)}{7} \quad (4)$$

Likewise, WIPI for the single decadal interval from 2001–2011 is given by:

$$WIPI_{\Delta 11} = \frac{\left(\frac{1}{3}\right)\left(\frac{\Delta A_t}{A_i} + \frac{\Delta SI_t}{SI_i} + \frac{\Delta FD_t}{FD_i}\right)}{1} \quad (5)$$

WIPI normalizes the persistence index for the effects of time, as the absolute value of a given patch's PI would be expected to increase as time passes.

Patch and class level analytics were performed in both ArcMap and SPSS, including exploratory regression, dependent, and independent t-tests. For comparative purposes, meadows were placed into one of the two previously described nominal categories, PVP or CVP. The CVP category comprised both previously confirmed vernal pool meadows and those discovered during this research. PVP were defined as any other persistent lowland meadow study site within the study area. For the 1941–2011 interval, it was possible to compare the groups of CVPs and PVPs because sufficient samples existed. However, between 2003 and 2011, approximately half of the study area was burned or masticated. As a consequence, PVP sites were reduced from 38 to seven. CVP sites suffered less, being reduced from 16 to 15. Thus WIPI was developed to facilitate a comparison between self-same CVP sites over time. Whereas the 70-year interval allowed for the comparison of two different groups—CVP and PVP—using the Student's (independent samples) t-test, the 10-year interval only allowed for CVP to be compared with themselves using the Paired (dependent) samples t-test.

Spatial analytics were attempted in addition to parametric statistics, but were ultimately dropped when an adequate model could not be constructed using exploratory regression. The datasets were not well-suited to the requirements of a regression analysis. Redundancy in some of the metrics manifested itself as multi-collinearity, while spatial autocorrelation of the residuals and small sample sizes further confounded the test. Moreover, a regression requires a continuous dependent variable, which the datasets in question did not adequately possess. Conversely, the data were amenable to parametric analysis, allowing the data collected from this OBIA to be analyzed with only the occasional logarithmic transformation or removal of an outlier.

CHAPTER 4: RESULTS

The results presented here are broken up into three parts. In Section 4.1, the accuracy reports for the classification procedures are given, while Section 4.2 contains the key statistical outputs from SPSS. The last section focuses on the observations resulting from the low altitude flyover.

4.1 Classification Results

Classification accuracy was assessed in eCognition using error matrices generated from TTA masks. Masks were created from MO level segments, using sample sets carefully chosen to represent the within-class variation inherent in the data. Error, or confusion, matrices (contingency tables) like the ones shown later in this section provide estimates of Type I and II errors on a per class basis. Classification errors can manifest in two basic ways. The former, Type I, happen when the correct action *was not* taken. The latter, Type II, arise when the incorrect action *was* taken.

Type I errors are errors of omission that occur when a pixel should have been included in a given class, but was mistakenly omitted instead. Omission errors are reflected in the columns of a contingency table. The sum of each column is actually the total number of pixels that should belong to that class in the real world, according to ground evidence. The Producer's accuracy is another way of describing Type I error, in that it gives the estimated proportion of the true number of pixels that were classified correctly into a given class. For example, consider a situation where an image contains 100 true pixels of grass; if 75 are classified as grass and 25

errantly classed into another category, the omission error would be 25% and the Producer's accuracy would be 0.75 (75%).

By comparison, Type II errors are related to User's accuracy and commission errors, and are interpreted from a table's rows. Type II commission errors are those that result from a pixel being classified into a class to which it does not belong. The way to distinguish between Type I and II errors is to recall that, for a given class, some proportion of pixels *were not* included that *should* have been (Type I) while other pixels *were* included that *should not* have been (Type II). Type II errors are caused when pixels are falsely counted in the class being examined. In the same manner that Producer's accuracy relates to Type I error, the User's accuracy is an alternate expression of Type II error. In essence, the User's accuracy gives the relative likelihood that someone visiting a pixel's real-world location would actually find the expected class of object.

4.1.1 1941 Panchromatic Classification and Accuracy

Classifying the 1941 B&W image required the fewest object classes, since its lower resolution and lack of color made classification to a higher granularity impossible. Only classes that were easily and unmistakably identifiable were included in the image semantics. The object classes included were Upland (UL), Fire Break/Burn (FB), Lowland (LL), Bare Ground/Dirt Track (BG), Oak Tree (OT), and Live Transition (LT). With this semantic scheme, it is possible that undetectable errors may have occurred if Dead Transition (DT) and Invasive (IV) objects were present in the image, as they were not incorporated in the class structure. Both classes would have been counted in the LT class by mistake. Such a determination would be impossible to make, however, without ground evidence—which does not exist for the 1941 dataset.

Figure 18 presents the classification results and Table 3 follows with the error matrix for the 1941 panchromatic image. A visual examination of the output map shows that the

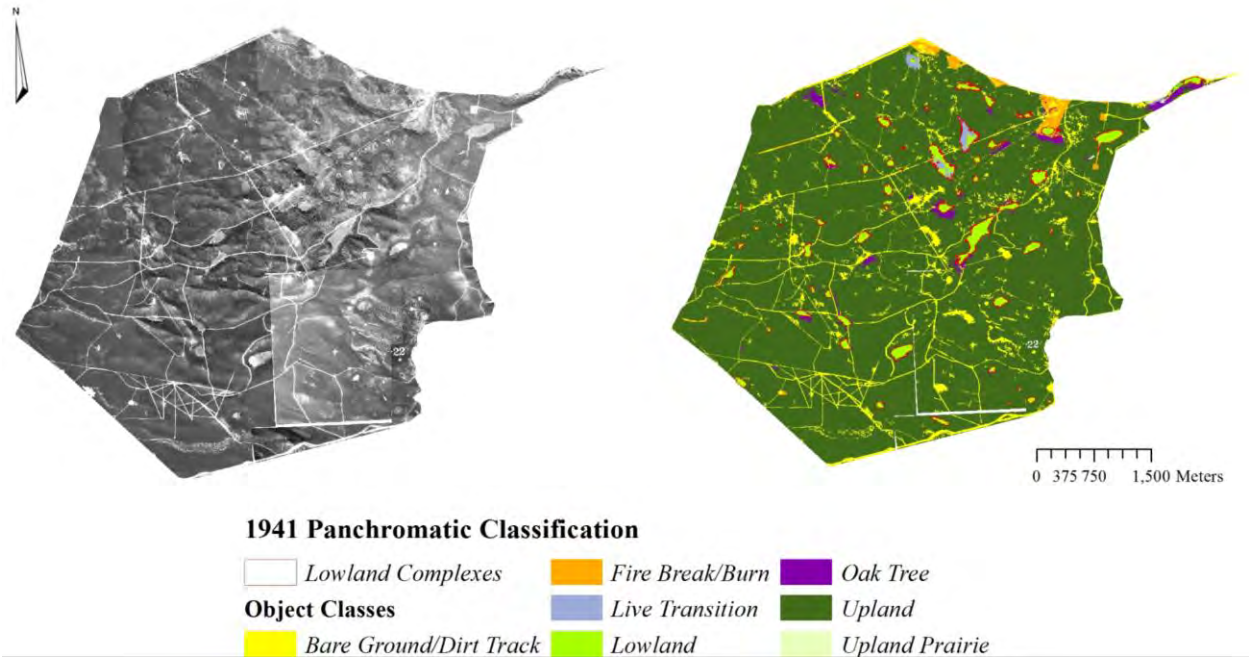

Figure 18: 1941 Panchromatic Image Classification Results

Table 3: Error Matrix (Contingency Table) for 1941 Panchromatic Classification

CLASS	UL	FB	LL	BG	OT	LT	SUM
UL	8,904,365	0	0	0	0	0	8,904,365
FB	0	149,975	0	0	0	0	149,975
LL	0	0	598,688	0	0	0	598,688
BG	0	0	0	72,254	0	0	72,254
OT	0	0	0	0	37,731	0	37,731
LT	0	0	0	0	0	325,437	325,437
SUM	8,904,365	149,975	598,688	72,254	37,731	325,437	10,088,450
Prod.	1	1	1	1	1	1	1
User	1	1	1	1	1	1	1
Overall	1						

classification proceeded with a high degree of accuracy. On the other hand, the error matrix overestimated the accuracy in calculating 0% types I and II errors for each object class. Since perfect classification performance is highly improbable, the accuracy results shown in Table 3 are dubious. The real accuracy could not have been 100%, but the reason for the overestimate is unclear. Nonetheless, the vector output results easily pass inspection when scrutinized with the human eye. It is reasonable to expect that the true accuracy may still be on par with the 2001 and 2011 results, which both exceeded 98% overall.

4.1.2 2001 Ikonos Classification and Accuracy

The 2001 Ikonos imagery was significantly more complex than the B&W from 1941. An additional six classes were needed, doubling the total from the first OBIA (Figure 19, next page). The combination of multispectral bands and increased spatial resolution led to an improved ability to distinguish between classes. However, the gain in sensitivity is also what necessitated the expansion of the semantic structure. The original MO classes were maintained, and six new classes were added, including Building, Dead Transition, Invasive, Paved Road (PR), Upland Prairie, and Water. Only three of the newly added classes were considered during the accuracy assessment. Building, upland prairie, and water objects were not evaluated in the error matrix because their occurrence rates were disproportionately low. In all, there were five classified building objects and one each of upland prairie and water, out of a total of 10,643 object segments. Since these three classes together occupied less than 0.1 percent of the total image area, their bearings on the overall accuracy of the OBIA were negligible.

The accuracy estimates produced using the remaining nine classes were very high (Table 4, next page), equaling the accomplishments of Frohn et al. (2011). Visually, the classification

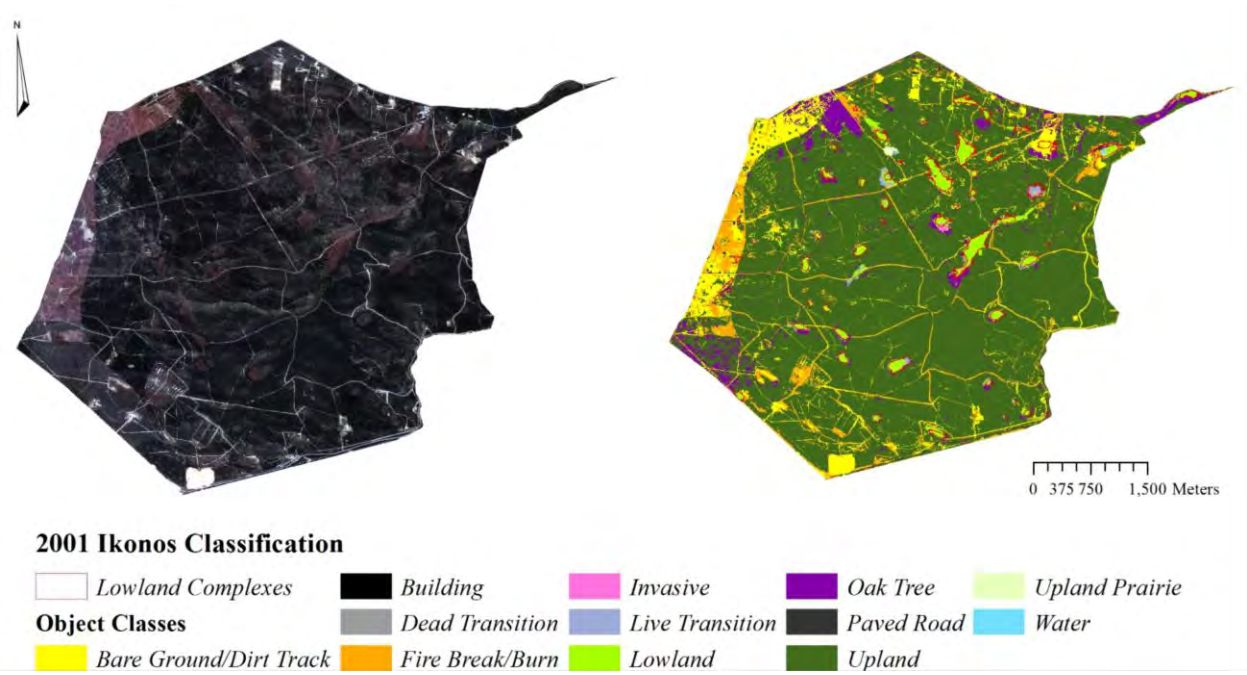

Figure 19: 2001 Ikonos Image Classification Results

Table 4: Error Matrix (Contingency Table) for 2001 Ikonos Classification

CLASS	LL	UL	DT	BG	FB	OT	PR	LT	IV	SUM
LL	68,186	0	0	0	0	0	0	0	0	68186
UL	0	1,515,886	0	1,928	14,210	1,145	0	0	0	1533169
DT	0	0	15,530	0	0	0	0	0	0	15530
BG	0	0	0	53,842	13,113	0	0	0	0	66955
FB	0	0	0	2,328	87,514	0	0	0	0	89842
OT	0	100	0	0	0	159,154	0	0	0	159254
PR	0	0	0	0	0	0	49,956	0	0	49956
LT	0	0	0	0	0	0	0	21,648	0	21648
IV	0	0	0	0	0	0	0	0	9,285	9285
SUM	68,186	1,515,986	15,530	58,098	114,837	160,299	49,956	21,648	9,285	201,3825
Producer	1	0.9999	1	0.9267	0.7621	0.9929	1	1	1	
User	1	0.9887	1	0.8042	0.9741	0.9994	1	1	1	
Overall	0.9837									

results showed an exceptional degree of fidelity to the original image. Like the 1941 results, there were some ostensibly error-free classes, such as Lowland, Paved Road, Live Transition, and Invasive. However, these results are somewhat more believable because those classes were either classified manually or, in the case of Paved Road, had a sizable separation in feature space. The most confusion transpired amongst the Upland, Oak Tree, Bare Ground/Dirt Track, and Fire Break/Burn classes. BG and FB pixels were most often confused for one another, with each class lending to the majority of Type I and II errors in the other. Consequently, the BG User's accuracy of 80.42% and the FB Producer's accuracy of 76.21% were significantly lower than those of the other classes. Upland, for instance, demonstrated high User's and Producer's accuracies (98.87% and 99.99% respectively), in spite of a slight propensity toward commission errors involving BG, FB, and OT pixels. Oak tree objects and their shadows were known confounding factors as they were too small and numerous to reliably segment as individuals. Not surprisingly, it was not unheard of for the occasional oak tree to go entirely unsegmented. Typically these oaks were encompassed within a larger upland object, which is reflected as Type I error for the Oak Tree class and Type II error for the Upland class.

4.1.3 2011 WorldView 2 Classification and Accuracy

The 2011 semantic structure had an extra class included, that of Athletic Field, to accommodate the addition of two small sod grass fields in an athletic compound at the southern tip of the study area. As there were numerous water features visible in this image (Figure 20), the Water class was incorporated into the classification accuracy assessment (Table 5). The Athletic Field, Building, and Upland Prairie classes were ignored for reasons similar to that of the 2001 evaluation. Altogether, 10 classes were included in the error matrix for the 2011 dataset, with nine being common to the 2001 image and six common to all three years.

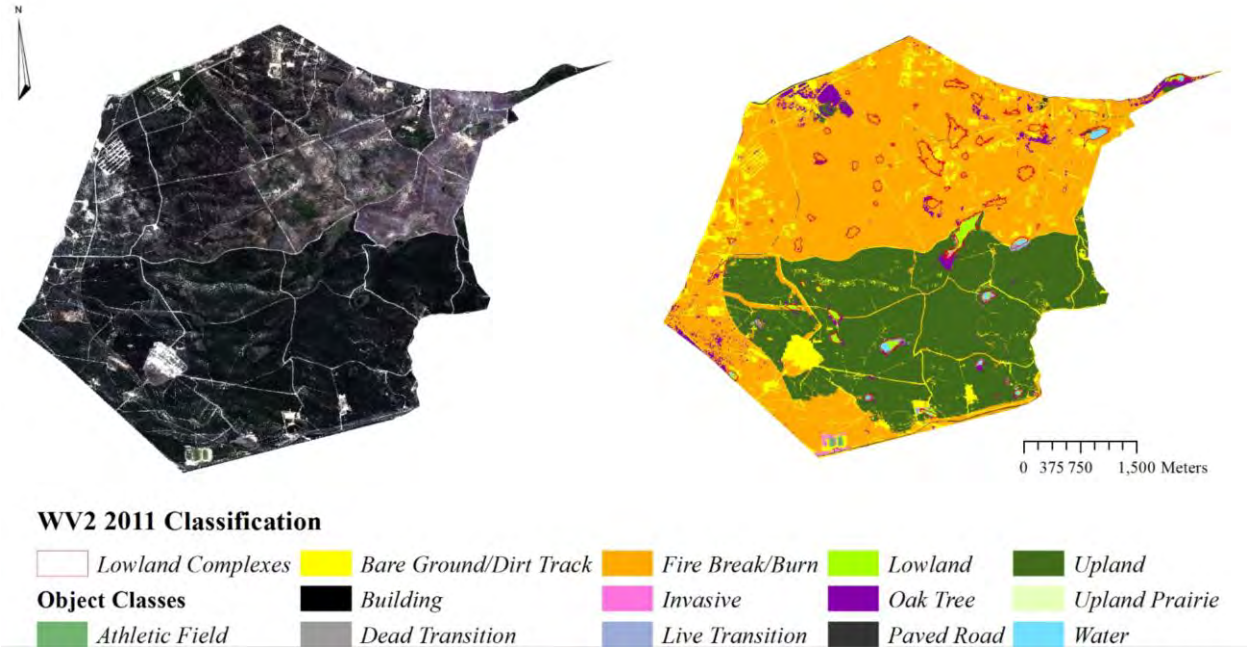

Figure 20: 2011 WV2 Image Classification Results

Table 5: Error Matrix (Contingency Table) for 2011 WV2 Classification

CLASS	LL	DT	BG	UL	FB	PR	OT	W	LT	IV	SUM
LL	235,207	0	0	0	0	0	0	0	0	0	235,207
DT	0	38,977	0	0	0	0	0	0	0	0	38,977
BG	0	0	170,946	0	25,099	0	0	0	0	0	196,045
UL	0	0	0	1,556,450	0	0	0	0	0	0	1,556,450
FB	0	0	0	0	3,209,234	0	0	0	0	0	3,209,234
PR	0	0	0	0	0	117,178	0	0	0	0	117,178
OT	0	0	0	0	0	0	168,586	0	0	0	168,586
W	0	0	0	0	0	0	0	106,129	0	0	106,129
LT	0	0	0	0	0	0	0	0	33,479	0	33,479
IV	0	0	0	0	0	0	0	0	0	44,999	44,999
SUM	23,5207	38,977	170,946	1,556,450	3,234,333	117,178	168,586	106,129	33,479	44,999	5,706,284
Prod.	1	1	1	1	0.9922	1	1	1	1	1	
User	1	1	0.8720	1	1	1	1	1	1	1	
Overall	0.9956										

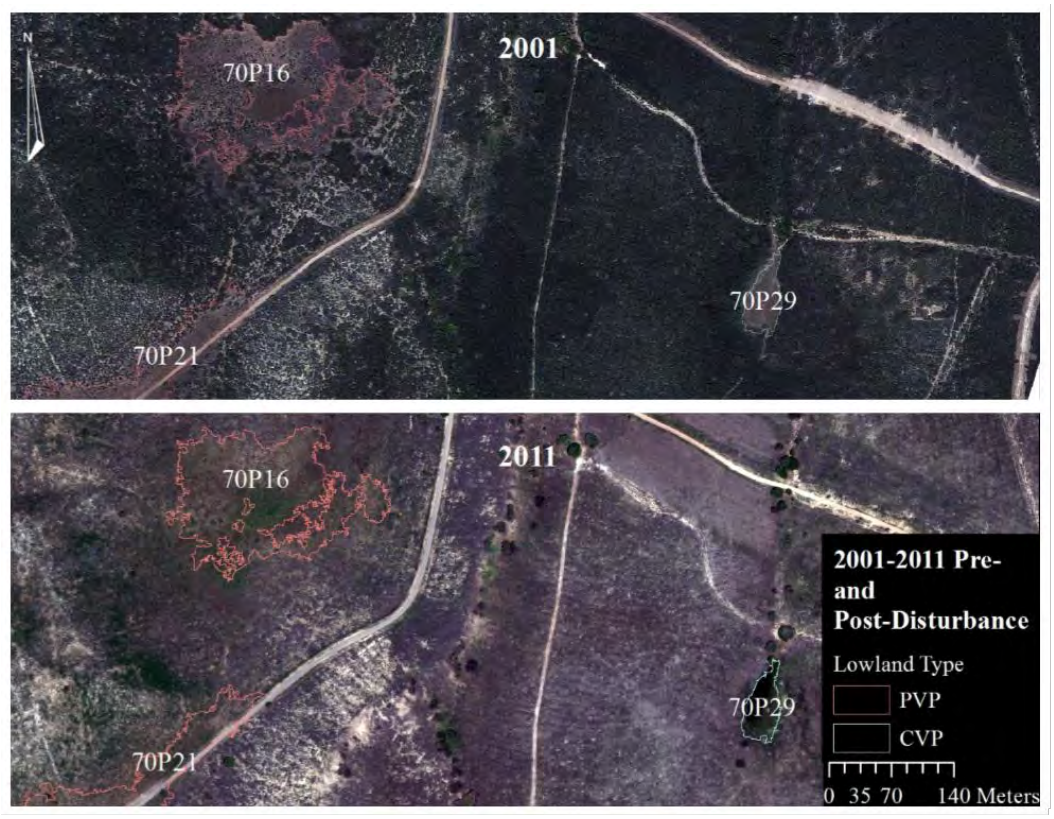

Figure 21: Landscape Conversion to Disturbance, from 2001 to 2011

The WV2 imagery presented a unique set of challenges for OBIA because widespread disturbance effects were visible throughout the study area (Figure 21). The disturbances were due to recent prescribed burns and manifested in a gradient of immature upland vegetation. The most recent and severe disturbances were concentrated at the northeast corner of the study area. Within the disturbed zone, immature upland chaparral graded from youngest to oldest in a westerly direction, echoing the chronology of the previous decade's land management practices. The total area of Fire Break/Burn class grew from an estimated 155.62 ha (384.54 acres) in 2001 to 1,350.32 ha (3,336.73 acres) in 2011, nearly an order of magnitude increase. In 2011, Fire Break/Burn coverage increased to about 52% of the study area, up from a modest 6% in 2001.

As so much of the study area had been mowed, masticated, or burned in the 10-year interval between datasets, the classification scheme was necessarily arbitrary. The most reasonable course of action was to set a criteria for minimum growth years, and place any areas that failed to reach the age-restriction into the Fire Break/Burn category. Doing so meant that, in 2011, FB was a class that included upland, lowland, invasive, and transitional vegetation. Segments not already classified as Oak Tree, Bare Ground/Dirt Track, Paved Road, or Water were classified into the FB class wherever they intersected a polygon shapefile of relevant controlled burn sites, or otherwise contained indicative visual cues (e.g. an obvious recent vegetation disturbance).

While painstaking care was applied to ensure the most accurate OBIA possible, the arbitrary nature of the FB class seems to have led to another overestimate of the procedure's performance. Like the results from 2001, the 2011 error matrix showed a similar, but less extreme tendency toward confusing FB with BG. The other classes again exhibited overestimated accuracies of 100%. The estimated overall accuracy of 99.56% is therefore believed to be higher than the true value as well.

4.2 Statistical Results

The Patch Analyst extension was used to derive the base geometry metrics described in Chapter 3, Section 6 (Area, Perimeter, PAR, SI, and FD), which were then used calculate PI, WIPI, percent area change, and percent perimeter change. Metrics were computed per lowland complex, for each year of analysis.

Since so many PVP areas were eliminated from the 2011 classification, the full short- and long-term analyses were not comparable. Therefore, the statistical analysis for each was conducted differently. For the 70-year interval, sufficient PVPs (n = 26-31, depending on

outliers) and CVPs (n = 16) were available to be able to compare the two as separate groups through independent samples t-tests. At the 10-year scale, there were not enough PVPs (n = 5) to enable their inclusion. Instead, 14 self-same CVPs were compared using dependent samples t-tests. Two sites, 70C29 and 80C11, presented water features but were eliminated because they were within burn areas. In this manner, a short- and long-term comparison of geometric changes in CVP sites was achieved. For PVP sites, only a comparison between these and CVP sites at the 70-year scale was possible. The results are summarized below, and a series of maps documenting more complete results are included in the appendices at the end of this document.

4.2.1 70-Year CVP/PVP Comparison

To evaluate CVP and PVP at the 70-year time scale, the two populations were compared using independent samples t-tests. Metric values measured in 1941 and again in 2001 were used to calculate the change in each for every site. The analysis included the following six metrics:

1) Change in Fractal Dimension (Δ_FD)
2) Change in Shape Index (Δ_SI)
3) Change in Perimeter-to-Area Ratio (Δ_PAR)
4) Percent Area Change (%Δ_AREA)
5) Percent Perimeter Change (%Δ_PERI)
6) Log base 10 of Persistence Index (Log(PI))

Area change and perimeter change were expressed in terms of a percentage to normalize them, since they do not scale equally. Persistence indices were transformed into normal distributions by a base 10 logarithmic transformation with a positive shift of 0.25. Table 6 provides the full set of group statistics. Table 7 summarizes the t-test results, including Levene's Test for Equality of Variances. The remaining graphical outputs, such as the box and whisker

Table 6: Group Statistics for 70-Year CVP/PVP Comparison

Metric	Type	N	Mean	Std. Deviation	Std. Error Mean
Δ_FD	PVP	31	.0342	.1101	.0198
	CVP	17	.0546	.0886	.0215
Δ_SI	PVP	31	.9358	1.6836	.3024
	CVP	17	1.0426	1.4661	.3556
Δ_PAR	PVP	28	.0150	.0792	.0150
	CVP	16	.0168	.0418	.0105
%Δ_AREA	PVP	26	22.7111	50.4222	9.8886
	CVP	17	33.5210	45.2974	10.9862
%Δ_PERI	PVP	27	40.1622	53.0898	10.2171
	CVP	17	65.7299	67.5221	16.3765
Log(PI)	PVP	29	-.3612	.2871	.0533
	CVP	16	-.2874	.1879	.0470

Table 7: Independent T-test Results for 70-Year CVP/PVP Comparison

		Levene's Test for Equality of Variances		t-test for Equality of Means						
									95% Confidence Interval of the Difference	
	Equal Variances	F	Sig.	t	df	Sig. (2-tailed)	Mean Diff.	Std. Error Diff.	Lower	Upper
Δ_FD	Assumed	.725	.399	-.655	46	.516	-.0204	.0311	-.0830	.0423
	Not			-.698	39.477	.489	-.0204	.0292	-.0794	.0386
Δ_SI	Assumed	.420	.520	-.219	46	.827	-.1067	.4863	-1.0856	.8721
	Not			-.229	37.148	.820	-.1067	.4668	-1.0524	.8389
Δ_PAR	Assumed	2.298	.137	-.081	42	.936	-.0017	.0212	-.0449	.0414
	Not			-.095	41.848	.925	-.0017	.0183	-.0386	.0351
%Δ_AREA	Assumed	.039	.844	-.715	41	.479	-10.8099	15.1233	-41.3520	19.7322
	Not			-.731	36.919	.469	-10.8099	14.7811	-40.7616	19.1418
%Δ_PERI	Assumed	1.524	.224	-1.400	42	.169	-25.5676	18.2689	-62.4358	11.3005
	Not			-1.325	28.246	.196	-25.5676	19.3023	-65.0911	13.9559
Log(PI)	Assumed	3.214	.080	-.923	43	.361	-.0738	.0800	-.2351	.0875
	Not			-1.039	41.572	.305	-.0738	.0711	-.2173	.0696

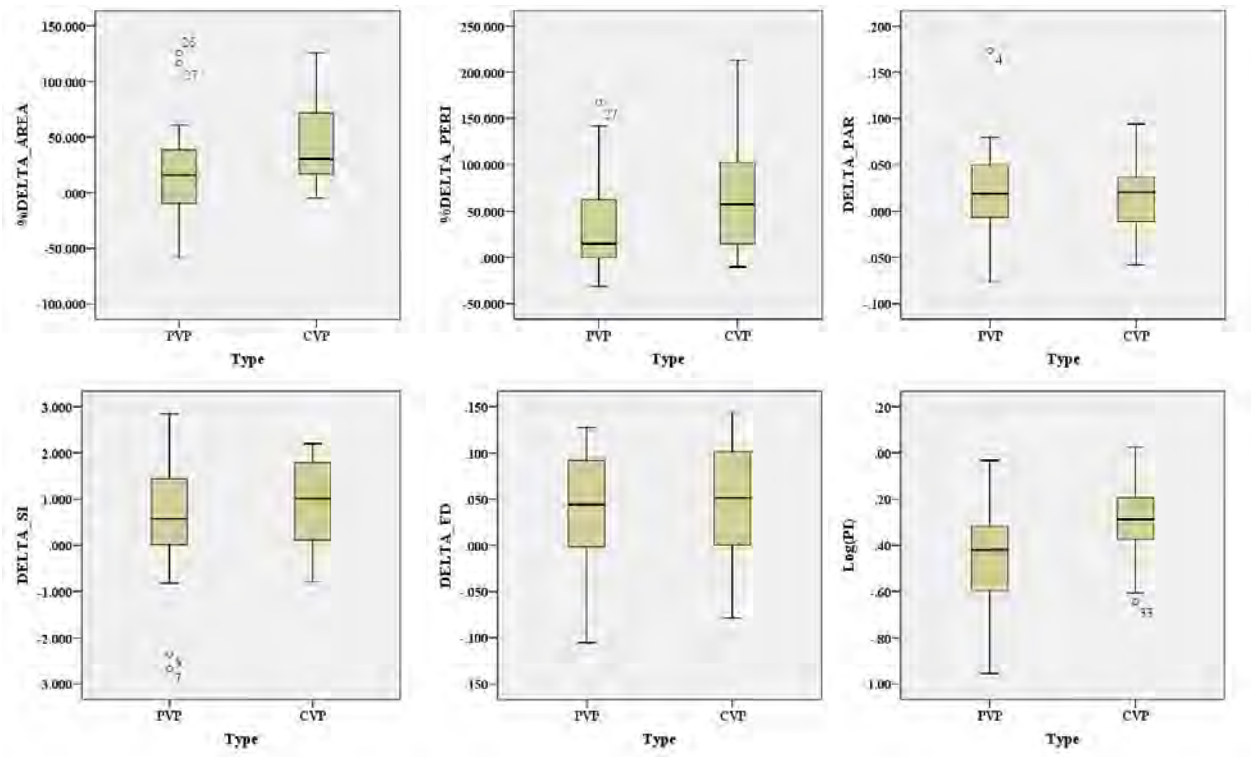

Figure 22: Box and Whisker Plots with Outliers, Comparing PVP to CVP, for Each Analyzed Metric

plots shown in Figure 22, are included in the appendices and were used to help ensure that each population met the assumptions of normality. The boxplots show the range of values for PVPs (leftmost box in each plot) and CVPs (rightmost box), for each metric analyzed in the study. The horizontal black bars represent, in order from lowest to highest, the minimum observed value, the first quartile, the median, the third quartile, and the maximum observation. The box itself highlights the interquartile range, while the small black circles depict outliers. Extreme outliers were removed prior to the final analysis.

The most important statistics provided are the means, standard deviations, and standard error means from Table 6, along with the p-values given by the Levene's Significance and the t-test Significance (2-tailed) in Table 7. A significant Levene's statistic ($p \leq 0.05$) would indicate that the assumption of equal variances was violated, necessitating the use of lower rows of values

(labeled "Not"). However, equal variances were met across all categories, so the upper rows (labeled "Assumed") were used. For values of Significance (2-tailed), a p-value of 0.05 or less would have indicated a significant difference in the PVP and CVP means.

There were no data categories with a statistically significant 2-tailed p-value at a 95% confidence interval. In fact, no metric would have passed at a 90% confidence interval either. The means, standard deviations, and standard error means appear to be comparable between site types as well, particularly for the transformed PI and the changes in FD, SI, and PAR. The percent changes in area and perimeter were non-significant as well, but did display greater relative discrepancies. Nonetheless, by the metrics and methods applied here, the CVP and PVP populations are indistinguishable from the vantage point of geometric change.

4.2.2 Short- and Long-Term Changes in Self-Same CVP Sites

CVP were compared to themselves in order to check for geometric instabilities that might have been discoverable at a finer temporal scale. The reasoning was that environmental variability might cause lowland boundaries to exhibit short-term spatial dynamism, with them eventually converging to a mean location as a result of geographic restrictions. Water could be the cause of such a restriction, but drought and climate instability might lead to variation only evident on shorter time scales.

Since the 2011 image contained so few PVP sites, a comparison using these data would have led to a dataset that was too small to be analyzed. To ensure a larger sample size, PVPs were eliminated from the short- and long-term comparison. The remaining CVPs were matched against their self-same sites, and compared at 10- and 70-year intervals. The change in approach necessitated a shift from independent to dependent sample t-tests. Logarithmic transformations similar to those previously described were used to create normal distributions, and the Weighted

Intervals Persistence Index was substituted for the non-weighted PI to normalize for interval length:

1) Log base 10 of change in FD, 10-year minus 70-year (Log(ΔFD10) – Log(ΔFD70))
2) Log base 10 of change in SI, 10-year minus 70-year (Log(ΔSI10) – Log(ΔSI70))
3) Log base 10 of change in PAR, 10-year minus 70-year (Log(ΔPAR10) – Log(ΔPAR70))
4) Percent Area Change, 10-year minus 70-year (%ΔAREA10 – %ΔAREA70)
5) Percent Perimeter Change, 10-year minus 70-year (%ΔPERI10 – %ΔPERI70)
6) Weighted Intervals Persistence Index, 10-year minus 70-year (WIPI_10 – WIPI_70).

The results of this part of the analysis are harder to interpret, mainly because they seem to conflict with one another. The group statistics given in Table 8 show that, on average, CVP area decreased over the shorter but increased over the longer of the two intervals. Interestingly, perimeter change increased over both intervals instead of similarly decreasing over the short-term. Percent area and percent perimeter change are cumulative, so the absolute value of either mean would be expected to greater over the longer interval. Area should change the most, as it scales faster in both directions when a polygon changes size. Accordingly, it is unclear how mean perimeter grew while mean area shrunk over the short interval. WIPI, on the other hand, was stable across both time periods.

The primary values of interest for the results of the dependent sample t-test presented in Table 9 are found in the significance (2-tailed) column. Like the previous t-tests, a 95% confidence interval for detecting differences in means is indicated by $p \leq 0.05$. Not surprisingly, percent area and percent perimeter changes showed significant differences between the two time intervals ($p = 0.003$ and $p = 0.018$, respectively). Even slow growth (positive or negative) would eventually lead to the same kinds of results. By contrast, low, stable WIPI values over both

Table 8: Group Statistics for Short- and Long-term Self-Same CVP Comparisons

Pair	Mean	N	Std. Deviation	Std. Error Mean
Log(ΔFD10) – Log(ΔFD70)	-.0775	14	.0239	.0064
	-.067	14	.0476	.0127
Log(ΔSI10) – Log(ΔSI70)	.2076	14	.6954	.1858
	.4160	14	.2363	.0632
Log(ΔPAR10) – Log(ΔPAR70)	-1.0979	14	.2253	.0602
	-1.2209	14	.5270	.1409
%ΔAREA10 – %ΔAREA70	-6.5806	14	15.6050	4.1706
	41.3330	14	43.3527	11.5865
%ΔPERI10 – %ΔPERI70	15.6284	14	33.6389	8.9904
	77.4321	14	65.7887	17.5828
WIPI_10 – WIPI_70	.0501	14	.1330	.0356
	.0474	14	.0333	.0090

Table 9: Dependent Samples T-test Results for Short- and Long-Term CVP Comparisons

				Paired Differences				
							95% Confidence Interval of the Difference	
	t	df	Sig. (2-tailed)	Mean	Std. Deviation	Std. Error Mean	Lower	Upper
Log(ΔFD10) – Log(ΔFD70)	-.670	13	.514	-.0106	.0591	.0158	-.0447	.0235
Log(ΔSI10) – Log(ΔSI70)	-.935	13	.367	-.2084	.8343	.2230	-.6901	.2733
Log(ΔPAR10) – Log(ΔPAR70)	.760	13	.461	.1229	.6051	.1617	-.2265	.47233
%ΔAREA10 – %ΔAREA70	-3.693	13	.003	-47.9136	48.5477	12.9749	-75.9442	-19.8830
%ΔPERI10 – %ΔPERI70	-2.714	13	.018	-61.8037	85.2204	22.7761	-111.0085	-12.5989
WIPI_10 – WIPI_70	.066	13	.949	.0027	.1532	.0410	-.0858	.0912

intervals are likely attributable to an overall stability in size and shape. Put another way, a small WIPI means that the spatial appearance of a shape has changed little over time. When the 10-year and 70-year WIPI means are so similar ($p = 0.949$), and so small ($\overline{X}_{10} = 0.0501$, $\overline{X}_{70} = 0.0474$), the interpretation is that size and shape are temporally fractal. That is, regardless of the length of the time interval, the sizes and shapes of the polygons appear unchanged.

The most vexing results are the non-significant differences between intervals in the FD, SI, and PAR change tests. Since the datasets were log transformed, their means are not useful in understanding the directionality of the changes. However, since each is also a cumulative metric, a longer interval should result in more change. Counterintuitively, similarity in FD, SI, and PAR changes over both intervals means that change was happening more quickly during the shorter time period. Such a result supports the idea that short-term dynamics are juxtaposed with long-term stability.

4.2.3 Performance of PI and WIPI

The Persistence Index equation was created to provide a useful description of wholesale changes in polygon dimensions, including area, shape index, and fractal dimension. The Weighted Intervals Persistence Index makes it possible to compare PI values across unequal time intervals. The Persistence Index equation minimizes the effect of minor changes so that major changes stand out more. PI can be likened to the human eye, which is able to gloss over minor differences in a polygon to see that the underlying shape is still the same.

In the first analysis, the performance of PI was in keeping with the other results. The logarithmic transformation came at the price of lost directional knowledge because all the PI values were first shifted to ensure none were less than zero. The shift was necessary to perform the transformation, but it also filtered out information about whether change was in the form of

expansion or contraction. Still, the finding that the PVP and CVP groups were not different was consistent with the findings of the analysis at large. Conversely, the results of the second analysis were cryptic. With the other results pointing to an overall increase in change over the short-term, the absolute value of WIPI would be expected to increase too. Yet the differences between the two intervals was non-significant. The 10- and 70-year WIPI values are mapped in Figures 23 and 24. The WIPI results can easily be reconciled with the area and perimeter results because the latter two are cumulative while the former is not. Since WIPI is normalized for the effects of time, it effectively tracks the change rate while area and perimeter changes are considered in gross. Hence a constant rate of change would give both a constant WIPI and changes in area and perimeter.

Reconciliation between WIPI and the other metrics is challenged by the fact that the index describes a slow, constant rate of change. FD, SI, and PAR changes indicate a different trend. They instead show that change appears to have sped up over the 10-year period. The reasons for the discrepancy in the results are unknown. One possible explanation is that WIPI is less sensitive to small changes in metric values that are more easily discerned by one of the more focused metrics.

4.3 Flyover Observations

Even the highest resolution aerial photography cannot substitute for the understanding an *in situ* visit can impart. Despite the fact that a request for ground access to the study sites was denied, the airspace above Fort Ord is not restricted and low-altitude flyovers are permitted. The primary goal in performing a flyover was to put real eyes on the study sites. Since the only vernal pool visible from a public road was inundated at the time of this study, there seemed to be

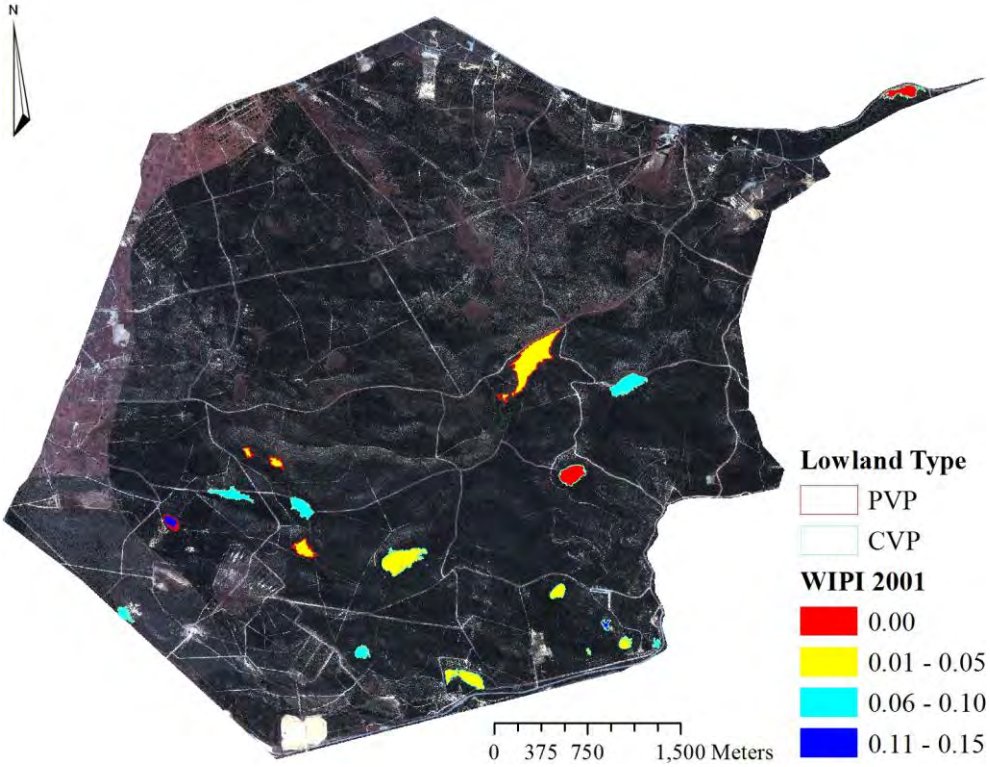

Figure 23: 70-Year WIPI for Self-Same CVP Sites

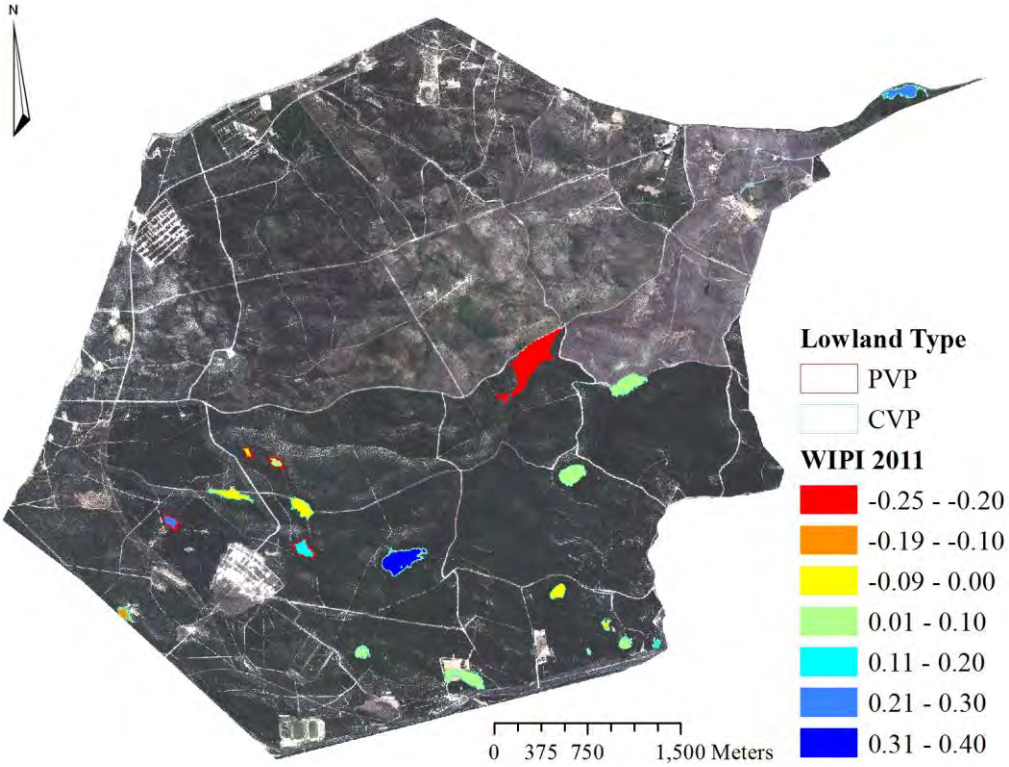

Figure 24: 10-Year WIPI for Self-Same CVP Sites

Figure 25: Erosion Scars Assisted in the Confirmation of Site ID# 80P07 as a CVP (Photo Credits: C. Hanley)

a reasonable possibility of other sites being inundated as well. The flyover was the only opportunity to collect ground evidence to verify classification results.

During the flight, there were seven CVP sites noted with visible water surfaces, along with an eighth site possessing a large erosion gully leading directly into its center. Of the seven sites with water in them, two were CVP confirmed for the first time during this study. The eighth site was a PVP that had a detectable water feature in 2011 to go along with the erosion drainage evident during the flyover, the combination of which was compelling enough to cause the type to be switched to CVP prior to the final SPSS analysis. Figure 25 shows the erosion feature (circled in red) in the eighth site (ID# 80P07) from opposite angles, with the aircraft wing visible in the foreground of the photo on the left.

Overall, the flyover confirmed several ideas that were considered during data exploration. First, one of the justifications used for reassigning PVPs as CVPs was the frequency of water sightings. The observation was made that certain PVPs had confirmed water features more often

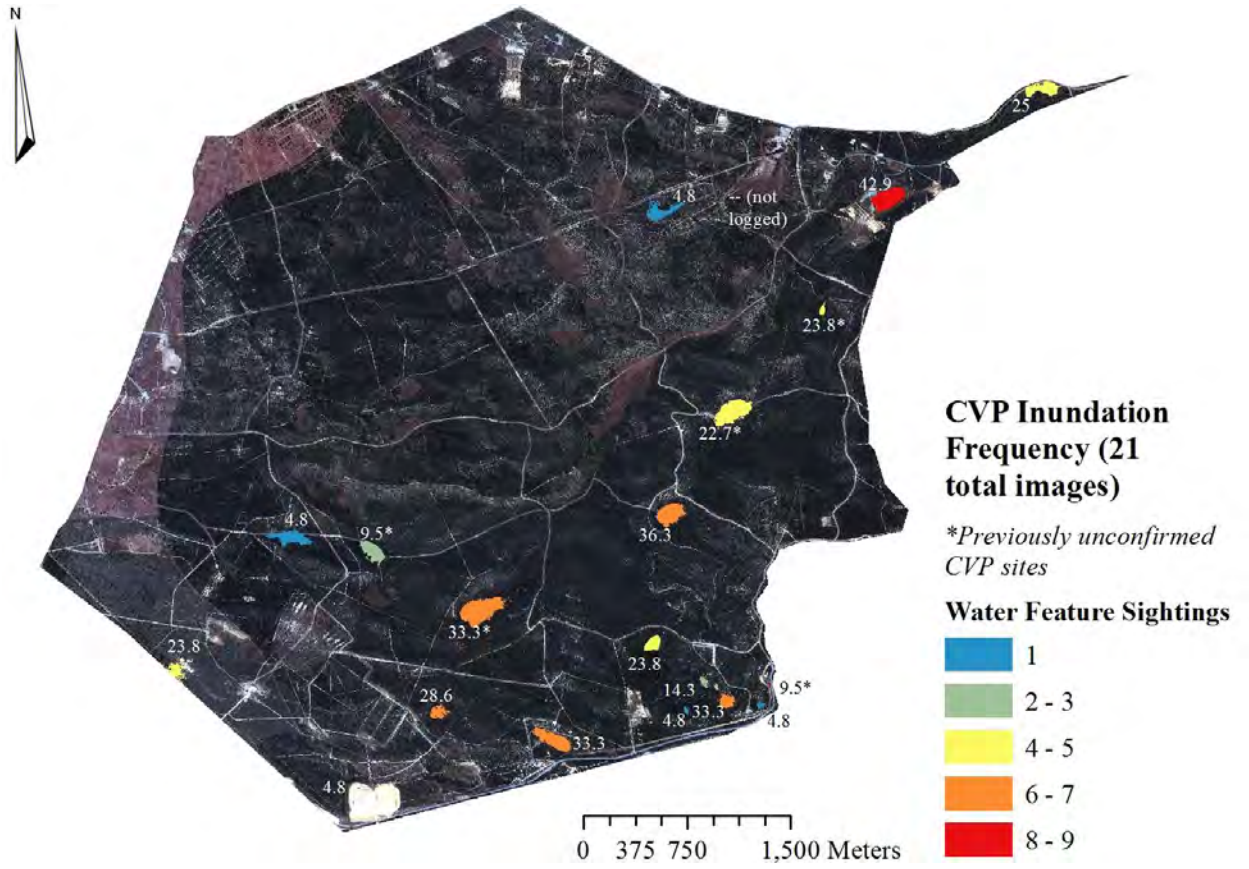

Figure 26: Inundation Frequencies, Compiled from a Review of 21 Historic Aerial Images

than some known vernal pools. By extension, it was also obvious that inundation did not occur equally across the landscape, nor predictably with time. In other words, there appeared to be no relationship between the filling of one pool and the filling of another in a given photo. The flyover substantiated the idea that some pools fill more often than others, or at least hold water for longer. Notably, when not inundated, CVP look superficially similar to PVP. Total inundation frequencies were calculated after the flyover for 21 historic and contemporary images (including flyover data), the results of which are presented in Figure 26.

A few PVPs, particularly toward the western margins, appeared to be converting into uplands. Most, however, were verdant grasslands that visibly stood out amongst the various age classes of chaparral. By the time of the flyover, around 75% of the study area's mature chaparral

Figure 27: CVP Site 80C01 Timeline Showing Persistent Dead Transition (DT) Vegetation Band (Data Sources: Google Earth 2015; DigitalGlobe Foundation 2014; US Army BRAC 2014)

had been removed. After burning or mastication, the only vegetation left standing were oak trees. Based on photographic evidence, it will take an estimated 8–10 years for the study area to return to a measurable state again, and 2–3 times as long as that for the chaparral to reach full maturity, when it can become decadent and exceed 5 m in height.

Unfortunately, the flyover did not settle matters of identifying invasive and dead transition species. The expedition did nothing to refute the assertion that the invasive class contained only pampas grass and ice plant, but neither did it provide confirmation. Dead transition vegetation, on the other hand, was given this name for the lack of a better description. The only new information provided by the flight was that dead transition appears to come from a taller species than first anticipated. The consistent shape and size of the DT band around some CVP is so striking that it almost looks artificial (Figure 27). At the risk of being speculative, it seems at least plausible that DT is a remnant of very old chaparral that was never removed during previous land management regimes. A mechanical clearing of the surrounding brush

Figure 28: Major Erosion Scars Divert Surface Waters within the Study Area (Photo Credits: C. Hanley)

could account for the smooth shape and consistent size, with the cleared areas slowly maturing into healthy chaparral again while the remaining plants buffering the lowland eventually senesce and die.

Certainly, vegetation removal is not the only anthropogenic scar visible on the landscape. The flyover revealed that wide, deep erosion gullies now crisscross the study area. These gullies, visible as ragged gashes in Figure 28, clearly alter the way that water flows through the environment, and could be responsible for changing or stopping inundation regimes in nearby lowlands. There also exist many leftover vehicles, buildings, bunkers, and rifle pits spread throughout study area that are sources of pollution, as well as physical disturbances.

CHAPTER 5: DISCUSSION AND CONCLUSIONS

In the Fort Ord study area, lowland complexes are akin to Burnett and Blaschke's "island patch[es] in a sea matrix" (2003, p. 238). For them to exist, they must combat the slow encroachment of maritime chaparral. This thesis pursued the explanation as to why lowland meadows, in the absence of a known vernal pool, are able to persist and not be swallowed up in the sea of upland vegetation by which they are surrounded. The evidence put forth here indicates that the upland-lowland border interactions are spatially stagnant. That is, when not artificially disturbed, they change very little whether measured over short or long time intervals. Lowland grasses do not invade manzanita or chamise chaparral, likely because the shrubs are allelopathic and poison the surrounding soils (Van Dyke, Holl, and Griffin 2001). On the other hand, persistent annual hydric cycles are the most plausible explanation as to why chaparral is repelled from the vernal and non-vernal pool lowlands with equal vigor.

According to the data presented here, the border interactions that vernal and non-vernal pool lowlands have with upland chaparral are similar, in terms of their spatial context. The empirical numbers confirm the observation that CVPs and PVPs are more than just superficially similar. PVPs respond in similar ways to the same environmental pressures as CVPs. That is not to suggest that all PVPs in the study are really vernal pools. Rather, vernal pools are probably common amongst the PVP group, in order for them to exhibit such holistic similarities to CVPs. To be sure, directly spotting water or visiting a site in person are the best, if not the only, ways to confirm that a PVP site is actually a vernal pool. Nonetheless, the evidence suggests that most of the PVP sites must at least exhibit damp soil conditions that favor the

development of grasslands, while simultaneously repelling upland vegetation. A few may actually display surface pools of water under the correct climatic conditions, although this is speculation based on suggestive but ultimately inconclusive visual evidence. Since the region is currently in the midst of a severe and prolonged drought, the likelihood of ascertaining the truth in the near future is low. If disturbances have re-routed water away from areas that were once vernal pools, they may now be relict or dormant instead. Dormancy is nevertheless reversible, so it is worthwhile to examine the feasibility of restoring the ecological potential of such areas.

In the field of ecology, it has been said that when the same phenomenon occurs in two places, the root cause is likely the same. Similarly in geography, the closer two instances of a phenomenon are in space, the more similar they are likely to be in character. Bearing these adages in mind, a collective of logic, observation, and empirical evidence stand in support of the assertions made in the closing paragraphs of this document. What follows now is the final discussion of the meaning behind the results this study produced. Though there are multiple possible interpretations, the principle of parsimony (Occam's razor) instructs that the simplest, most succinct explanation is the best. In this case, the best explanation is that water is the driving environmental force behind lowland vegetation patterns in Fort Ord's MRS-BLM zone. The final arguments as to why are presented below.

5.1 On OBIA Accuracy

Converting raw image data into useful intelligence requires considerable domain knowledge of the subject matter being interpreted. Image interpretation demands much technical skill of the analyst as well. Naturally, the results of an image analysis need to somehow be vetted *post-hoc* to judge their quality. Where the object-based extraction algorithms used in this study differ from those typically described in the literature is in the use, or lack thereof, of the nearest

neighbor approach. NN uses object class samples, select feature space components, and a horizontally moving window to evaluate object pixels and their spatial relationships. To reduce the semantic gap, the methods used to segment and classify the Fort Ord imagery employed a higher-degree of supervision than is typical of NN. Consequently, the manual adjustments made to segments and class assignments somewhat negated the efficacy of generating an error matrix, which is better suited to estimate the performance of automatic classification algorithms.

In terms of the accuracy assessment itself, experience has proven that the cohort of samples inputted into a TTA mask can have an effect on the subsequent error matrix. Accuracy is also tied in with segmentation performance and semantic structure, and so is subjective in several ways. In the cases where MO classes were infrequently represented, occupied a small percentage of the total area, or incurred unusual amounts of manual intervention, the trend was to exhibit 100% accuracy. In short, the overestimation of accuracy was likely to occur whenever the sample size was small or the classification not fully-automated. Water features detected in the 2011 data illustrate this principle well, since they were rare and isolated to a few known areas. There was little likelihood of a Type I or II error occurring in the water class because water features were classified manually, and no other objects had mixed water features in them. The segmentation also fared well at determining shorelines—the areas that were most susceptible to errors. It is easy to understand, then, why the Water class had an estimated 100% accuracy. Between the ways the OBIA was conducted and the TTA samples selected, there was virtually no chance of detecting an error, even if it did exist.

While it is clear that a few errors went unnoticed in the accuracy assessment, upon looking at the results with the eye, it is equally clear that very reliable classifications were achieved. Importantly, the boundaries of MO classes with lowland associations were thoroughly

examined and corrected to ensure accurate measurements would be taken. For these reasons, the OBIA results were deemed appropriate for analytical use.

5.2 Comparing 70-Year Changes in PVPs and CVPs

The ability to observe landscape processes in action is limited to the moments when a sensor or an observer are present to record a snapshot. It follows that the study of such processes must rely heavily on whatever evidence is left behind. In this case, since inundation events are inconsistent at best, vegetation patterns were seen to be a good proxy for the presence of water in lowland meadows. As many of the meadows with known vernal pools exhibit long-term spatial persistence in floral patterns, it was inferred that patterns in vernal pool meadows must be different than patterns in non-vernal meadows. Both types of lowland complex are shown on the following page in Figure 29. Suffice to say, if two things are not the same, there must be a way to tell them apart. A belief that this difference exists is what compelled this analysis.

Although CVPs and PVPs are similar in many respects, they do differ greatly in the singularly important category of confirmed water sightings. Notwithstanding the obvious difference, many non-vernal lowlands bear the hallmarks of a hidden hydric soil regime. The initial data exploration uncovered two different types of pattern that were associated with vernal lowlands. One involved the way in which some vernal pools had wide margins of dead vegetation that clearly defined the meadow's perimeter and appeared to never move. This patterning may not be natural since it was not evident in all CVPs, nor in most other lowland study sites, but certain PVPs did exhibit the same conditions. Coincidently or not, these few PVP were subsequently confirmed to be vernal pools after numerous logged water sightings enabled their proper reassignments as CVPs. In so doing, the second type of pattern emerged as the fixed nature of upland/lowland boundaries was observed.

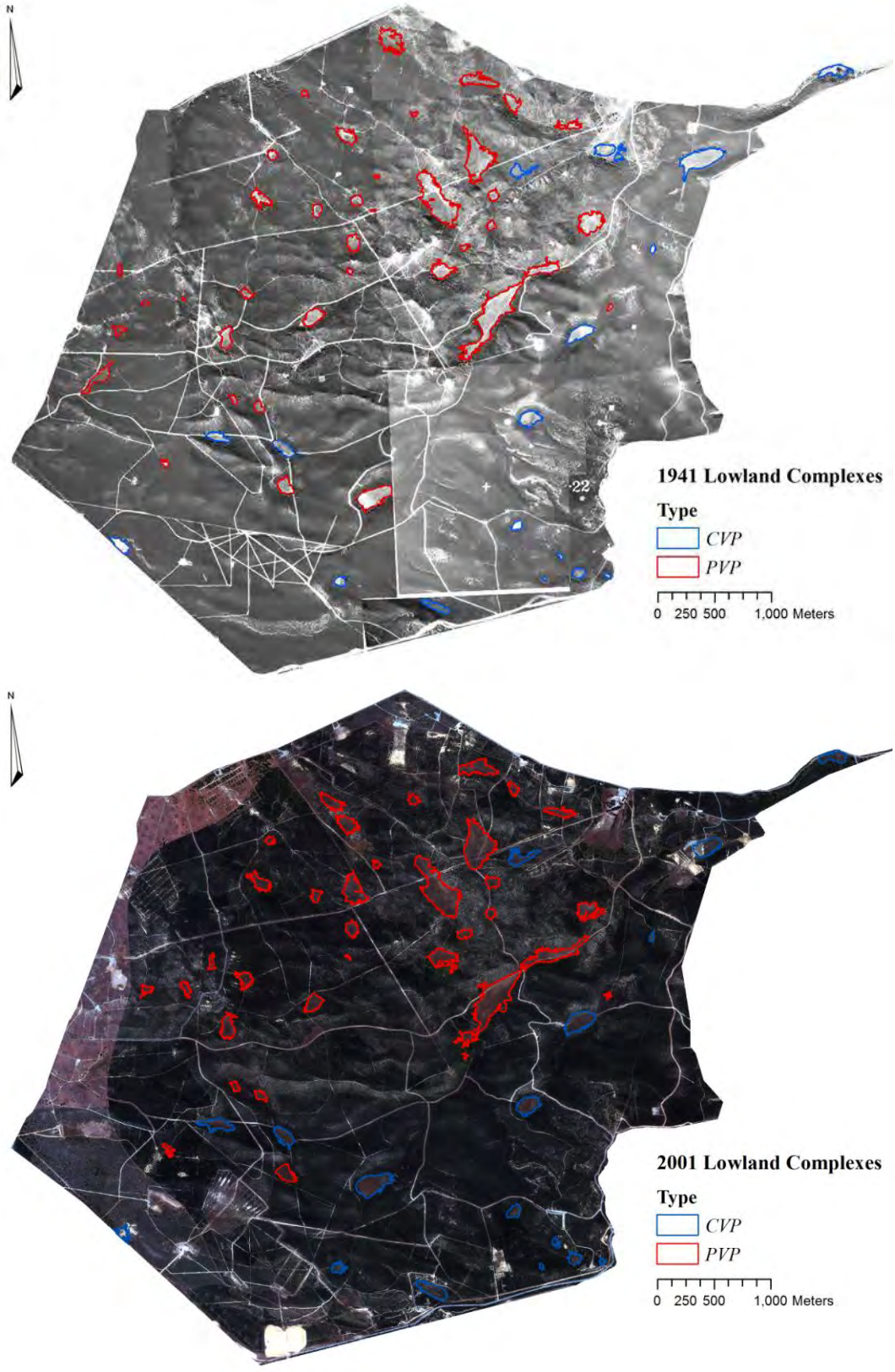

Figure 29: PVP and CVP Complexes in 1941 (top) and 2001 (bottom)

CVPs and PVPs were compared at the population level across six size- and shape-related metrics, using the independent samples t-test. The test compares the means of two populations for a given parameter, provided that the datasets are normally distributed and display equal variances. To accept the hypothesis that CVPs and PVPs in the study area are fundamentally different is to reject the null hypothesis that they are the same. Statistically speaking, rejecting a hull hypothesis with a 95% confidence interval ($p \leq 0.05$) is making the statement that there is less than a 5% probability that the pattern evident in the data is the result of chance. Accepting the null hypothesis does not denote the same thing as does rejecting it, though. The former simply acknowledges that any differences in the two populations are not significant enough to be thought of as different with 95% confidence, while the latter states that, with 95% confidence, the two populations are significantly different. Rejecting a null hypothesis is therefore a stronger statistical statement. That said, accepting the null hypothesis for all of the metrics is a strong result in itself. It is clear that in the context of shape and size changes, statistical differences between the PVP and CVP sites are not evident in these data.

Indeed, there *must* be a difference in plant patterning around meadows containing and not-containing vernal pools. The distributions of 70-year SI and FD differences for CVPs and PVPs were not expected to be similar. That fact that they were not different still supports the original assertion of this thesis though; namely that water is the ultimate arbiter of plant distributions at the upland-lowland interface. The preponderance of evidence presented in the scientific literature supports this notion as well. P-values for SI and FD of 0.514 and 0.397, respectively, suggest these datasets are undoubtedly alike. The similarity is confirmed by the results of the PI t-test. Although a log transformation was required, the p-value of 0.781 underscores the similarity of the two distributions. From these data, there is no reason to suggest

that boundary changes occur differently in PVP meadows than in CVP meadows. These results are compelling, and difficult to attribute to anything other than flooded lowland soils that sharply give way to xeric upland conditions at slightly higher elevations.

5.3 Comparing Short- and Long-Term Patterns of Change in Self-Same CVPs

The rate of change analysis for self-same CVP produced inconclusive results. The meaning behind the results could be something as profound as an unforeseen ecological mechanism, or as mundane as variation in the smoothness of drawn boundaries. Even occasional edge effects caused by road cuts might have been enough to throw off the results (visible as long, thin, whitish features adjacent to several lowlands illustrated in Figure 30, next page). The data provides little insight into what is really happening.

Qualitatively, it is apparent that, year after year, CVPs have similar appearances as past versions of themselves. Some images show that there are locations where stretches of a CVP boundary may move slightly back and forth. There are also almost always well-defined portions of the depression where upland or transitional vegetation break in long, smooth, stationary arcs. The arc-like pool edges appear virtually unmoved over time, the imprint of a flood cycle that has continued for millennia. Mima mounds within pool margins also create small depressions between them that can harbor lesser vernal pools in years that lack enough rainfall to fill the greater pool to capacity. Even though the distributions and characteristics of transitional vegetation vary from pool to pool, there is always a central region that is the flood zone within which only grass can survive. As the neighboring chaparral matures but is unable to encroach upon the flood zone, the vernal meadow appears to be cut into the surrounding brush, as if it has been carved into the land surface itself.

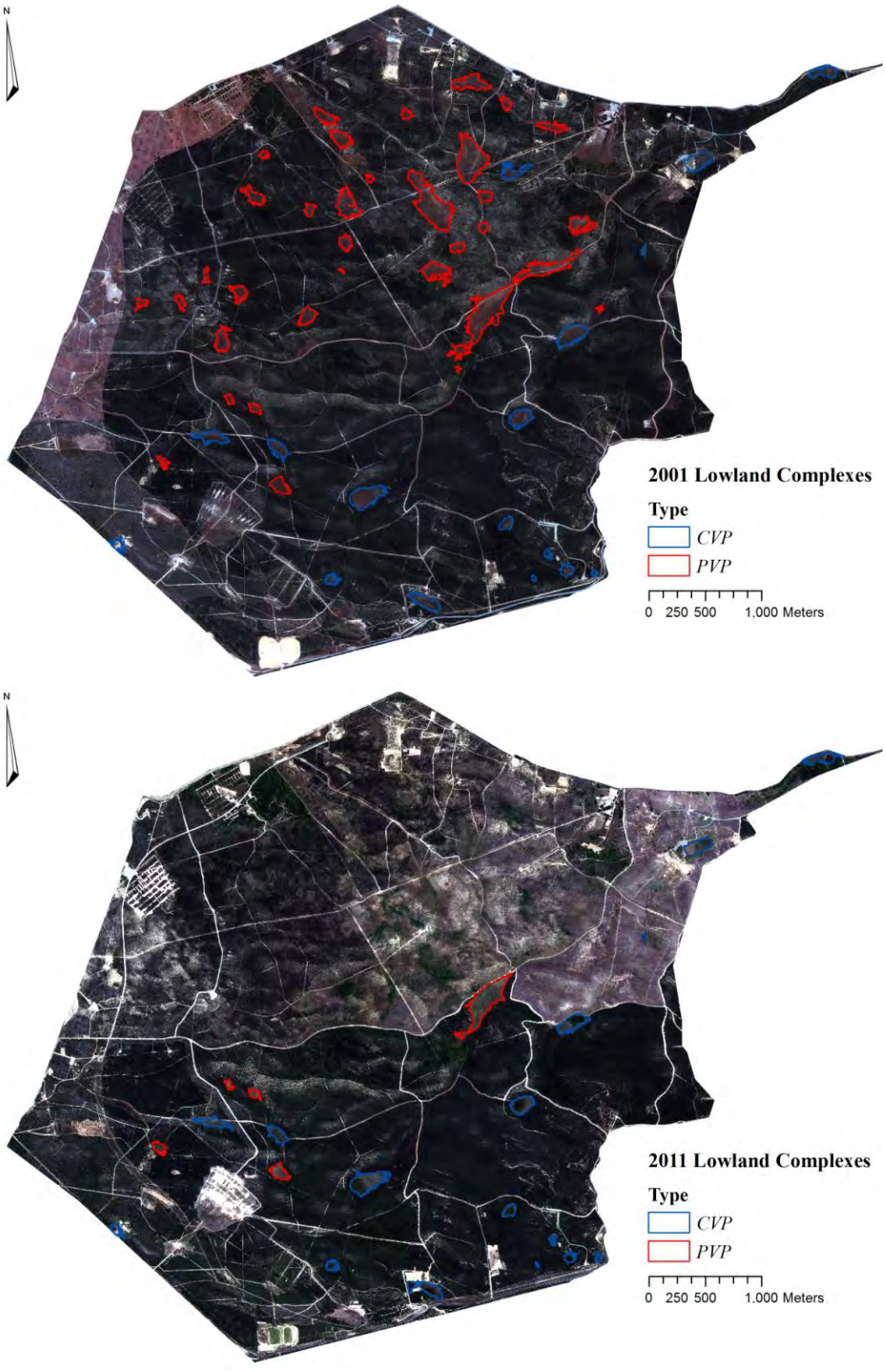

Figure 30: PVP and CVP Complexes in 2001 (top) and 2011 (bottom)

In a very real sense, pool boundaries are inscribed on the landscape. Yet, typical meadows encompass more than just the flood zone. Usually there is a subtly elevated terrace where grasslands eventually grade into transitional or upland vegetation. These elevated areas are presumably affected by the flooding as well. During inundation, the water table rises enough to be above ground in the flood zone, and should be close to the surface at slightly higher elevations nearby. Thus the flooding effects more than just the areas that are visibly submerged. Upland vegetation may suffer as much for being near a pool as it would for being in one. It is logical to assume that, in drier years without surface pools, the water table may still rise enough to create the damp soil conditions necessary to rebuff upland encroachment.

The observed consistency of vernal meadow margins is supported by the mean differences in WIPI, but does not match the results from the other metrics. The performance of PI in the 70-year analysis lends it credibility as a measurement. However, low standard errors and standard error means across the board in the self-same comparison suggest that none of the data is random. Since the visual appearance of the study sites denotes both short- and long-term stability, as does the WIPI t-test result, the sensible conclusion is that CVPs are geometrically stable over an indefinite time frame. The most likely explanation for the remaining results is that they have been interpreted incorrectly, possibly because the relationships between the metrics is more complicated than expected. The numbers are too self-consistent to be discounted, but they also do not match the most obvious explanation. Therefore, there is likely a mistake in final interpretation of the meaning.

5.4 Sources of Error

In any research endeavor, there are opportunities for errors to inject uncertainty into the results. Even in a well-designed study there are avenues by which errors can arise. For instance, the

photographs that were used in this analysis were not perfectly co-registered. It is possible that distortions, particularly in the base photograph from 1941, resulted in classifications that were not true to life at the time. Yet, such an error would actually be all the more reason to accept the results of this study, since unequal distortion across an image would lead to a more randomized pattern of change in the data than was actually present. In regards to the 1941 photo specifically, the individual mosaic tiles were not all of equal spatial resolution. Prior to its use here, however, the entire mosaic had clearly been resampled to a 0.5 m pixel size.

The most likely place for error to have occurred would have been in the image analysis. Both segmentation and classification require thorough examination to eliminate gross errors, but for large rasters, optical revue is only practical on a cursory scale. Fortunately, since lowland meadows and the immediately adjacent upland chaparral were the only targets of the analysis, manually scanning for and correcting errors was feasible. The highest probability for error in the entire study was in the classification semantics and their individual applications. The landscape was much more mixed in the later images than first anticipated, owing greatly to disturbances and successional vegetation. There were instances where determining the proper classification for an object was difficult without ground evidence. Inputs from higher resolution imagery (0.25 m) added marginal clarification, but also led to a point of diminishing returns as the objects became more and more spectrally mixed. In point of fact, a slight reduction in resolution of the segmented image might have improved results more because objects would have appeared more blurry at the edges. The blur would have had an anti-aliasing effect that would generalize the appearance of objects and their boundaries. Increasing resolution does the opposite; objects turn spectrally intricate and become fractal at their edges.

Resolution discrepancies may have also accounted for the unexplained growth in mean perimeter that contrasted with the shrinkage of the mean area for CVPs at the 10-year interval. The higher resolution image acquired in 2011 made it possible to more accurately segment the irregular edges of many meadows, which would have had a much greater effect on measures of perimeter than area. Moreover, this effect was probably exacerbated by minor changes in plant composition at meadow boundaries.

Another problem related to boundary edges come from edge effects. Edge effect, in essence, is the influence an environmental type has on its neighbors, which typically penetrates some distance into the neighboring landscapes and affects their ecosystems. There are two potential manifestations of edge effect that were probable in this study. The first, the edge effect happening at lowland/upland boundaries, was the primary focus of this research. Where the slope angle was the steepest, the edge effect was narrow. Simply put, the transitional band between upland and lowland vegetation had a thin width when the soil moisture gradient (i.e. slope angle) was steep. When the slope angle was lower, as was often the case in the upper terrace of a meadow, the soil moisture gradient was obviously shallower and the transition band was wider and visibly more diverse. The identities of transitional flora were not known for certain at the time of this writing, making it difficult to create an adequate name in the classification scheme. Suspected constituents included annual and native grasses, sandmat manzanita (*A. pumila*), chamise, Monterey ceanothus, poison oak (*Toxicodendron diversilobum*), ice plant, and pampas grass.

The other type of edge effect of concern here is evident in areas where a road has been maintained close enough to the boundary of a lowland to become part of the edge itself. Most of the time, the road is cut just inside or just outside of a boundary, as opposed to right up against it.

Either way, the result is sometimes a narrow band of upland sandwiched between a road and a lowland, or vice versa; both grass and chaparral that are caught in the middle are subjected to extra environmental pressure from the isolation and the nearby road. In the end roads were not judged to be problematic enough to account for them in this study, but they easily could have contributed some error, especially to falsely support the findings of geometric stability presented herein.

The true identities of the lowland grasses might also be a source of error, as there is undoubtedly some mixture of non-vernal, non-native species combined with natives. The native grasses themselves may be of either vernal or non-vernal varieties, as well. Since this study treated all grasses equally, there is a deeper level of granularity to be sought after. Imagery was available to this study with sufficiently high accuracy to identify individual grass and possibly even indicative wildflower species. Such an effort in the future could provide definitive evidence for vernal pool presence in the absence of water, yet was unachievable here because commensurate ground evidence did not exist and could not be acquired.

Finally, the ground evidence that was captured during the flyover brought to light a type of classification error that was unanticipated. The severity of erosion gullies, and their ostensible coincidence with roads and trails, made it clear that many of the linear structures classified as Bare Ground/Dirt Track were better classified into a separate erosion category. Yet, since Bare Ground was not considered in the statistical analysis, unclassified erosive features probably did not skew the results. At the same time, there can be no question that the true classification accuracies for the 2001 and 2011 analyses were marginally lower than estimated.

5.5 Final Thoughts

There exists a phenomenon that prevents chaparral and oak trees from encroaching upon the bottoms of lowland depressions in the Fort Ord study area. For known vernal pools, the reason is self-evident. The cyclical presence of water in the form of seasonal flooding prevents upland vegetation from competing in the lowland areas. Thus the vernal lowlands are able to exist as grassy meadow islands surrounded by a dense matrix of manzanita and coast live oak.

This study has provided reasonable argument that a similar hydric process is occurring in many of the other lowland sites as well. Five previously unrecognized vernal pools have been discovered and reported for the first time here (Figure 31). Each of these sites now requires consideration as protected wetland habitat for California tiger salamander, fairy shrimp, and Contra Costa goldfields wildflowers. Tiger salamanders in particular require a 2 km upland habitat buffer, so the importance of these findings should not be overlooked.

In addition, a wide variety of empirical and observational evidence has been provided to warrant a more extensive study of the PVP sites at Fort Ord. On average, CVP and PVP margins change about the same amount over time. They both appear as lush and verdant grasslands during the spring if no water features are present, and each repels the encroachment of upland vegetation equally well. The similarities between PVPs and CVPs are noteworthy.

A strong case has been made that there remain vernal pools in the Fort Ord study area that are as yet unrecognized. Other PVPs studied here could be the remnants of lost vernal pools, having suffered too much nearby disturbance to become vernally active of late, but maintaining a hydric soil cycle that keeps them still thriving as grasslands. This study was unable to identify relict CVPs specifically without seeing an inundation event or collecting ground evidence *in situ*. In the absence of direct confirmation, future studies should focus

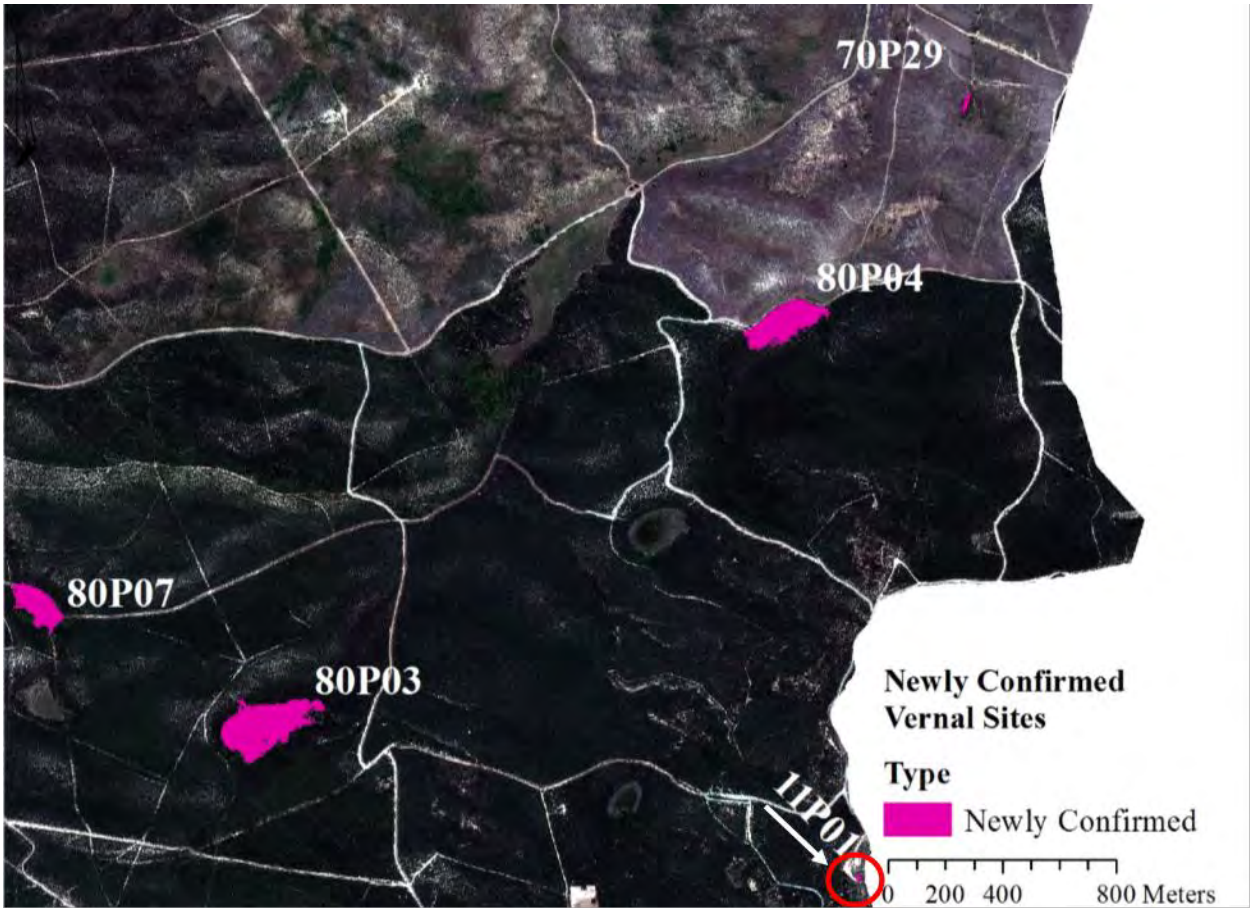

Figure 31: Five Previously Unconfirmed Vernal Sites within MRS-BLM

efforts toward assessing the PVPs with similar vegetative persistence as CVP. Such studies would be particularly impactful if they combined soil moisture testing to check for latent hydric potential with observations of flora. Sites identified as having unusually damp soils may be good candidates for restoration efforts aimed at returning the land to a more natural state. Soil samples could also be collected for ground evidence, to be included in a spectral analysis that uses remote sensing data to compare vernal and non-vernal soil compositions.

The remote sensing study of Fort Ord's vernal and non-vernal lowlands presented in this thesis was, to the author's knowledge, the first of its kind. This work presented a method for integrating historic and contemporary remote sensing data with GIS and parametric statistics,

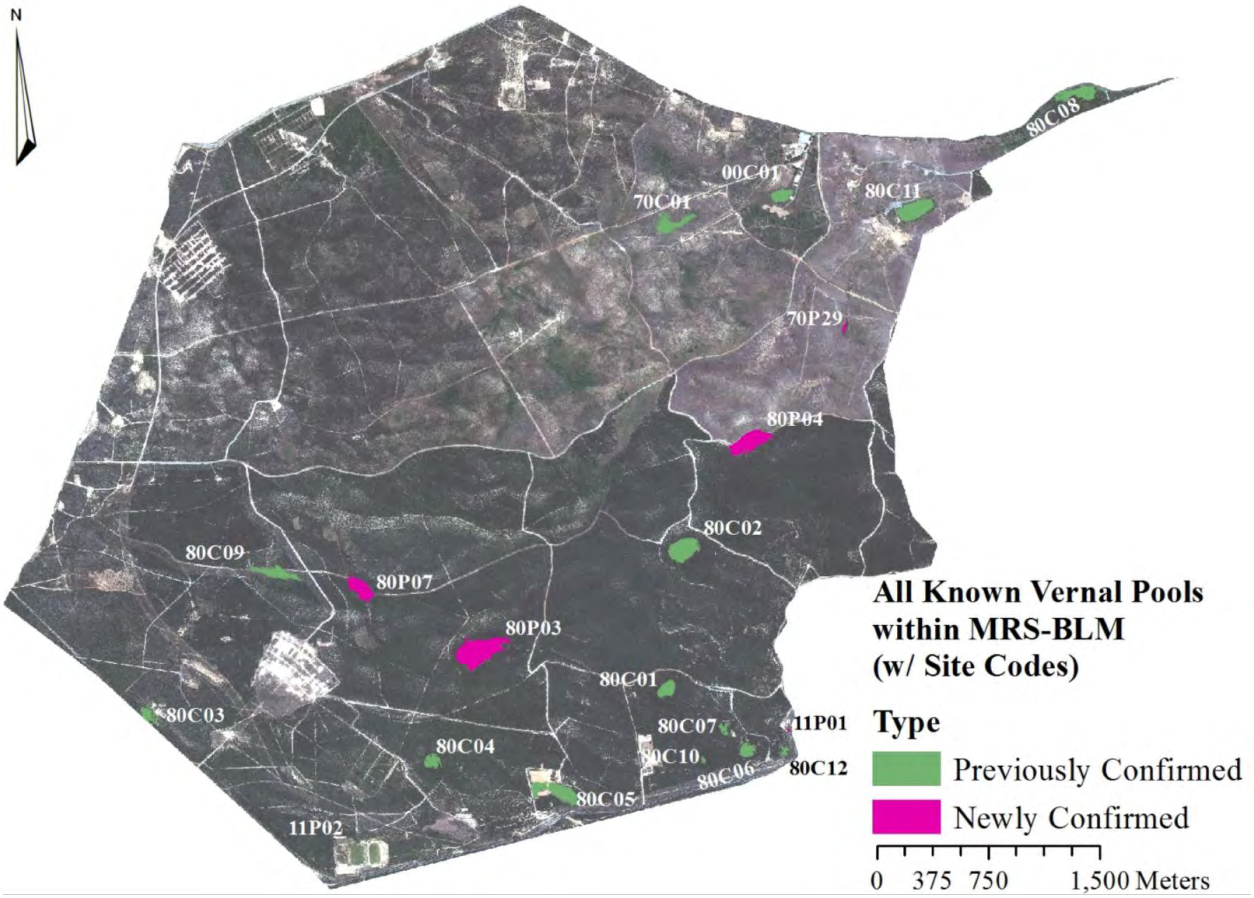

Figure 32: The First Ever Comprehensive Map of MRS-BLM Vernal Sites

to achieve a novel, spatiotemporal perspective on the interactions between upland and lowland plant communities. Additionally, a new metric, the Persistence Index, was created from patch data derived in a GIS. PI was demonstrated to be a valid blanket descriptor of the degree of change in patch geometry. Over a 70-year period at Fort Ord, vernal meadow patches changed about the same amount as non-vernal patches, indicating an underlying similarity between them. Finally, through incidental observation, five new vernal pools were discovered and identified during the image exploration and analysis portion of the study. In Figure 32 these five, along with all 15 other known vernal pools in the impact area, have now been compiled to reveal the first complete map of vernal sites within the MRS-BLM boundaries. The work the map

represents was applied for the first time here, but it should not be the last effort. If the legacy of this project is to simply be a link in the chain that advances the field of spatial ecology with clarity, then it will have achieved its prime directive.

REFERENCES

Andrew, Margaret E. and Susan L. Ustin. 2008. The role of environmental context in mapping invasive plants with hyperspectral image data. *Remote Sensing of Environment*, 112: 4301–4317.

Baatz, Martin and Arno Schäpe. 2000. Multiresolution segmentation: an optimization approach for high quality multi-scale image segmentation. In *Angewandte Geographische Informations-Verarbeitung*, edited by Josef Strobl, Thomas Blaschke, and Gerald Griesebner, XII. Wichmann Verlag, Karlsruhe: 12–23.

Backoulou, Georges F., Norman C. Elliott, Kristopher Giles, Mpho Phoofolo, and Vasile Catana. 2011. Development of a method using multispectral imagery and spatial pattern metrics to quantify stress to wheat fields caused by *Diuraphis noxia*. *Computers and Electronics in Agriculture,* 75: 64–70.

Bagella, Simonetta, Maria Carmela Caria, and Vincenzo Zuccarello. 2010. Patterns of emblematic habitat types in Mediterranean temporary wetlands. *Comptes Rendus Biologies*, 333(9): 694–700.

Bauder, Ellen T. 2000. Inundation effects on small-scale plant distributions in San Diego, California vernal pools. *Aquatic Ecology*, 34: 43–61.

----. 2005. The effects of an unpredictable precipitation regime on vernal pool hydrology. *Freshwater Biology*, 50: 2129–2135.

Barbour, Michael, Ayzik Solomeshch, Carol Witham, Robert Holland, Rod MacDonald, Sarel Cilliers, Jose A. Molina, Jennifer Buck, and Janelle Hillman. 2003. Vernal pool vegetation of California: variation within pools. *Madroño*, 50(3): 129–146.

Blaschke, Thomas. 2010. Object-based image analysis for remote sensing. *ISPRS Journal of Photogrammetry and Remote Sensing*, 65: 2–16.

Burnett, Charles and Thomas Blaschke. 2003. A multi-scale segmentation/object relationship modelling methodology for landscape analysis. *Ecological Modelling*, 168: 2–249.

BLM (Bureau of Land Management). 2010. Vascular plants of Fort Ord. Last modified 10/12/2010. http://www.blm.gov/style/medialib/blm/ca/pdf/hollister.Par.93735.File.dat/FtOrdPlantsAlph12Aug10_c.pdf.

Burleson Consulting, Inc. 2006. Wetland monitoring and restoration plan for munitions and contaminated soil remedial activities at Former Fort Ord. *Prepared for the U.S. Army Corps of Engineers*, Sacramento, CA.

Burne, Matthew R. 2001. Massachusetts aerial photo survey of potential vernal pools. *Prepared for the Massachusetts Division of Fisheries & Wildlife*.

Carpenter, Laurel, Janice Stone, and Curtis R. Griffin. 2011. Accuracy of aerial photography for locating seasonal (vernal) pools in Massachusetts. *Wetlands*, 31: 573–581.

Coburn, Craig and Arthur C.B. Roberts. 2004. A multiscale texture analysis procedure for improved forest stand classification. *International Journal of Remote Sensing*, 25(20): 4281–4308.

Cooper, Daniel S. and Dan L. Perlman. 1997. Habitat conservation on military installations. *Fremontia*, 25(1): 3–8.

Cormier, Tina A. 2001. Statistical and cartographic modeling of vernal pool locations: Incorporating the spatial component into ecological modeling. MS Thesis, University of New Hampshire.

Corcoran, Padraig, Adam Winstanley, and Peter Mooney. 2010. Segmentation performance evaluation for object-based remotely sensed image analysis. *International Journal of Remote Sensing*, 31(3): 617–645.

Cox, George W. 1986. Mima mounds as an indicator of the presettlement grassland-chaparral boundary in San Diego County, California. *American Midland Naturalist*, 116(1): 64–77.

Cutler, Justin Elliot. 2006. Accuracy assessment of high-resolution multispectral satellite imagery for remote sensing identification of wetlands and classification of vernal pool in Eastern Sacramento County, California. MS Thesis, California State University at Sacramento.

Dissanska, Maria, Monique Bernier and Serge Payette. 2009. Object-based classification of very high resolution and panchromatic images for evaluating recent change in the structure of pattern peatlands. *Canadian Journal of Remote Sensing*, 35(2): 189–215.

Drăgut, Lucian, and Thomas Blaschke. 2006. Automated classification of landform elements using object-based image analysis. *Geomorphology*, 81: 330–344.

EMC Planning Group. 2012. Final reassessment report: Fort Ord reuse plan final reassessment. *Prepared for Fort Ord Reuse Authority*, 165 pp.

EMC Planning Group and EDAW, Inc. 2001a. Fort Ord reuse plan, volume I: context and framework. *Prepared for Fort Ord Reuse Authority*, 211 pp.

----. 2001b. Fort Ord reuse plan, volume 4: final EIR. *Prepared for Fort Ord Reuse Authority*, 352 pp.

Fallon, Michael. 2013. Spectral mixture analysis of EO-1 Hyperion imagery in the channeled scablands of Eastern Washington. MS Thesis, Northwest Missouri State University.

Ferren Jr., Wayne R., David M. Hubbard, Sheila Wiseman, Anuja K. Parickh, and Nathan Gale. 1998. Review of ten years of vernal pool restoration and creation in Santa Barbara, California. *Ecology, Conservation, and Management of Vernal Pool Ecosystems—Proceedings from a 1996 Conference*, California Native Plant Society: 206–216.

Fernández-Aláez, Camino, Margarita Fernández-Aláez, and Eloy Bécares. 1999. Influence of water level fluctuation on the structure and composition of the macrophyte vegetation in two small temporary lakes in the northwest of Spain. *Hydrobiologica*, 415: 155–162.

Forestier, Germaine, Anne Puissant, Cédric Wemmert, and Pierre Gançarski. 2012. Knowledge-based region labeling for remote sensing image interpretation. *Computers, Environment, and Urban Systems*, 36: 470–480.

Frohn, Robert C., Ellen D'Amico, Charles Lane, Brad Autrey, Justicia Rhodus, and Hongxing Liu. 2012. Multi-temporal sub-pixel Landsat ETM+ classification of isolated wetlands in Cuyahoga County, Ohio, USA. *Wetlands*¸32: 289–299.

Frohn, Robert C., Molly Reif, Charles Lane, and Brad Autrey. 2009. Satellite remote sensing of isolated wetlands using object-oriented classification of Landsat-7 data. *Wetlands*, 29(3): 931–941.

Gibbes, Cerian, Sanchayeeta Adhikari, Luke Rostant, Jane Southworth, and Youliang Qiu. 2010. Application of object based classification and high-resolution satellite imagery for savanna ecosystem analysis. *Remote Sensing*, 2: 2748–2772.

Gopal, B. 1986. Vegetation dynamics in temporary and shallow freshwater habitats. *Aquatic Botany*, 23: 391–396.

Gordon, Sarah P., Christina M. Sloop, Heather G. Davis and J. Hall Cushman. 2012. Population genetic diversity and structure of two rare vernal pool grasses in central California. *Conservation Genetics*, 13: 117–130.

Grant, Evan H.C. 2005. Correlates of vernal pool occurrence in the Massachusetts, USA landscape. *Wetlands*, 25(2): 480–487.

Haas, Eva M., Etienne Bartholomé, and Bruno Combal. 2009. Time series analysis of optical remote sensing data for the mapping of temporary surface water bodies in sub-Saharan western Africa. *Journal of Hydrology*, 370: 52–63.

Halounova, Lena. 2004. The automatic classification of B&W aerial photos. *The International Archives of the Photogrammetry, Remote Sensing and Spatial Information Sciences*, 34(XXX): 455–460.

Highfield, Linda, Michael P. Ward, Shawn W. Laffan. 2008. Representation of animal distributions in space: how geostatistical estimates impact simulation modeling of foot-and-mouth disease spread. *Veterinary Research*, 39(17): 1–14.

Hsu, Wynne, Tat-Seng Chua, and Hung K. Pung. 2000. Approximating content-based object-level image retrieval. *Multimedia Tools and Applications*, 12: 59–79.

Jiang, Zhenlan, Shiliang Su, Changwei Jing, Shengpan Lin, Xufeng Fei, and Jiaping Wu. 2012. Spatiotemporal dynamics of soil erosion risk for Anji County, China. *Stochastic Environmental Research and Risk Assessment*, 26: 751–763.

Johansen, Kasper, Nicholas C. Coops, Sarah E. Gergel, and Yulia Stange. 2007. Application of high spatial resolution satellite imagery for riparian and forest ecosystem classification. *Remote Sensing of Environment*, 110: 29–44.

Jones & Stokes Associates. 1992. Flora and fauna baseline study of Fort Ord, California. *Prepared for U.S. Army Corps of Engineers,* Sacramento, CA: 290 pp.

Keeler-Wolf, Todd, Diane R. Elam, Kari Lewis, and Scott A. Flint. 1998. California vernal pool assessment preliminary report. *Prepared for the California Department of Fish and Game*, 161 pp.

Kneitel, Jamie M. 2014. Inundation timing, more than duration, affects the community structure of California vernal pool mesocosms. *Hydrobiologica*, 732: 71–83.

Lane, Charles R., Ellen D'Amico, and Brad Autrey. 2012. Isolated wetlands of the southeastern United States: abundance and expected condition. *Wetlands*, 32: 753–767.

Lathrop, Richard G., Paul Montesano, Jason Tesauro, and Brian Zarate. 2005. Statewide mapping of vernal pools: a New Jersey case study. *Journal of Environmental Management*, 76(2005): 230–238.

LFR, Weston Solutions, and Westcliffe Engineers, Inc. 2008. FORA ESCA remediation program; final community involvement and outreach program plan. *Prepared for the Fort Ord Reuse Authority*.

Lichvar, Robert W., David C. Finnegan, Stephen Newman, and Walter Ochs. 2006. Delineating and evaluating vegetation conditions of vernal pools using spaceborne and airborne remote sensing techniques, Beale Air Force Base, CA. *Prepared for: U.S. Army Corps of Engineers*, 1–18.

Longcore, Travis and Catherine Rich. 2008. Invertebrate conservation at the gates of hell. *Wings*, Spring 2008: 9–13.

Mallinis, Giorgos, Magdalini Pleniou, and Nikos Koutsias. 2010. Object-based vs pixel-based mapping of fire scars using multi-scale satellite data. *The International Archives of the Photogrammetry, Remote Sensing and Spatial Information Sciences*, XXXVIII-4(C7): 1–5.

Mattoni, Rudi and Travis R. Longcore. 1997. The Los Angeles coastal prairie, a vanished community. *Crossosoma*, 23(2): 71–102.

Mayer, Alex S., Patrick P.E. Carriere, Claudio Gallo, Kurt D. Pennell, Tammy P. Taylor, Glenn A. Williams, and Lirong Zhong. 1997. Groundwater Quality. *Water Environment Research*, 69(4): 777–844.

Montrone, Ashton. 2013. Hydrologic and vegetative modeling of vernal pools in the Sierra Nevada. MS Thesis, University of Nevada, Reno.

Moore, Craig, Monica Bastian, and Harold Hunt. 2001. Long-term vegetational and faunal succession in an artificial Northern California vernal pool system. *Prepared for California Department of Transportation*, FHWA/CA/TL-2001/36: 1–49.

Munoz, Breda, Virginia M. Lesser, John R. Dorney, and Rick Savage. 2009. A proposed methodology to determine accuracy of location and extent of geographically isolated wetlands. *Environmental Monitoring and Assessment*, 150: 53–64.

Rhazi, Laila, Mouhssine Rhazi, Patrick Grillas, and Driss El Khyari. 2006. Richness and structure of plant communities in temporary pools from western Morocco: influence of human activities. *Hydrobiologica*, 570: 197–203.

Reed, Sarah and Ronald Amundson. 2007. Sediment, gophers, and time: a model for the origin and persistence of mima mound—vernal pool topography in the Great Central Valley. *Vernal Pool Landscapes*. In *Studies from the Herbarium*, edited by R.A. Schlising, and D.G. Alexander, 14: 15–27.

Rempel, Robert S., Daniel Kaukinen, and Angus P. Carr. 2012. Patch analyst and patch grid. *Ontario Ministry of Natural Resources*. Centre for Northern Forest Ecosystem Research, Thunder Bay, Ontario.

Schlising, Robert A. and Ellen L. Sanders. 1982. Quantitative analysis of vegetation at the Richvale Vernal Pools, California. *American Journal of Botany*, 69(5): 734–742.

Smeulders, Arnold W.M., Marcel Worring, Simone Santini, Amarnath Gupta, Ramesh Jain. 2000. Content-based image retrieval at the end of the early years. *IEEE Transactions on Pattern Analysis and Machine Intelligence*, 22(12): 1349–1380.

Smith, Douglas, Bob Curry, Donald Koslowski, Regina Williams, Fred Watson, Leslie Turrini-Smith, and Wendi Newman. 2002. Watershed and riparian assessment report: Bureau of Land Management lands, former Fort Ord, Monterey County, California. *Prepared for the Watershed Institute, California State University at Monterey Bay*, WI-2002-01: 151 pp.

Stone, Janice S. 1992. Vernal pools in Massachusetts: aerial photographic identification, biological and physiographic characteristics, and state certification. MS Thesis, University of Massachusetts Amherst.

Tannourji, Danielle N. 2009. Ecological factors suitable for the endangered *Lasthenia conjugens* (Asteraceae). MS Thesis, San José State University.

Tetra Tech Inc. and EcoSystems West Consulting Group. 2014. 2013 biological monitoring report for units 7, 5E, and 23E; units 15, 21, 32, and 34; units 18 and 22; and Ranges 43–48 Former Fort Ord. *Prepared for U.S. Army Corps of Engineers,* Sacramento, CA: 1–209.

Thompson, Shanley D. and Sarah E. Gergel. 2008. Conservative implications of mapping rare ecosystems use high spatial resolution imagery: recommendations for heterogenous fragmented landscapes. *Landscape Ecology*, 23: 1023–1037.

Tiner, Ralph W. 2003. Estimated extent of geographically isolated wetlands in selected areas of the United States. *Wetlands*, 23(3): 636–652.

USGS. Earth Explorer Application. 2014. U.S. Geological Survey.

USFWS (U.S. Fish and Wildlife Service). 2005. Recovery plan for vernal pool ecosystems of California and Southern Oregon. Portland, Oregon. xxvi + 606 pages.

Van Dyke, Eric. and Karen Holl. 2003. Mapping the distribution of maritime chaparral species in the Monterey Bay area. *Prepared for U.S. Fish and Wildlife Service*, Ventura Fish and Wildlife Office: 22 pp.

Van Dyke, Eric, Karen D. Holl, and James R. Griffin. 2001. Maritime chaparral community transition in the absence of fire. *Madroño*, 48:221–229.

Van Meter, Robin, Larissa L. Bailey, and Evan H.C. Grant. 2008. Methods for estimating vernal pool habitat in the northeastern United States. *Wetlands*, 28(3): 585–593.

Van Thomme, Eric. 2001. Restored vernal pools in California and post-creation monitoring and management. *Student On-Line Journal, Department of Horticultural Science, University of Minnesota*, 7(4): 1–6.

Wang, Ian J., Jarret R. Johnson, Benjamin B. Johnson, and H. Bradley Shaffer. 2011. Effective population size is strongly correlated with breeding pond size in the endangered California tiger salamander, *Ambystoma californiense*. *Conservation Genetics*, 12: 911–920.

Yu, Huan and Shu-Qing Zhang. 2008. Application of high resolution satellite imagery for wetlands cover classification using object-oriented method. In *The International Archives of the Photogrammetry, Remote Sensing and Spatial Information Sciences*, edited by Chen Jun, Jiang Jie, and John van Genderen, Vol. XXXVII. Part B7: 521–526.

Zedler, Paul H. 1987. The ecology of Southern California vernal pools: a community profile. *Biological Report, Prepared for the U.S. Fish and Wildlife Service*, 85(7.11): 137 pp.

----. 2003. Vernal pools and concept of "isolated wetlands." *Wetlands*, 23(3): 597–607.

Zhang, Yun and Travis Maxwell. 2006. A fuzzy logic approach to supervised segmentation for object-oriented classification. *ASPRS Annual Conference, Reno, NV*.

APPENDIX A: SUPPORTIVE IMAGERY

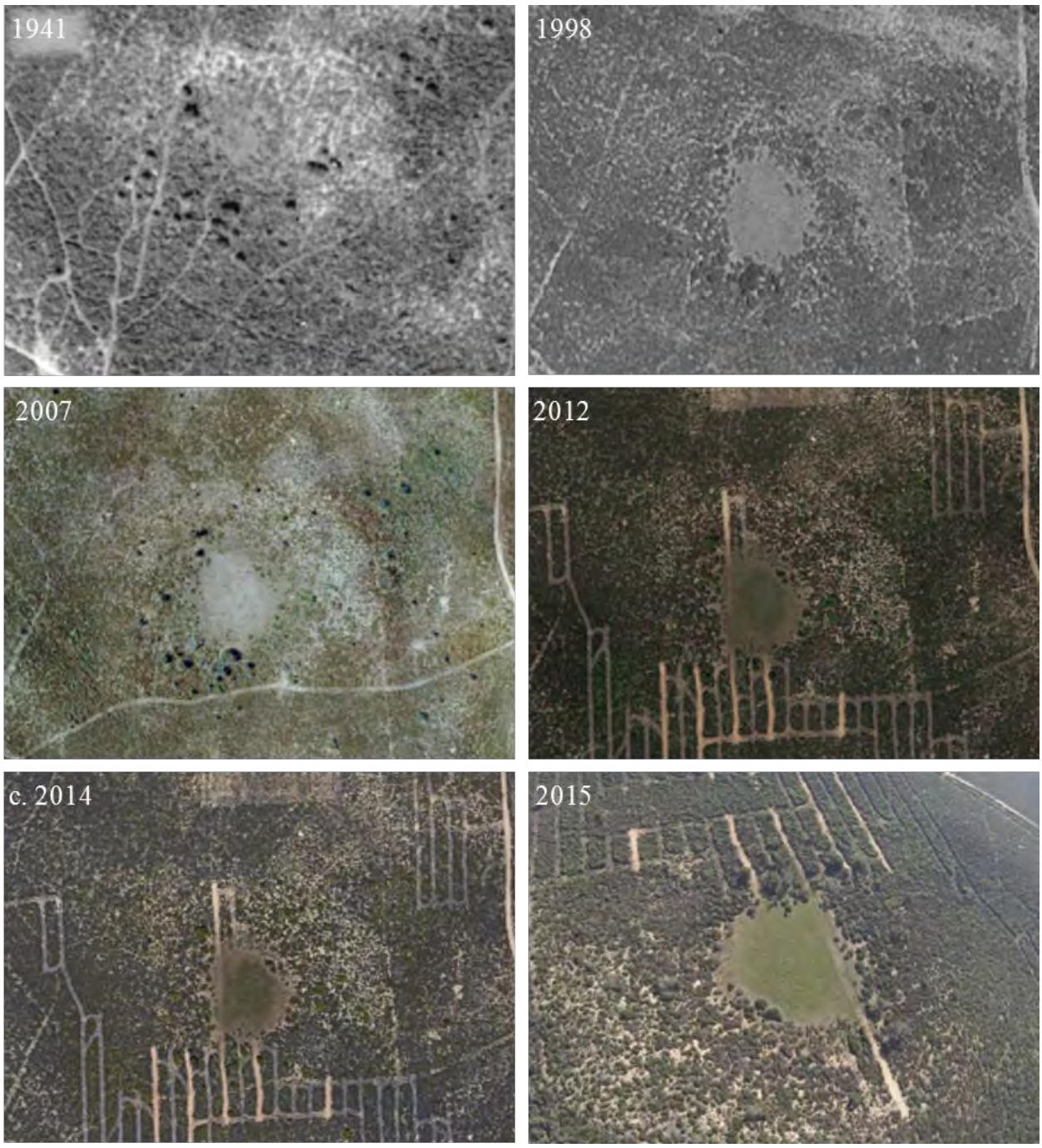

Figure 33: PVP Site 70P05 Displays Floral Persistence Similar to that of Study Area CVP (Source Imagery: Google Earth, C. Hanley—bottom right)

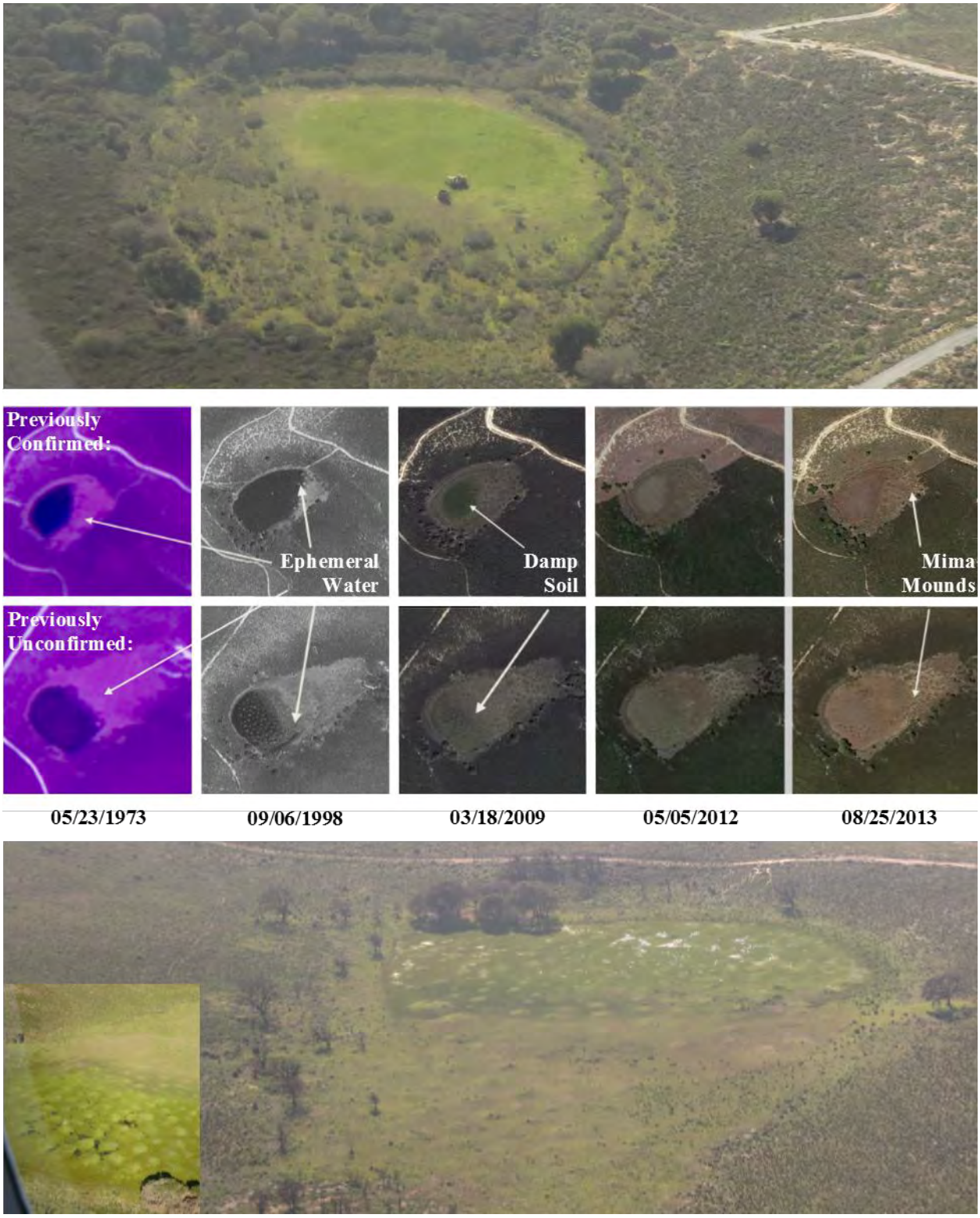

Figure 34: Previously Unconfirmed CVP 80P03 (bottom row) Was Flooded During the Flyover While Known CVP 80C02 Was Not (Source Imagery: USGS EarthExplorer, Google Earth, C. Hanley—top and bottom)

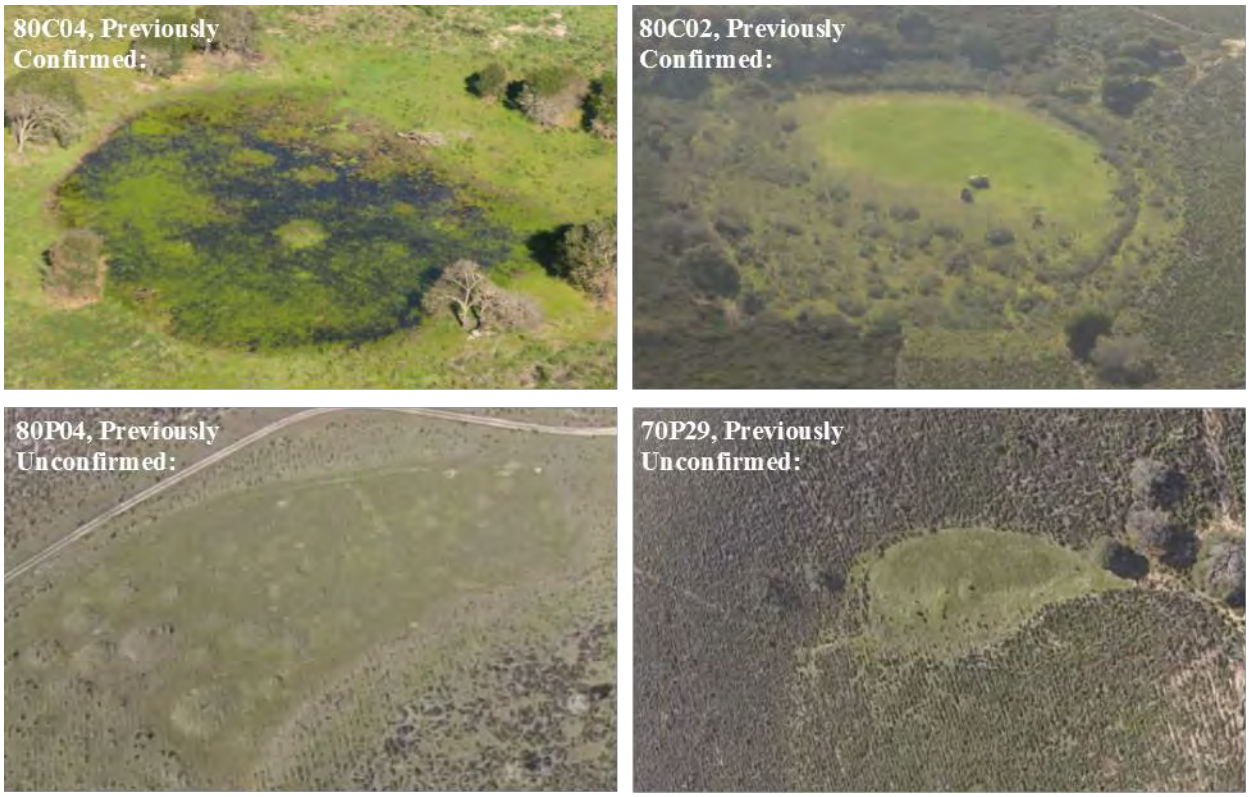

Figure 35: Comparative Shoreline Shapes for Known and Previously Unconfirmed CVP (Photo Credits: C. Hanley)

Figure 36: Inundated CVP Site 11P01 (Previously Unknown), Likely Created by Disturbance (Photo Credits: C. Hanley)

Figure 37: Enlargement of Erosion Drainage Scar in Site ID# 80P07 (Photo Credits: C. Hanley)

APPENDIX B: ENLARGEMENTS OF CLASSIFICATION RESULTS

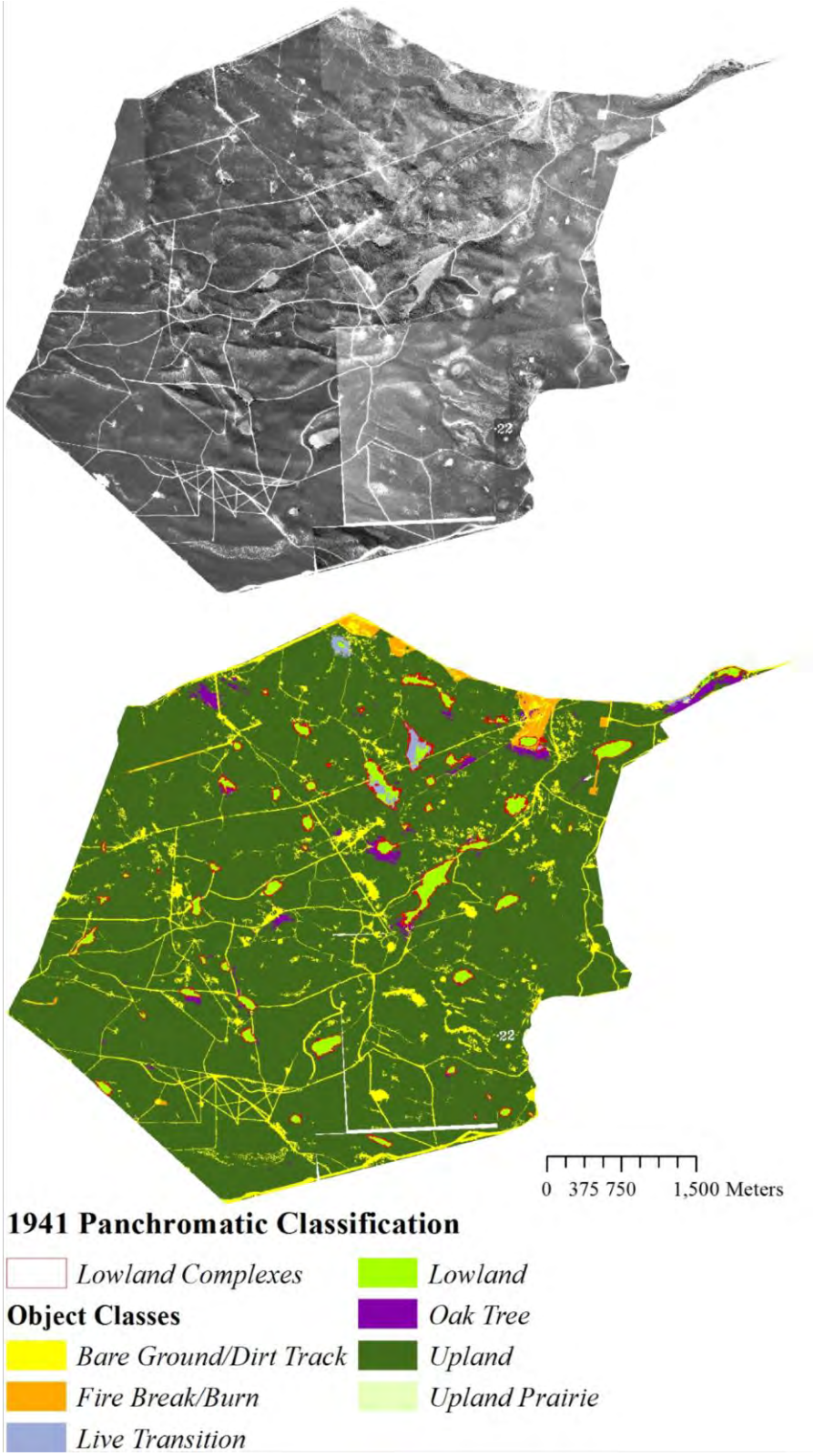

Figure 38: Enlargement of 1941 Classification Results

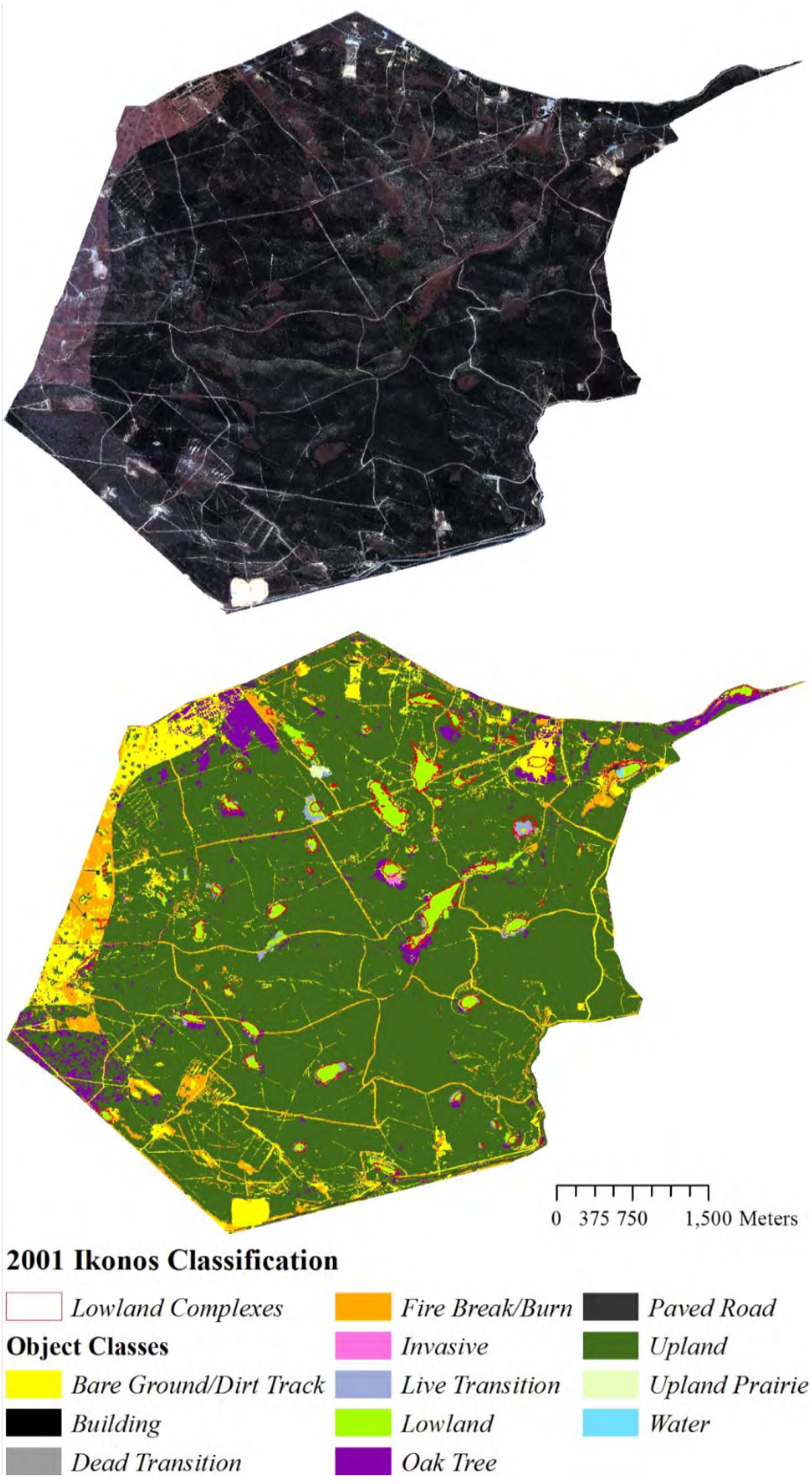

Figure 39: Enlargement of 2001 Classification Results

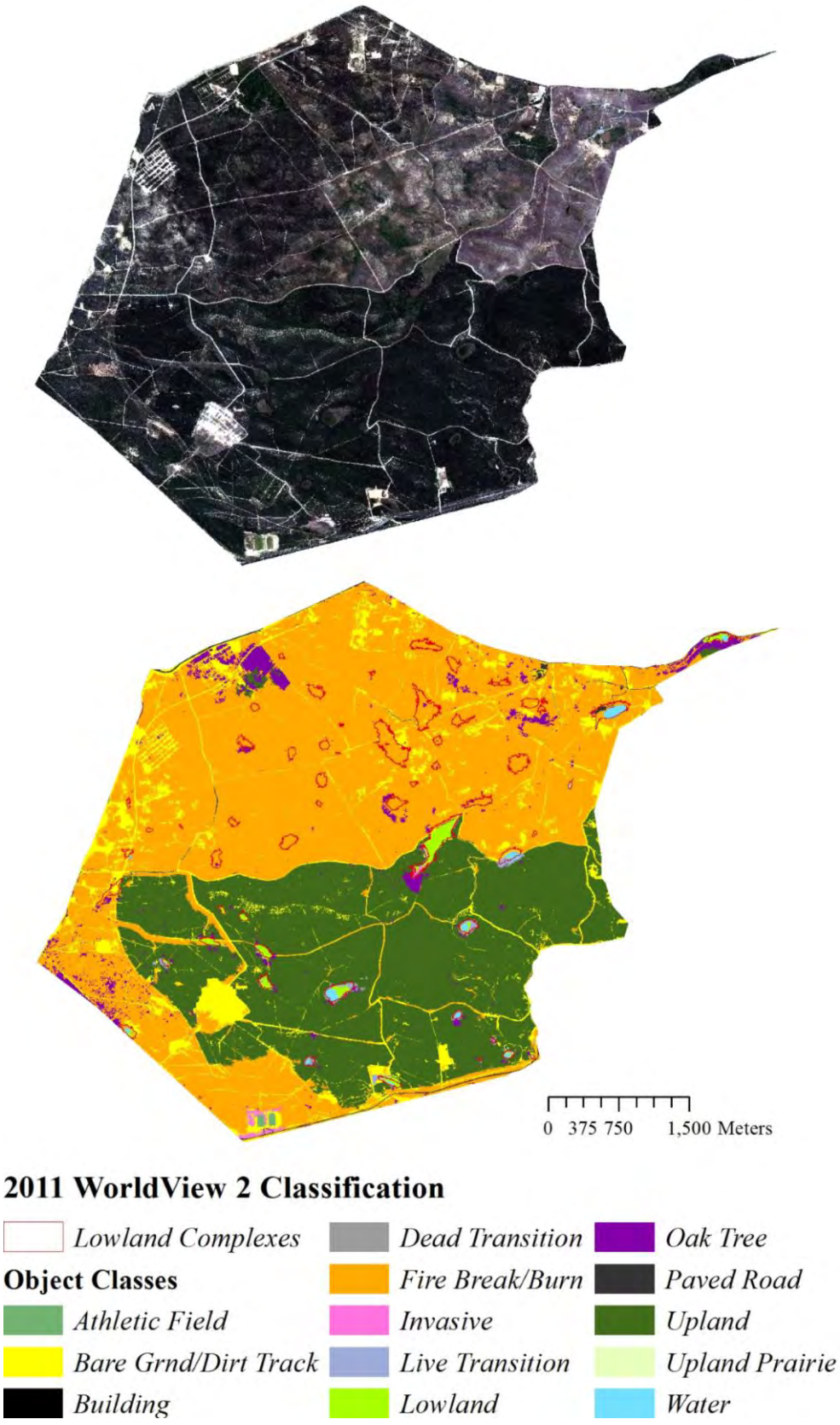

Figure 40: Enlargement of 2011 Classification Results

APPENDIX C: MAPS OF MEASURED METRICS

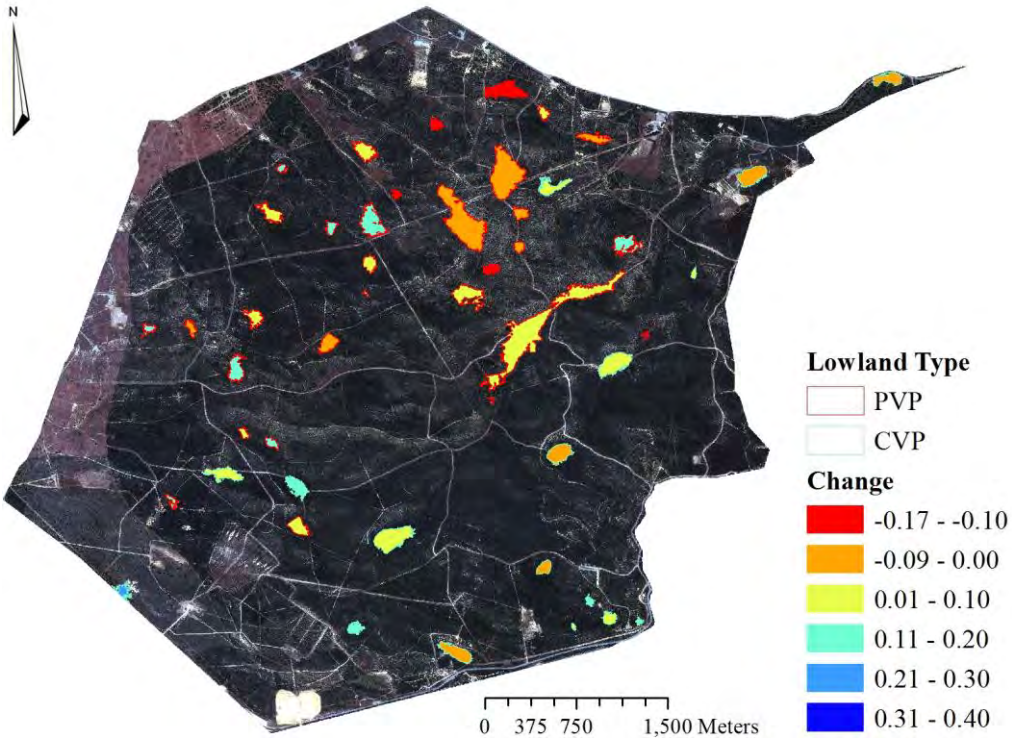

Figure 41: Lowland Complex FD Changes by Type, 1941-2001

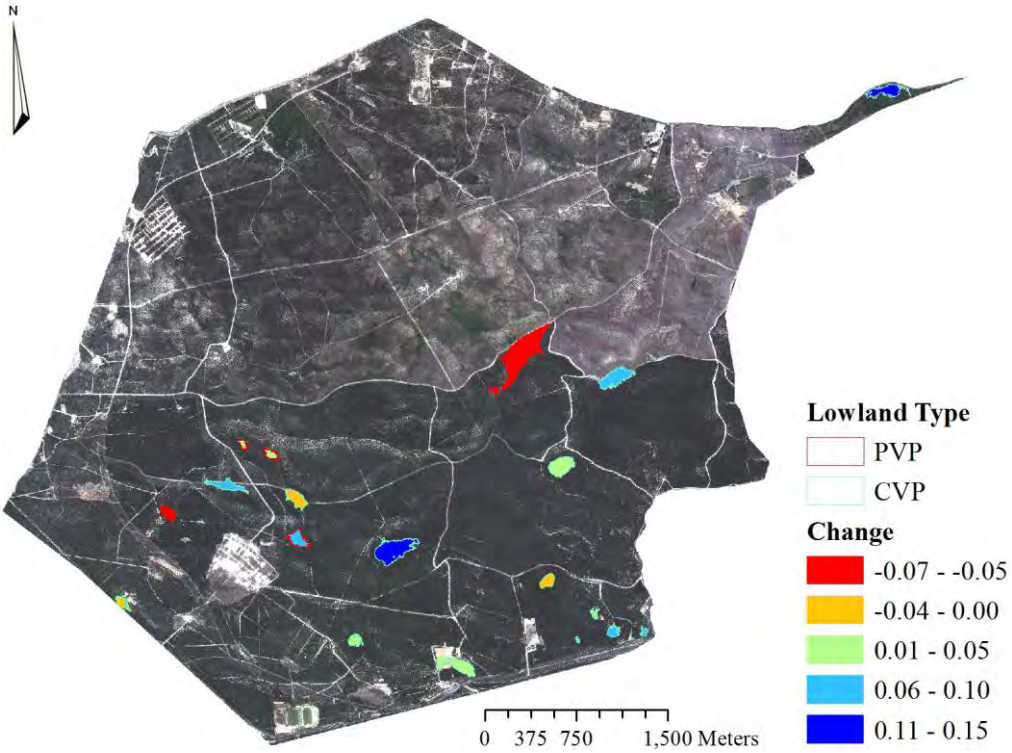

Figure 42: Lowland Complex FD Changes by Type, 2001-2011

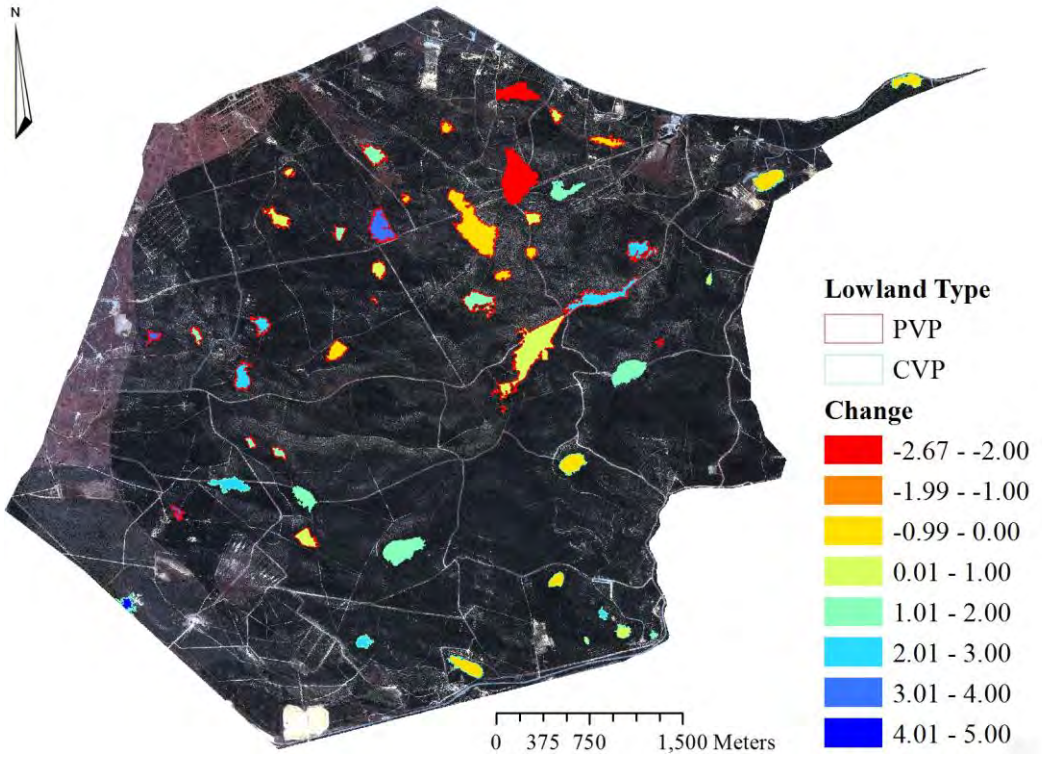

Figure 43: Lowland Complex SI Changes by Type, 1941-2001

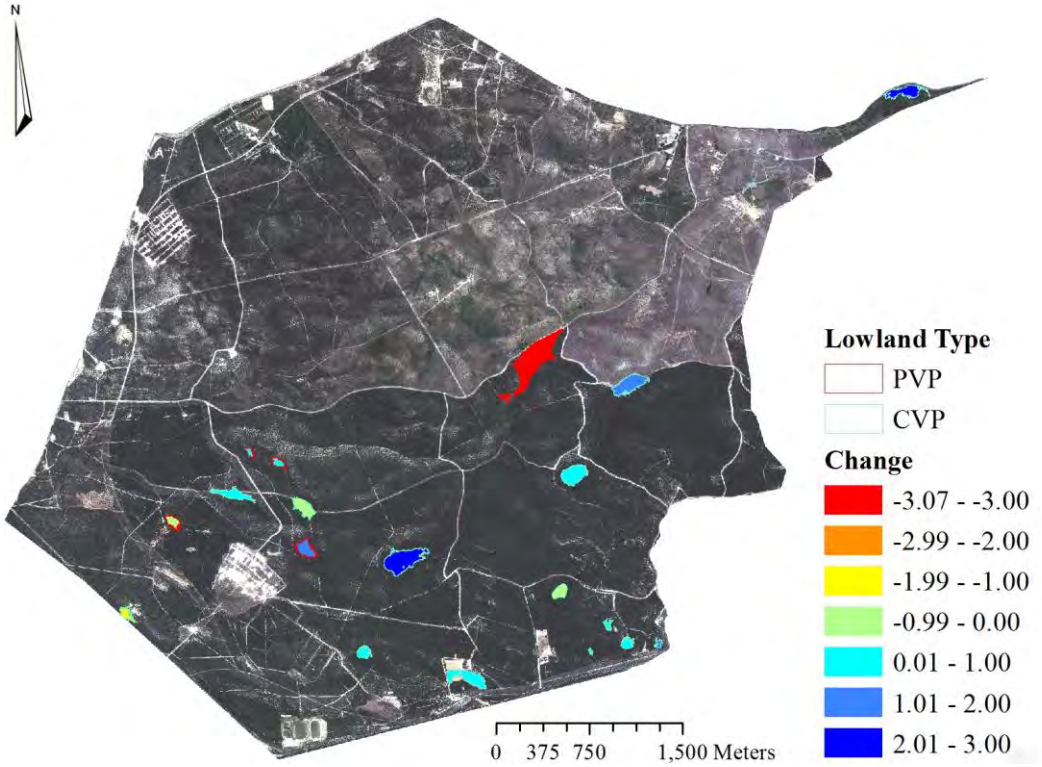

Figure 44: Lowland Complex SI Changes by Type, 2001-2011

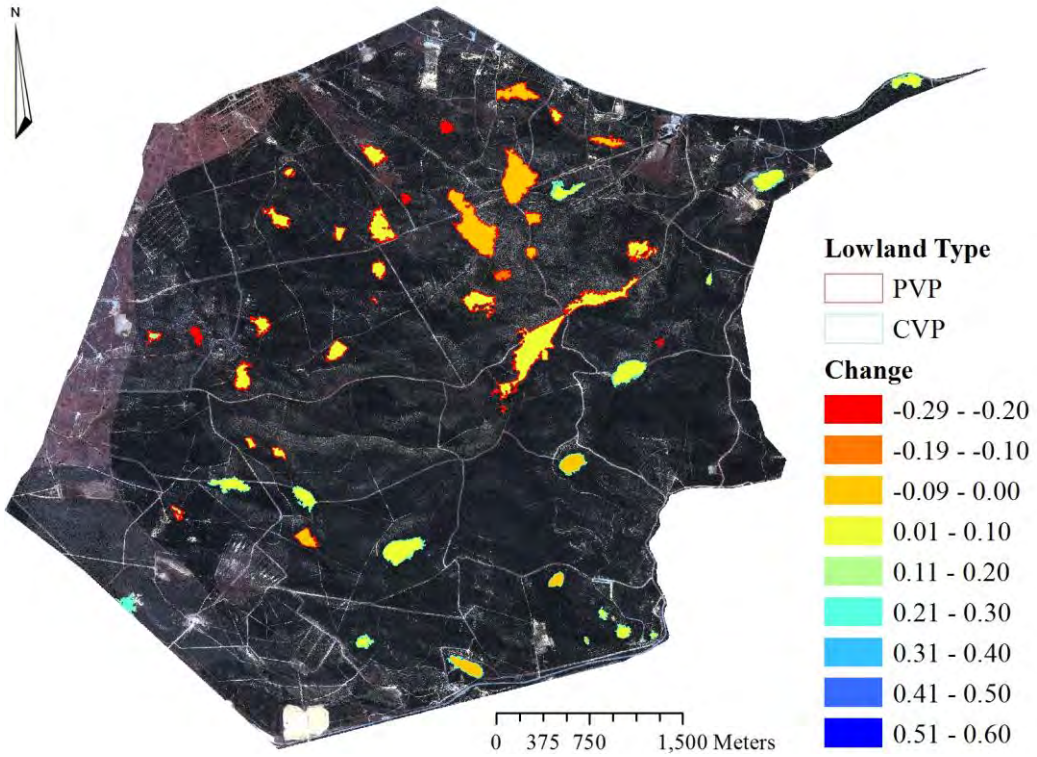

Figure 45: Lowland Complex PAR Changes by Type, 1941-2001

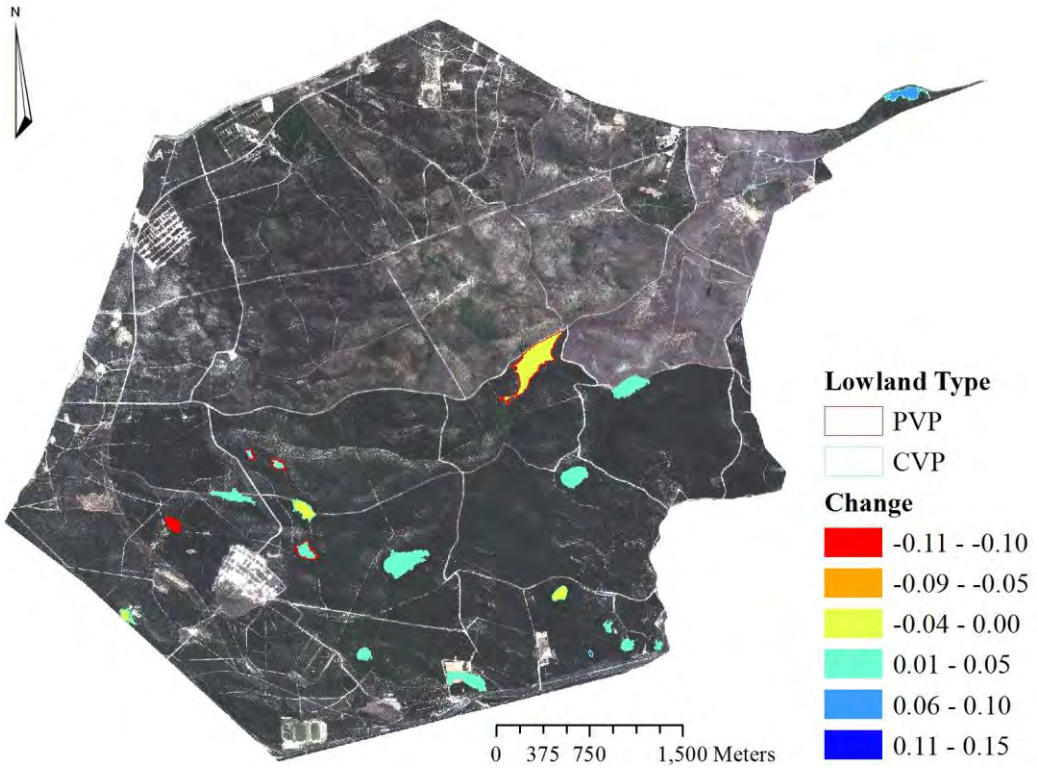

Figure 46: Lowland Complex PAR Changes by Type, 2001-2011

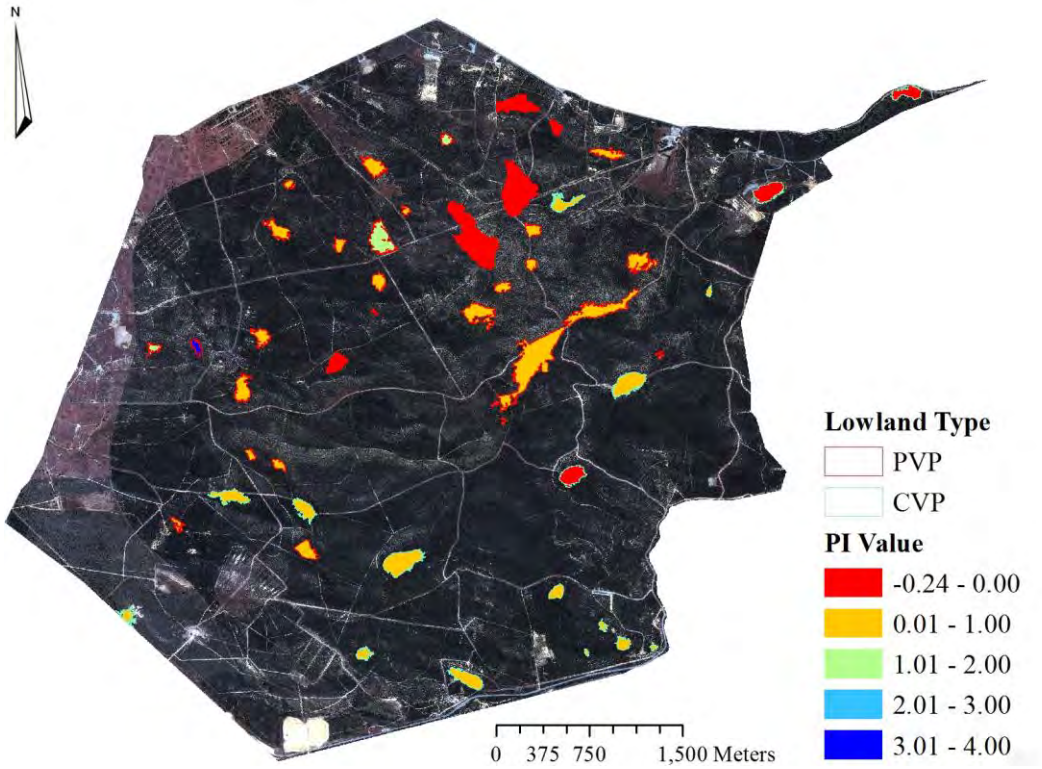

Figure 47: Lowland Complex PI Values by Type, 1941-2001

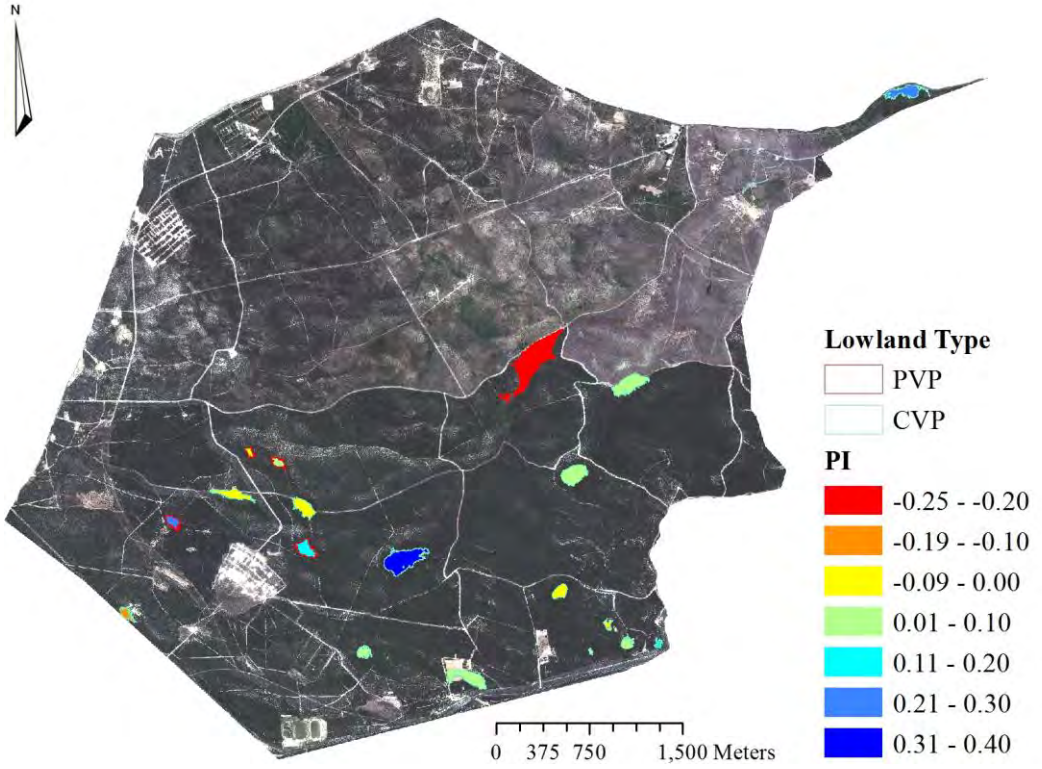

Figure 48: Lowland Complex PI Values by Type, 2001-2011

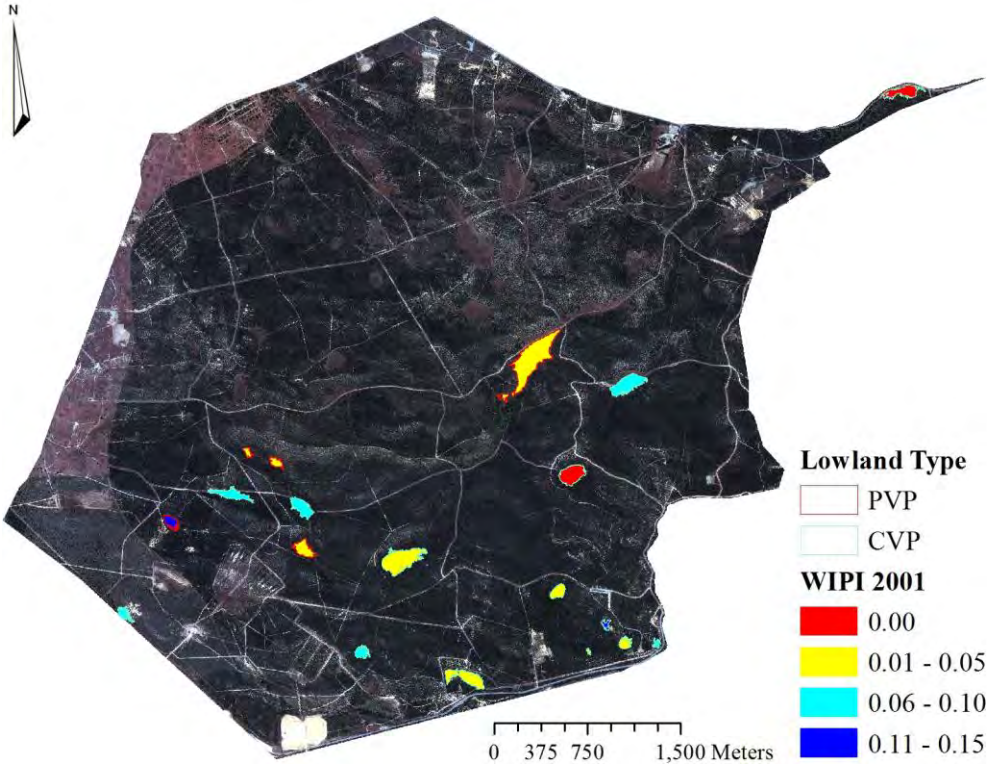

Figure 49: 70-Year WIPI for Self-Same CVP

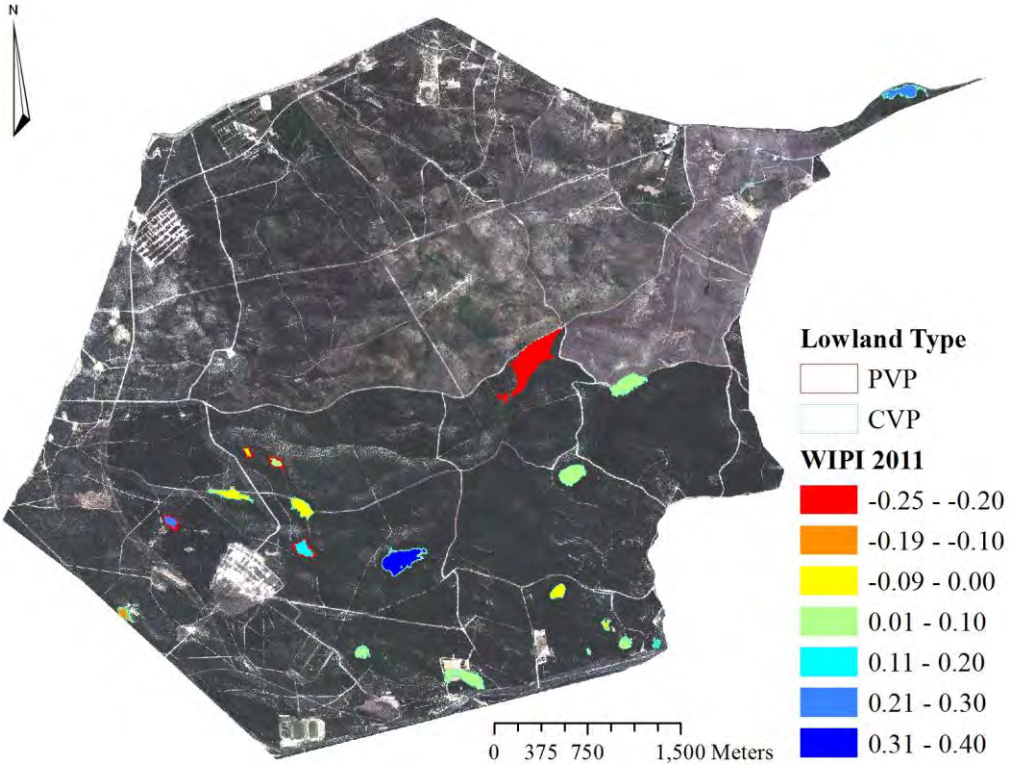

Figure 50: 10-Year WIPI for Self-Same CVP

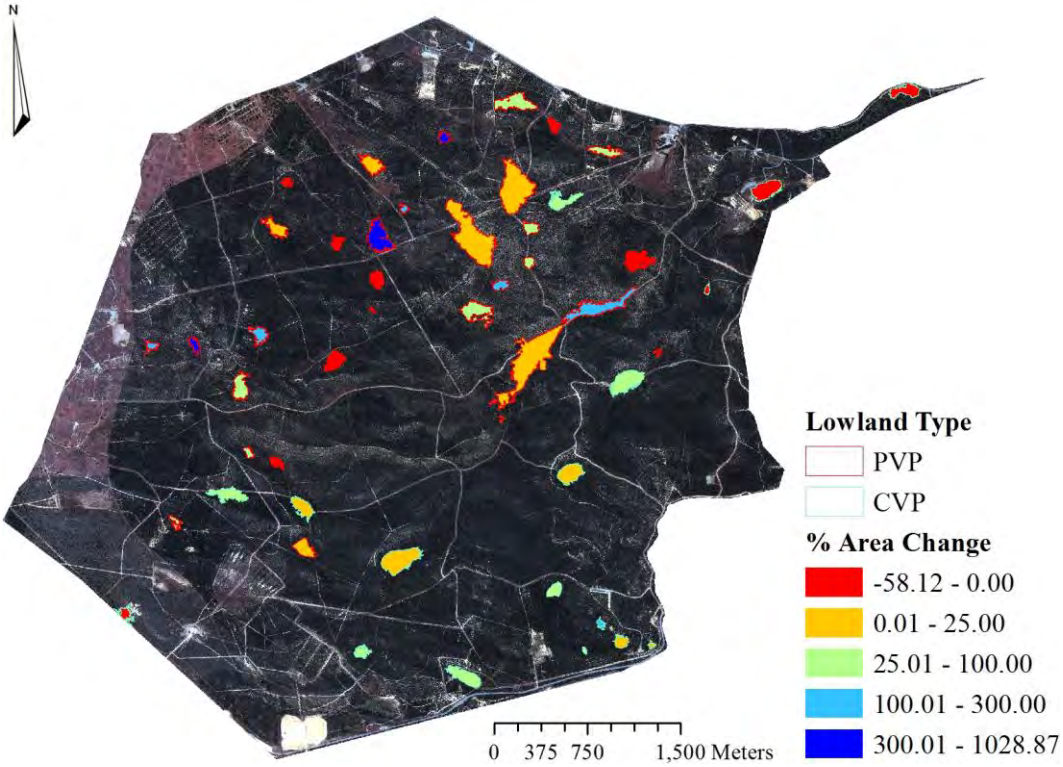

Figure 51: Lowland Complex Percent Area Changes by Type, 1941-2001

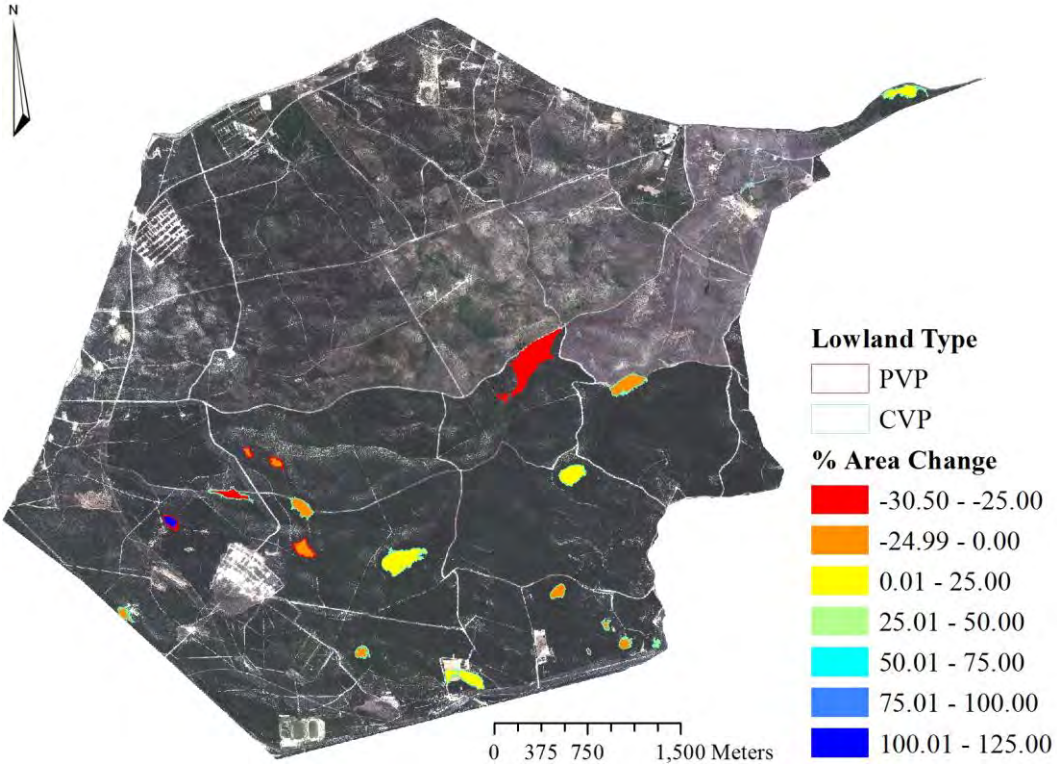

Figure 52: Lowland Complex Percent Area Changes by Type, 2001-2011

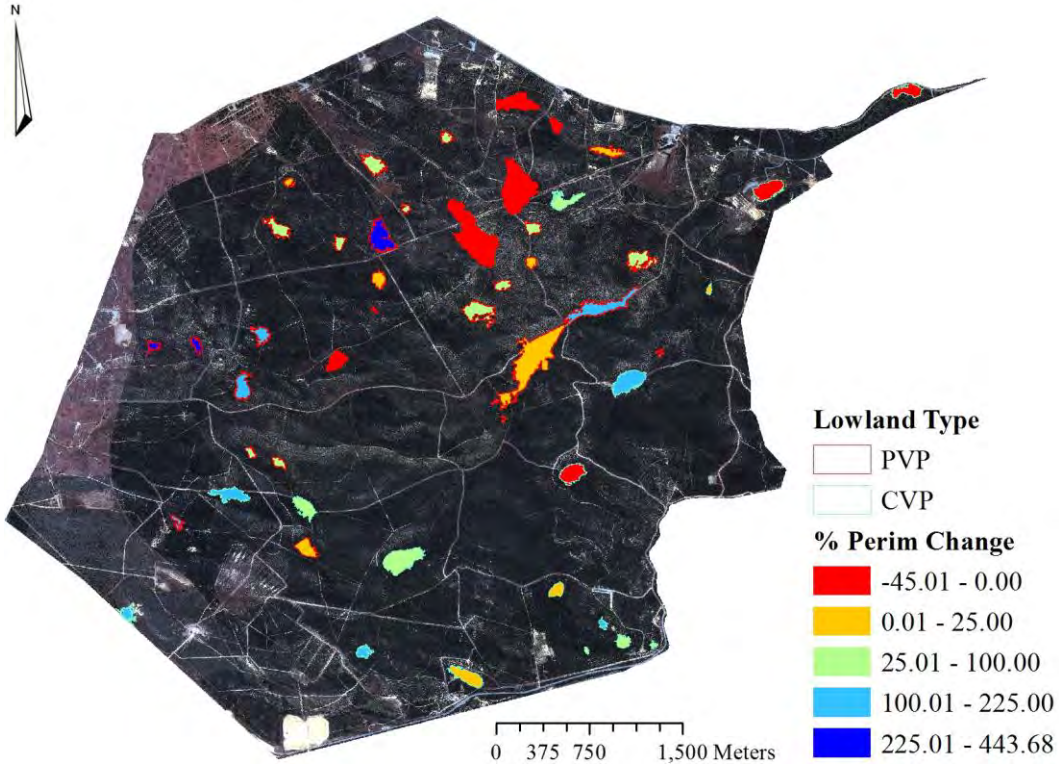

Figure 53: Lowland Complex Percent Perimeter Changes by Type, 1941-2001

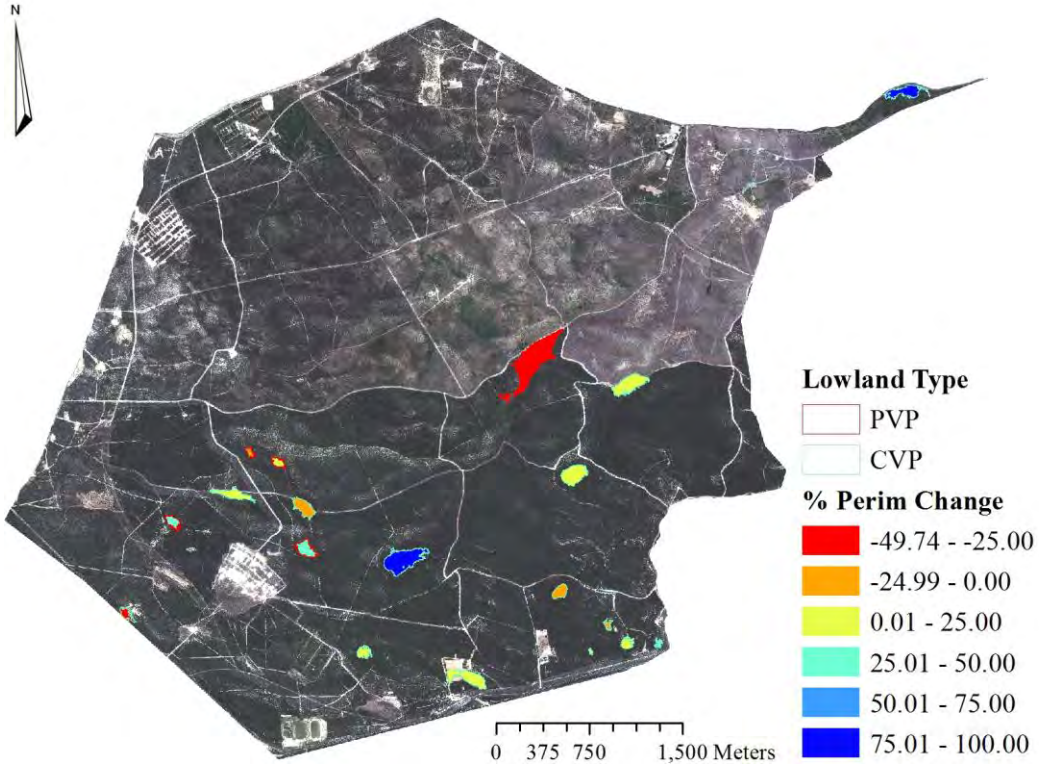

Figure 54: Lowland Complex Percent Perimeter Changes by Type, 2001-2011

APPENDIX D: EXPLORATORY STATISTICS RESULTS

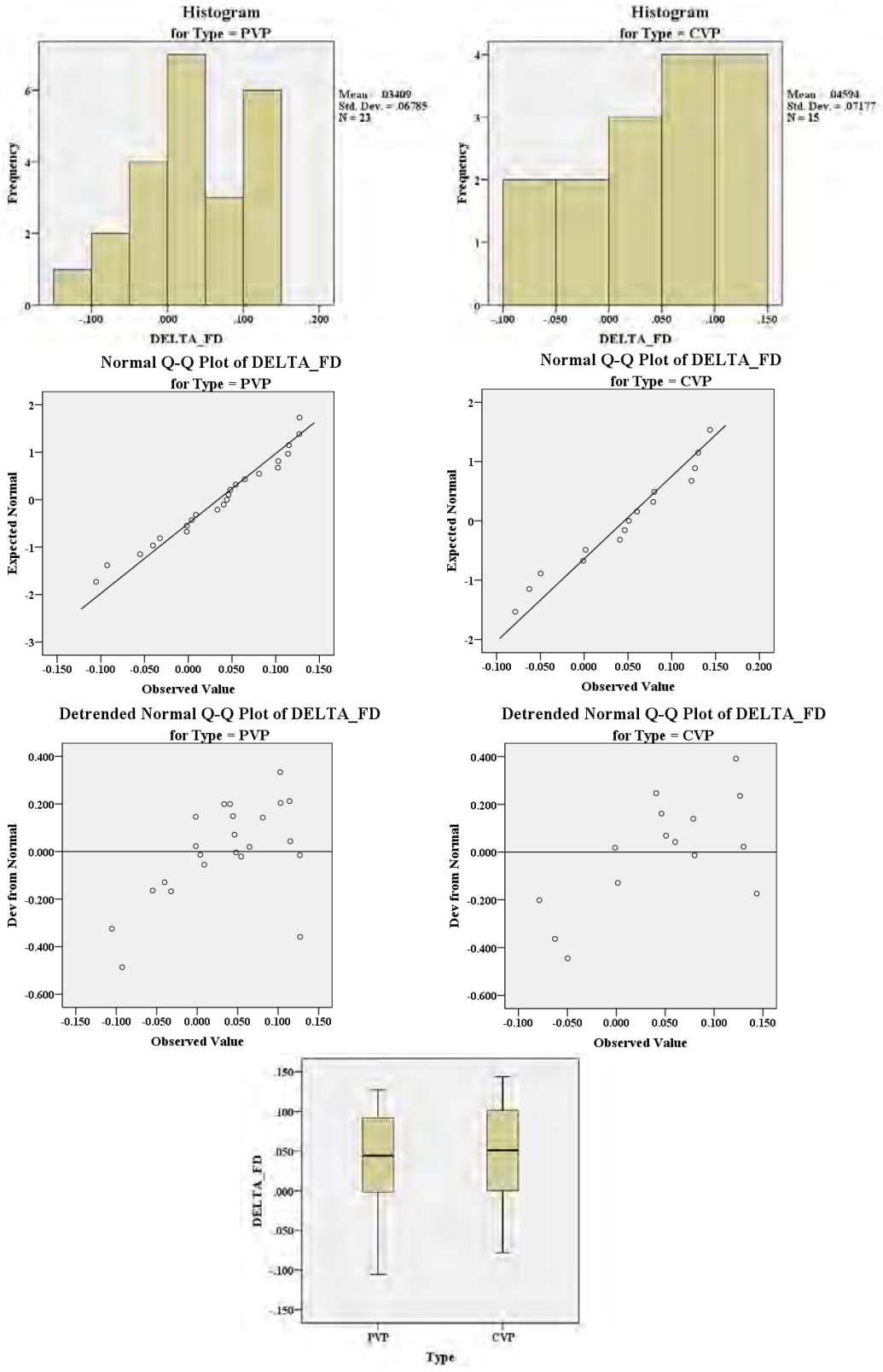

Figure 55: Exploratory Statistics for Change in FD, 1941-2001

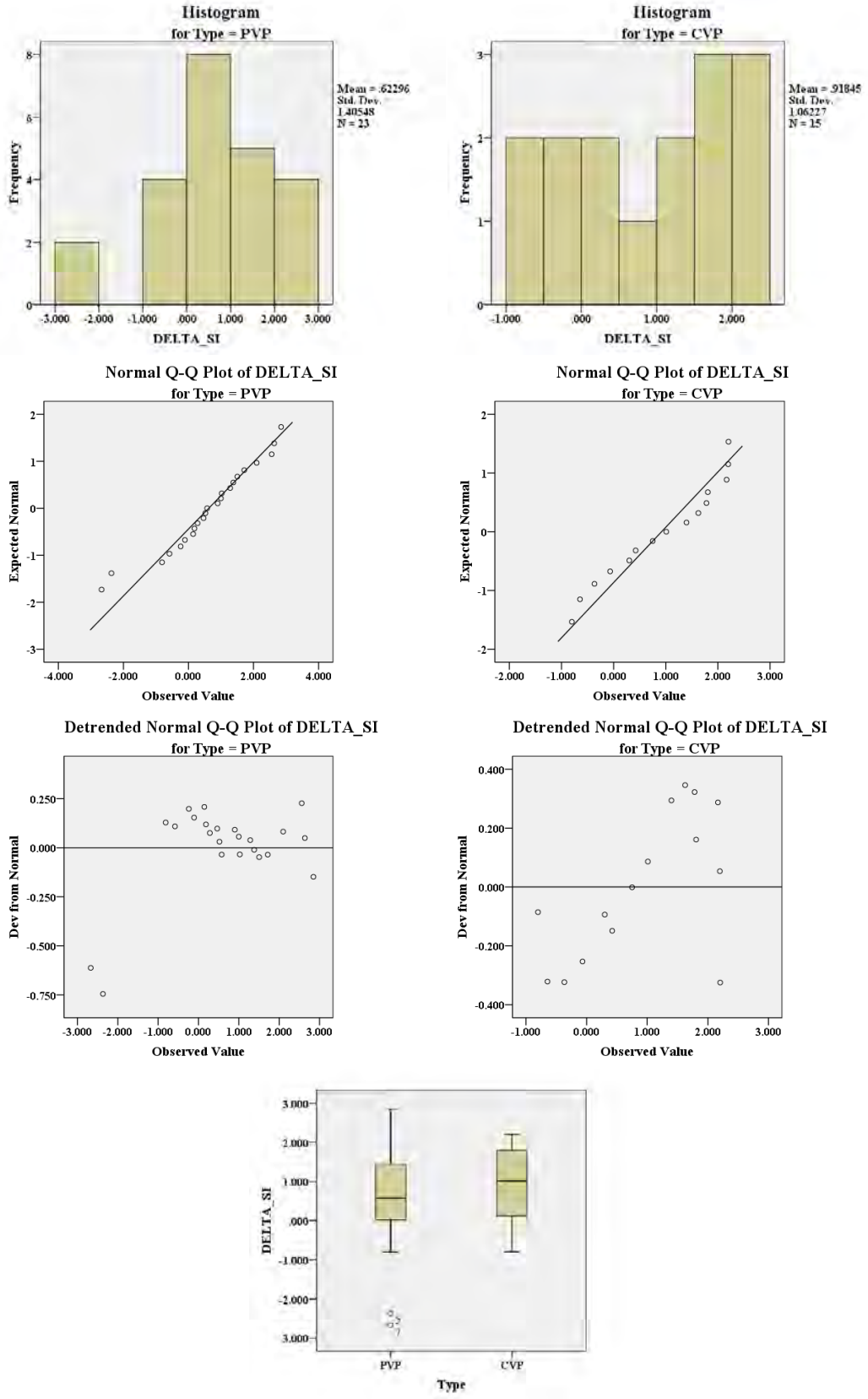

Figure 56: Exploratory Statistics for Change in SI, 1941-2001

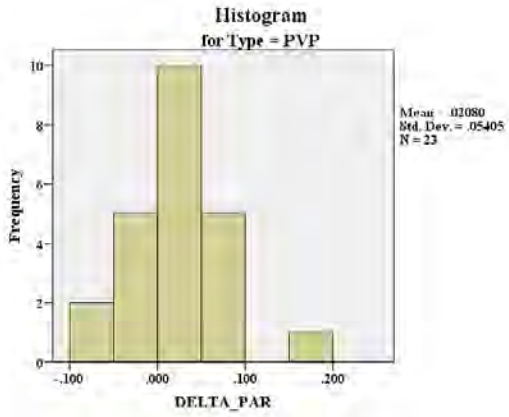
Histogram
for Type = PVP
Mean = .02080
Std. Dev. = .05405
N = 23
Frequency
DELTA_PAR

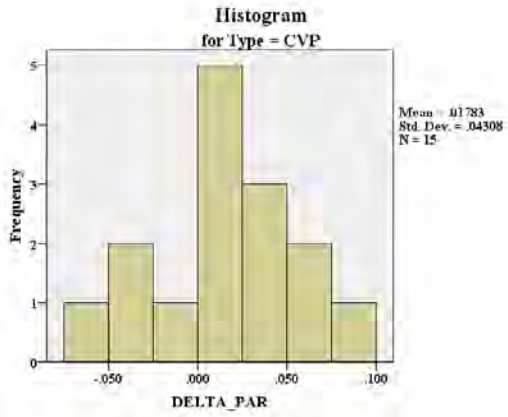
Histogram
for Type = CVP
Mean = .01783
Std. Dev. = .04308
N = 15
Frequency
DELTA_PAR

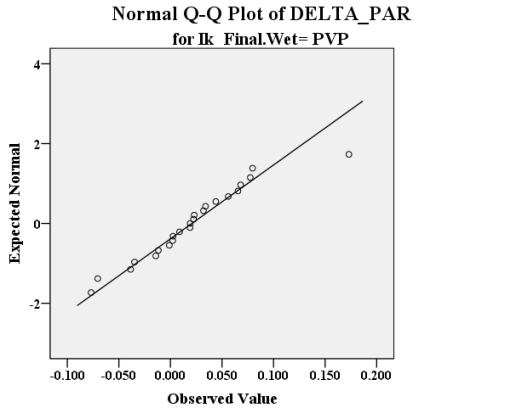
Normal Q-Q Plot of DELTA_PAR
for Ik_Final.Wet= PVP
Expected Normal
Observed Value

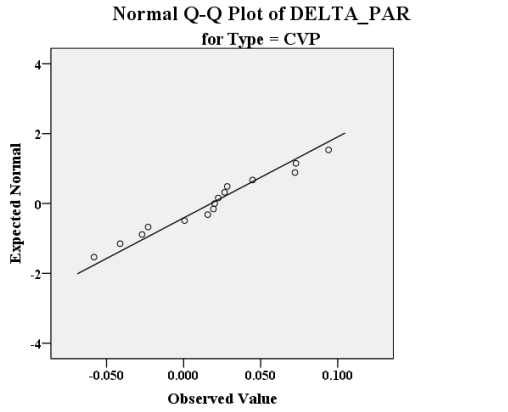
Normal Q-Q Plot of DELTA_PAR
for Type = CVP
Expected Normal
Observed Value

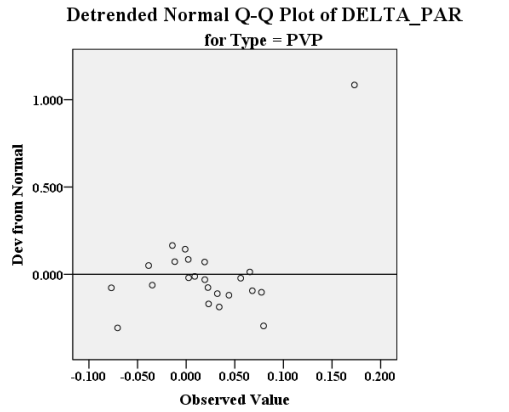
Detrended Normal Q-Q Plot of DELTA_PAR
for Type = PVP
Dev from Normal
Observed Value

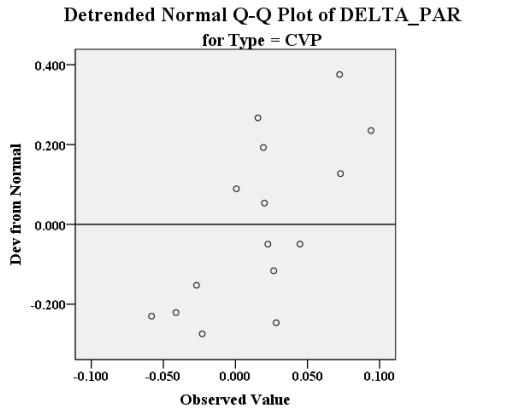
Detrended Normal Q-Q Plot of DELTA_PAR
for Type = CVP
Dev from Normal
Observed Value

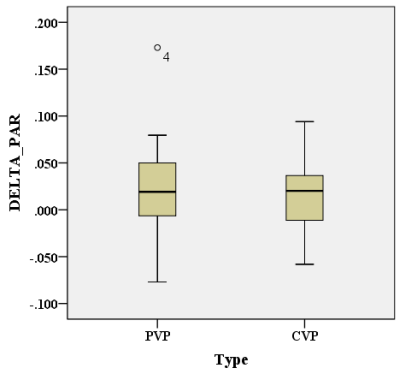
DELTA_PAR
PVP
CVP
Type

Figure 57: Exploratory Statistics for Change in PAR, 1941-2001

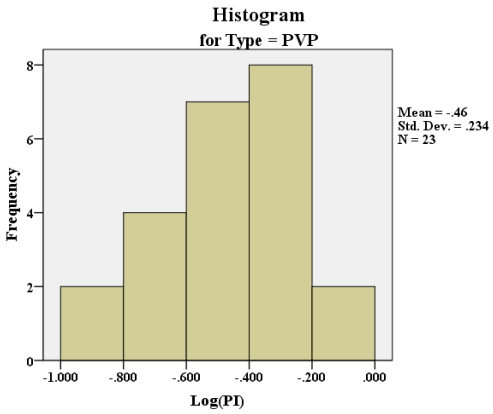
Histogram
for Type = PVP
Mean = -.46
Std. Dev. = .234
N = 23
Frequency
Log(PI)

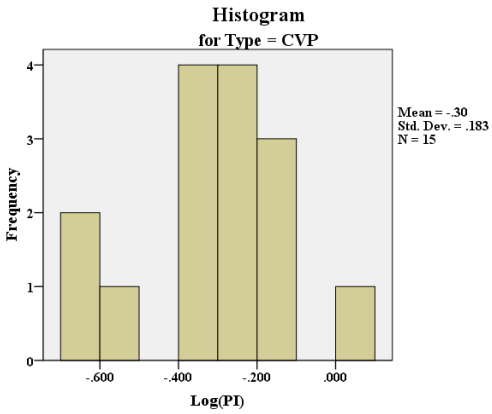
Histogram
for Type = CVP
Mean = -.30
Std. Dev. = .183
N = 15
Frequency
Log(PI)

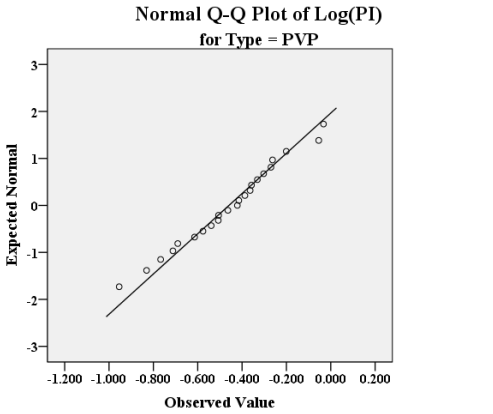
Normal Q-Q Plot of Log(PI)
for Type = PVP
Expected Normal
Observed Value

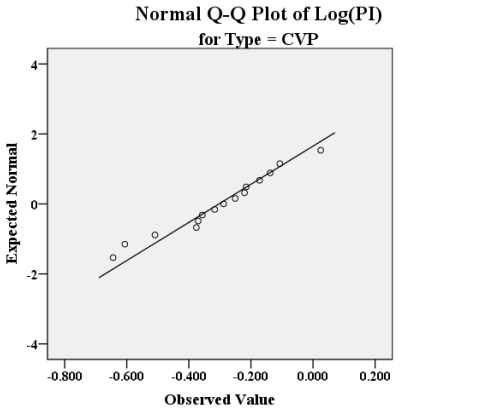
Normal Q-Q Plot of Log(PI)
for Type = CVP
Expected Normal
Observed Value

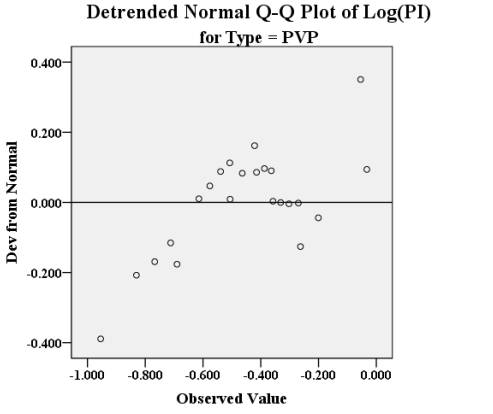
Detrended Normal Q-Q Plot of Log(PI)
for Type = PVP
Dev from Normal
Observed Value

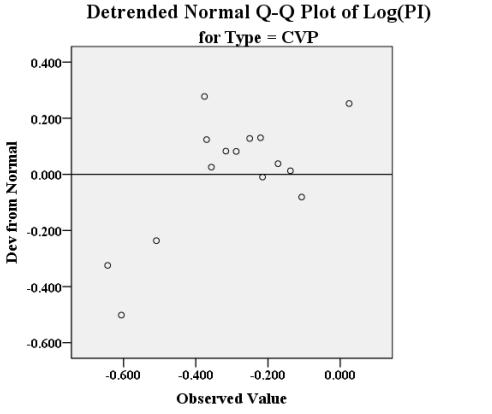
Detrended Normal Q-Q Plot of Log(PI)
for Type = CVP
Dev from Normal
Observed Value

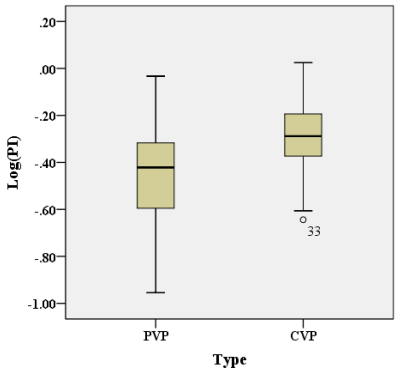
Log(PI)
33
PVP
CVP
Type

Figure 58: Exploratory Statistics for Log(PI), 1941-2001

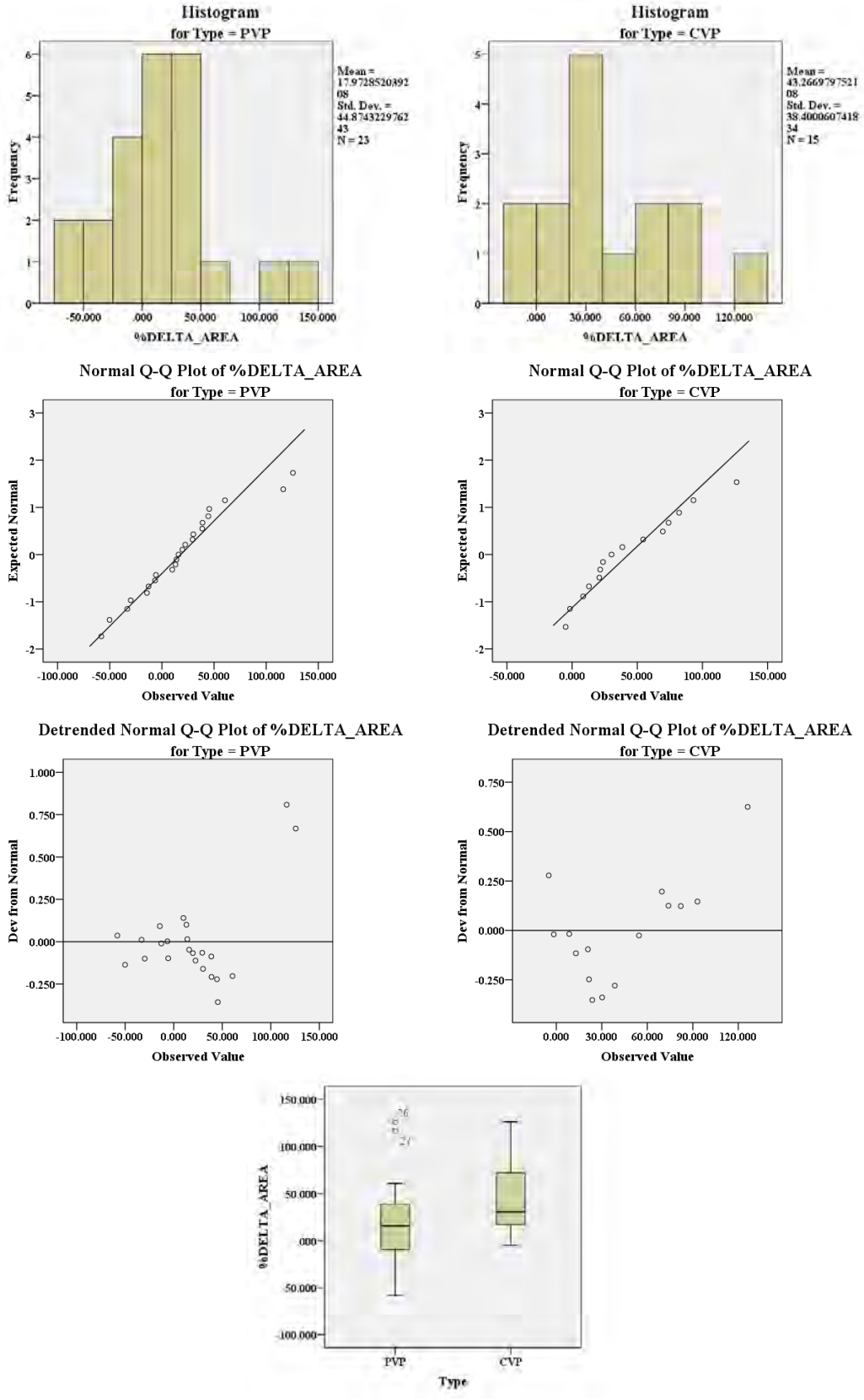

Figure 59: Exploratory Statistics for % Area Change, 1941-2001

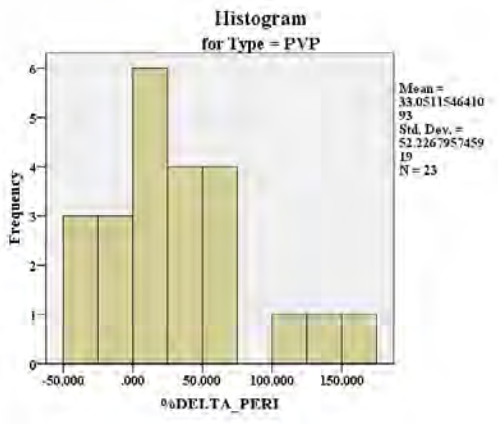
Histogram
for Type = PVP
Mean = 33.0511546410 93
Std. Dev. = 52.2267957459 19
N = 23
Frequency
%DELTA_PERI

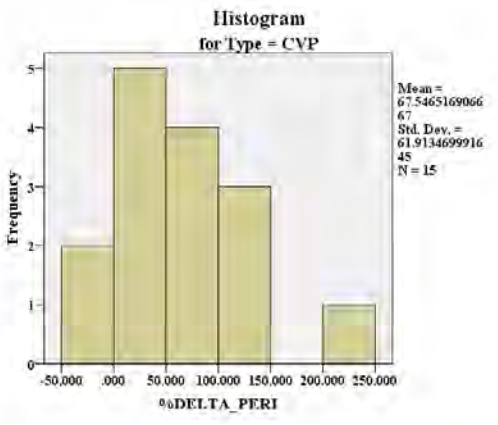
Histogram
for Type = CVP
Mean = 67.5465169066 67
Std. Dev. = 61.9134699916 45
N = 15
Frequency
%DELTA_PERI

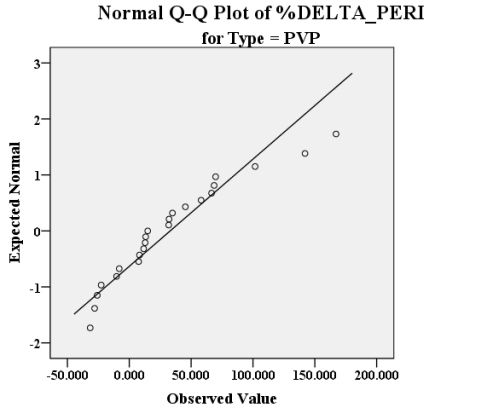
Normal Q-Q Plot of %DELTA_PERI
for Type = PVP
Expected Normal
Observed Value

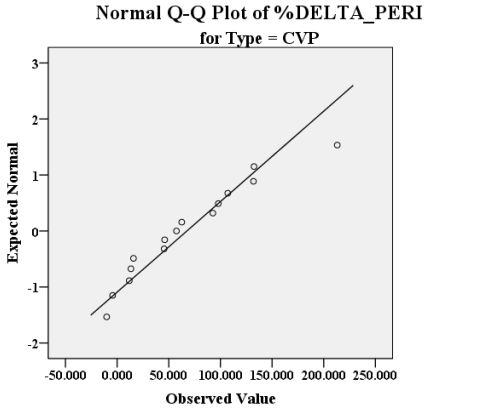
Normal Q-Q Plot of %DELTA_PERI
for Type = CVP
Expected Normal
Observed Value

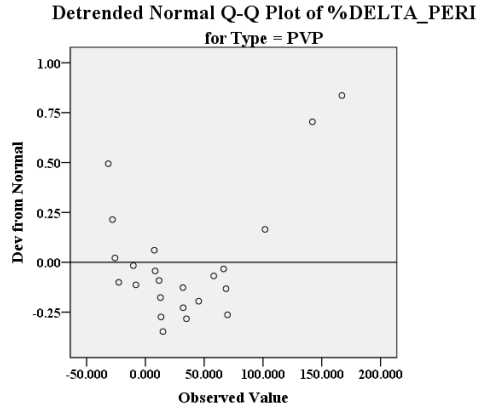
Detrended Normal Q-Q Plot of %DELTA_PERI
for Type = PVP
Dev from Normal
Observed Value

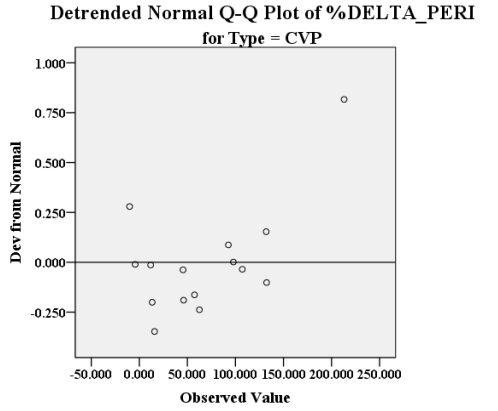
Detrended Normal Q-Q Plot of %DELTA_PERI
for Type = CVP
Dev from Normal
Observed Value

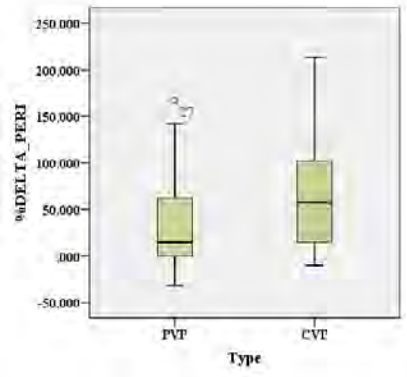
%DELTA_PERI
PVP
CVT
Type

Figure 60: Exploratory Statistics for % Perimeter Change, 1941-2001

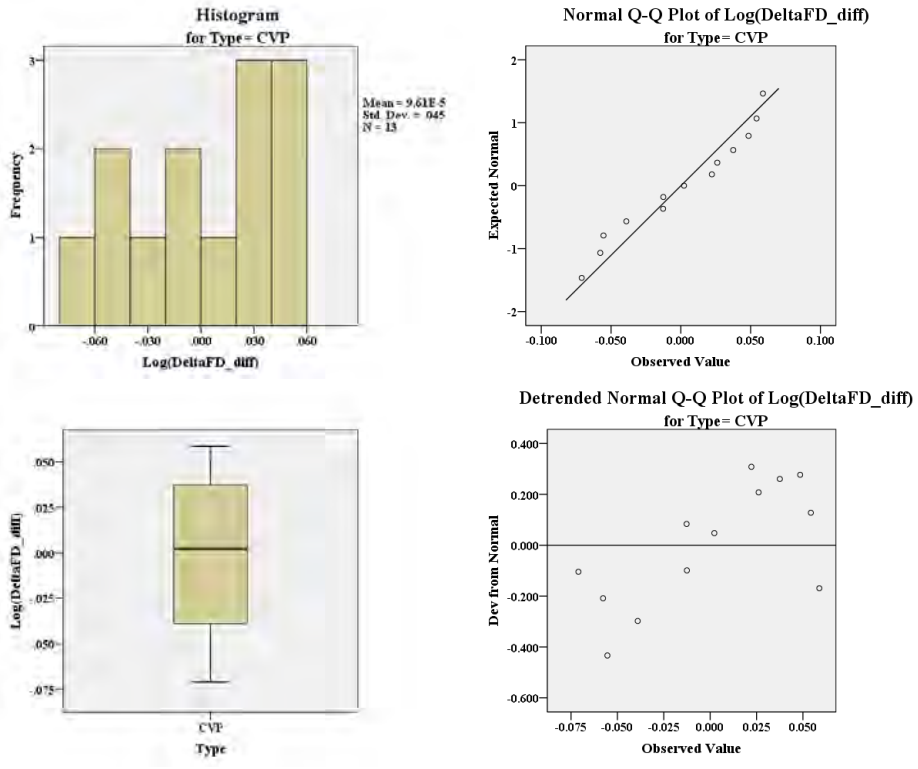

Figure 61: Exploratory Statistics Self-Same CVP FD Differences

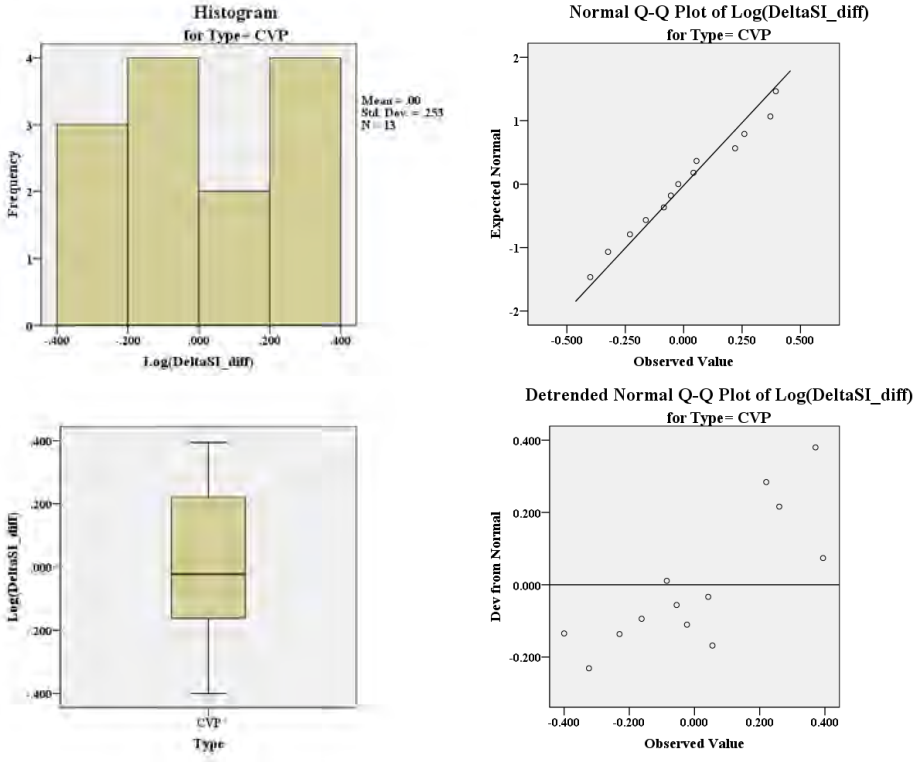

Figure 62: Exploratory Statistics Self-Same CVP SI Differences

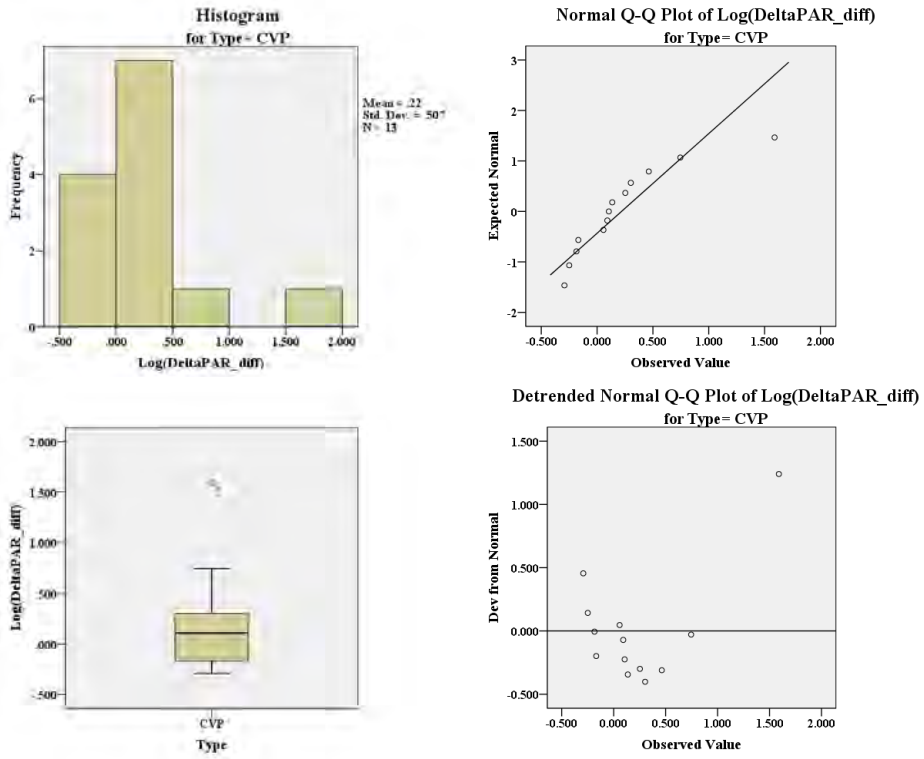

Figure 63: Exploratory Statistics Self-Same CVP PAR Differences

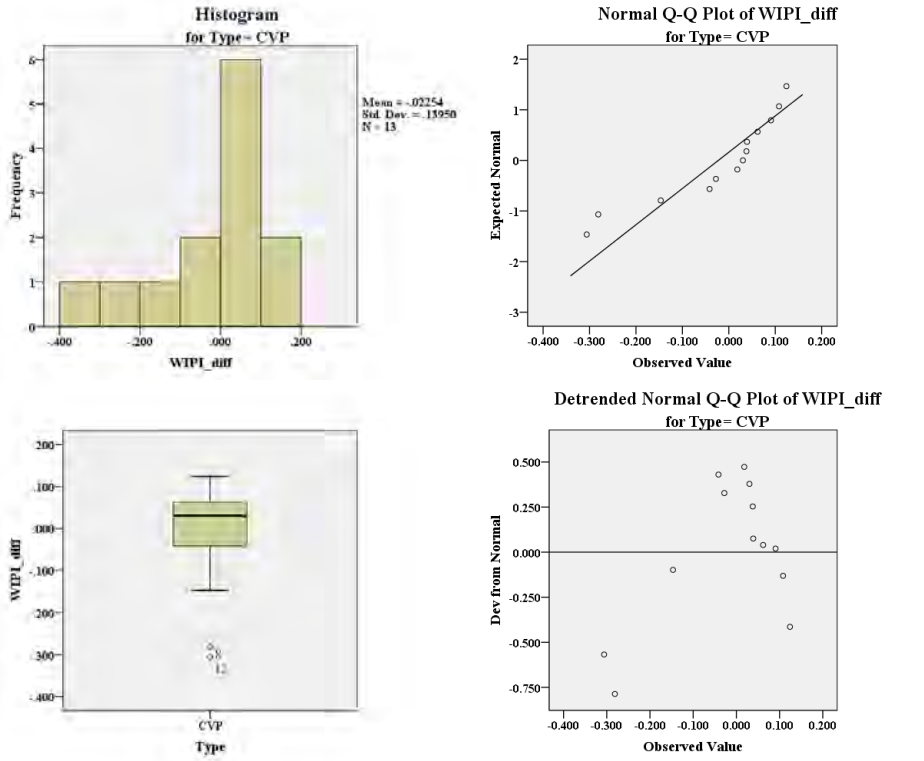

Figure 64: Exploratory Statistics Self-Same CVP WIPI Differences

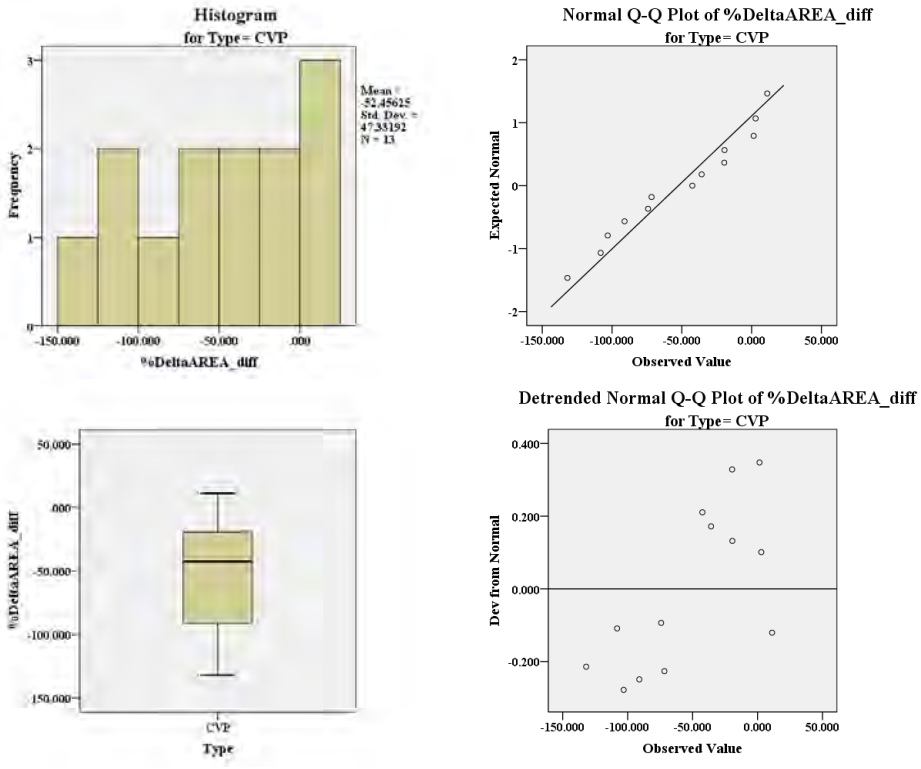

Figure 65: Exploratory Statistics Self-Same CVP % Area Differences

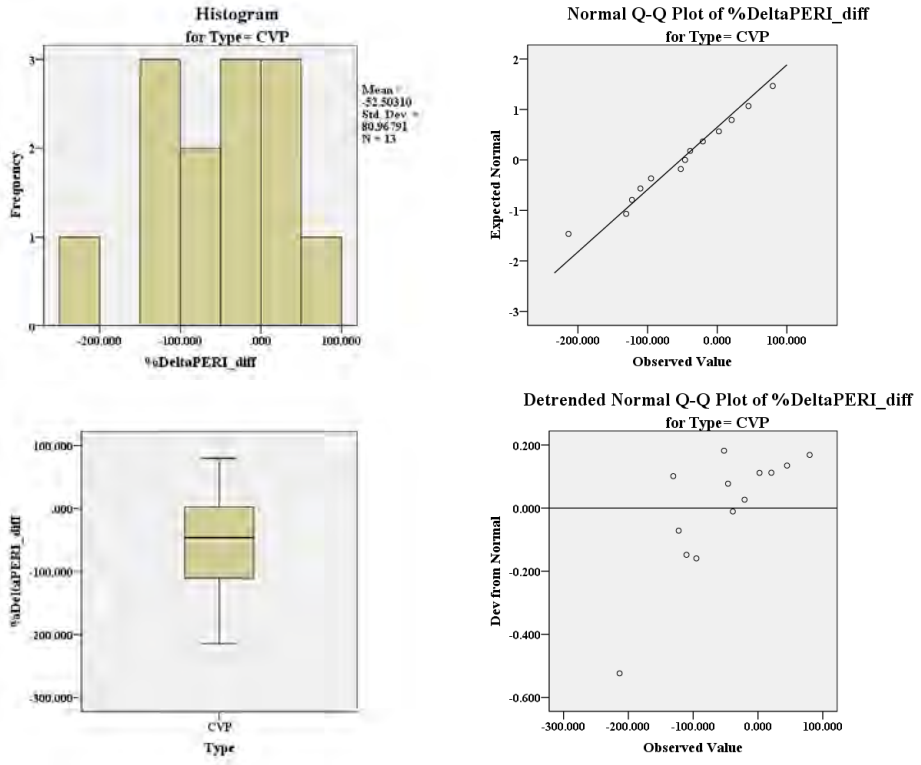

Figure 66: Exploratory Statistics Self-Same CVP % Perimeter Differences